UNIVERSITY OF L'AQUILA

DEPARTMENT OF BIOTECHNOLOGICAL AND APPLIED CLINICAL SCIENCES

PhD in Experimental Medicine

Curriculum Medical Biotechnology

XXXIV cycle

Thesis title

"Study of the regulation of mitochondrial function by the C-terminal fragment of the M_2 muscarinic receptor"

SSD BIO/14

Candidate

_____

Coordinator

Prof. _____

Tutor

Prof. _____

a.a. 2020/2021

Contents

List of abbreviations

A: Adenine

ACh: Acetylcholine

cAMP: Cyclic adenosine monophosphate

cGMP: Cyclic guanosine monophosphate

C-terminal: carboxyl-terminus

CaM: Calmodulin

Cys: Cysteine

COS-7: Fibroblast-like cell lines derived from monkey kidney tissue

COX8A: Cytochrome c oxidase subunit 8A

CNS: Central nervous system

DAG: Diacylglycerol

DMEM: Dulbecco's modified Eagle's medium

EC_{50}: Half maximal effective concentration

EGFP: Enhanced green fluorescent protein

ER: Endoplasmic reticulum

ERK: Extracellular signal-regulated kinase

p-ERK: Extracellular signal-regulated kinase phosphorylated

FAD: Flavin adenine dinucleotide

ETC: Electron transport chain

FBS: Fetal bovine serum

FCS: Fetal calf serum

G: Guanine

GDP: Guanosine diphosphate

GPCRs: G-protein coupled receptors

GTP: Guanosine triphosphate

H: Hairpin

HBSS: Hanks' Balanced Salt Solution

HEK: Human embryonic kidney cells

HT: Heterozygous

hiPSCs: Human induced pluripotent stem cells

HRP: Horseradish peroxidase

IC_{50}: Half maximal inhibitory concentration

eIF: Eukaryotic initiation factors

IP_3: Inositol trisphosphate

IRES: Internal ribosome entry site

ITAFs: IRES trans-acting factors

i3: Third intracellular domain

K_d: Dissociation constant

MAPK: Mitogen-activated protein kinase

mAChR: Muscarinic acetylcholine receptors

Met/M368: Methionine 368

mRNA: Messenger ribonucleic acid

NAD: Nicotinamide adenine dinucleotide

NMS: N-Methylscopolamine

N-terminal: amino-terminus

N.C.: Negative control

Nt: nucleotide

OCR: Oxygen consumption rate

ORF: Open reading frame

PAGE: Polyacrylamide gel electrophoresis

PBS: Phosphate-buffered saline

PIP_2: Phosphatidylinositol diphosphate

PKC: Protein kinase C

PLC: Phospholipase C

PNS: Parasympathetic nervous system

RPMI: Roswell Park Memorial Institute medium

ROS: Reactive oxygen species

sgRNA: Single guide ribonucleic acid

rRNA: Ribosomal ribonucleic acid

SDS: Sodium dodecyl sulphate

Ser: Serine

SMAC: Second mitochondria-derived activator of caspases

ssODNs: Single-stranded oligodeoxynucleotides

T: Timine

tdTomato: Tandem dimer Tomato

Thr: Threonine

TM: Transmembrane

TOM: Translocase of outer membrane

tRNA: Transfer ribonucleic acid

UAE: Ubiquitin activating enzyme

UPS: Ubiquitin-proteasome system

WT: Wild type

5'-UTR: 5' untranslated region

Aim of the thesis

In eukaryotes the translation process occurs in most cases through a cap-dependent mechanism, in which translation initiation factors bind the 5' terminal of the mRNA and induce recruitment of the ribosome, which starts the mRNA scanning process up to the first AUG start codon. The AUG codon is not always read in the correct open reading frame (ORF) context, in these cases, alternative translation initiation mechanisms are activated, including the cap-independent translation process mediated by nucleotide sequences that serves as the internal ribosome entry site (IRES). The IRES sequences form long and ordered RNA structures which alone or together with canonical eIF (eukaryotic initiation factors) and specific activation factors called ITAFs (IRES trans-acting factors), recruit ribosomes to initiate translation at an internal start codon of the mRNA sequence, bypassing the canonical scanning mechanism of the untranslated region at 5'-UTR.

This IRES-dependent translation has not been fully understood yet, but it had been shown that it is important in guiding protein synthesis in particular cellular contexts where cap-dependent translation is impaired, such as stressful conditions (apoptosis, response to hypoxia and ischemia), disease or during embryogenesis and development.

IRES elements have also been identified in G protein-coupled receptors (GPCRs), a family of transmembrane receptors involved in numerous physiological and pathological processes, present in different tissues and systems, that are essential for the proper functioning of the living organism. GPCRs have a typical serpentine structure, with a single polypeptide chain crossing the membrane seven times; the seven transmembrane domains are connected to each other by intracellular and extracellular loops. The third cytoplasmic loop and the carboxy-terminal domain are responsible for the interaction with the G protein, determining its activation, which causes a series of phosphorylation in order to promote a cellular response. To the GPCRs family belongs the subfamily of the mAChR, muscarinic acetylcholine receptors, activated by the endogenous neurotransmitter acetylcholine.

Radioligand binding, biochemical and molecular biology experiments have shown that the carboxyl terminal fragment of the muscarinic M_2 receptor, containing the transmembrane regions VI and VII (M_2tail), can be expressed by virtue of an IRES.

Mutations in the DNA sequence corresponding to the third cytoplasmic loop of the M_2 receptor, allowed us to identify the third in-frame methionine, Met368, as the alternative starting point of the translation of C-terminal portion, triggered by the IRES sequence. Therefore in this thesis, starting from this assumption, we have seen through fluorescence microscopy that the M_2tail doesn't follow the normal route to the plasma membrane, as the wild-type receptor does, but it is sorted into the mitochondria.

The use of a construct in which we have marked the sequence of the third cytoplasmic loop of the M_2 receptor with a fluorescent protein, the GFP, has allowed us to observe the expression mediated by IRES of the labelled carboxyl terminal domain, its different and precise localization in the mitochondria and we have been able to indicate the inner mitochondrial membrane as the subcellular localization; the presence in the mitochondria induces a considerable decrease in oxygen consumption by impairing oxidative phosphorylation that leads to a reduced cell growth and affects the oxygen radical formation.

In this thesis I present data concerning the expression of the C-terminal region of M_2 muscarinic receptor, as well as of other GPCRs, that can regulate mitochondrial function, that represents a novel mechanism that cells could activate for controlling their metabolism under variable environmental conditions; this data are available to be examined in depth in a pre-printed version of the paper [1]**(Petragnano et al., 2022)**.

Chapter 1: Key elements overview

1.1 Mechanism of translation in Eukaryotes

The genetic information contained in the DNA is transcribed into a messenger RNA (mRNA) molecule via an RNA polymerase. The mRNA is organized in nucleotide sequence based on codons units, each one codes for specific amino acids that will constitute the protein. The primary transcript mRNA undergoes post-transcriptional modifications that allow it to reach maturation through three processes: the insertion of a 7-methylguanylate cap (m7GpppN) at 5' (capping), the addition of the polyadenine tail at 3' (polyA) and the splicing of exons due to the presence of introns. Transfer RNA (tRNA), the protein responsible for identifying the codon and adding the corresponding amino acid, together with ribosomal RNA (rRNA), constitute the machinery complex behind the protein translation.

The genetic information is under the control of a regulatory sequence containing a promoter and an operator. The typical organization of polycistronic mRNA - mRNA is called polycistronic if it carries the information for several genes that are common in prokaryotes - is due to the characteristic setting of genes in operons, a series of genes displayed in succession along the chromosome encoding protein products with related functions. Usually, they are involved in the same metabolic pathway and are controlled by a single promoter. The genes arranged in sequence do not have transcription termination signals except for the last gene, which leads to the generation of a long molecule of polycistronic mRNA.

This can represent an important advantage, in situations where prokaryotes may need immediate adaptation to the surrounding environment, and polycistronic mRNA gives them the ability to synthesize most of the necessary proteins in a single step starting from a mRNA.

In eukaryotic cells, polycistronic mRNAs are less present, but clusters of genes with related functions can be observed. The first example of a eukaryotic polycistronic cellular mRNA is the gene for murine differentiation/growth factor 1 (GDF-1).

In eukaryotes, the most common mechanism of translation is the cap-dependent process, which requires the interaction of several key proteins at the 5' end (5′ cap) of

mRNA molecules. Protein biosynthesis is a complex process that consists of three phases: initiation, elongation and termination. In eukaryotes, the initiation phase - the most complex - can occur through different pathways that include translation depending on the cap 5' or scanning model - non-canonical pathways such as ribosomal shunting - cap-independent translation mediated by the internal ribosome entry site (IRES) [2]**(Komar & Hatzoglou, 2011).**

The canonical cap-dependent translation is mediated by eukaryotic initiation factors (eIFs) recruited in the untranslated region at the 5' (5'-UTR) of the mRNA, a sequence upstream of the start codon. The first step is the recruitment of the cap-binding protein eIF4E to cap 5' and the assembly of a protein complex called eIF4F; this complex also includes other functional proteins in the complex, such as eIF4G, responsible for the recruitment and binding of initiating factors and the ATP-dependent RNA helicase eIF4A. The latter has the task of unraveling the secondary structures of the mRNA, promoting the translation process.

The eIF4B factor acts together with the eIF4A factor by unrolling the messenger RNA in the 5'-UTR and aiding the binding of the 40S ribosomal subunit, in this phase dissociated from the 60S subunit.

The union of eIF4B and the 40S subunit leads to the formation of the 43S pre-initiation complex, accompanied by a ternary complex containing a tRNA initiator molecule together with factor eIF2 and a molecule of GTP (eIF2-GTP-Met-tRNAi^{Met}), both from the initiation factor eIF3 which acts as a bridge for the link between the 40S subunit and the eIF4G factor linked to mRNA. The ATP-dependent helicase eIF2, provide the anticodon for the initiator Met-tRNAiMet directly to the peptidyl site of the ribosomal subunit. The hydrolysis of GTP is carried out by eIF5 which in turn activates eIF2 and only at this point does the release of the initiating factors occur [3](**Jackson & Hellen, 2010)** The factors eIF1, eIF1A and eIF5 facilitate the recognition of the start codon.

The 43S pre-initiation complex moves from the 5'-UTR in the 5′ to 3′ direction to the starting AUG codon, where the 48S pre-initiation complex will be formed. The last important protein for the initiation of translation is the GTP-ase eIF5B which promotes the binding of the major 60S subunit with the minor subunit, forming the 80S complex: elongation phase start from this point.

After the termination of protein synthesis, the 40S subunit and the eIF2-GDP factor are recycled allowing the complex to interact again with Met-tRNAi^{Met} and to start a new protein translation more quickly [3]**(Jackson & Hellen, 2010,** Figure 1**).**

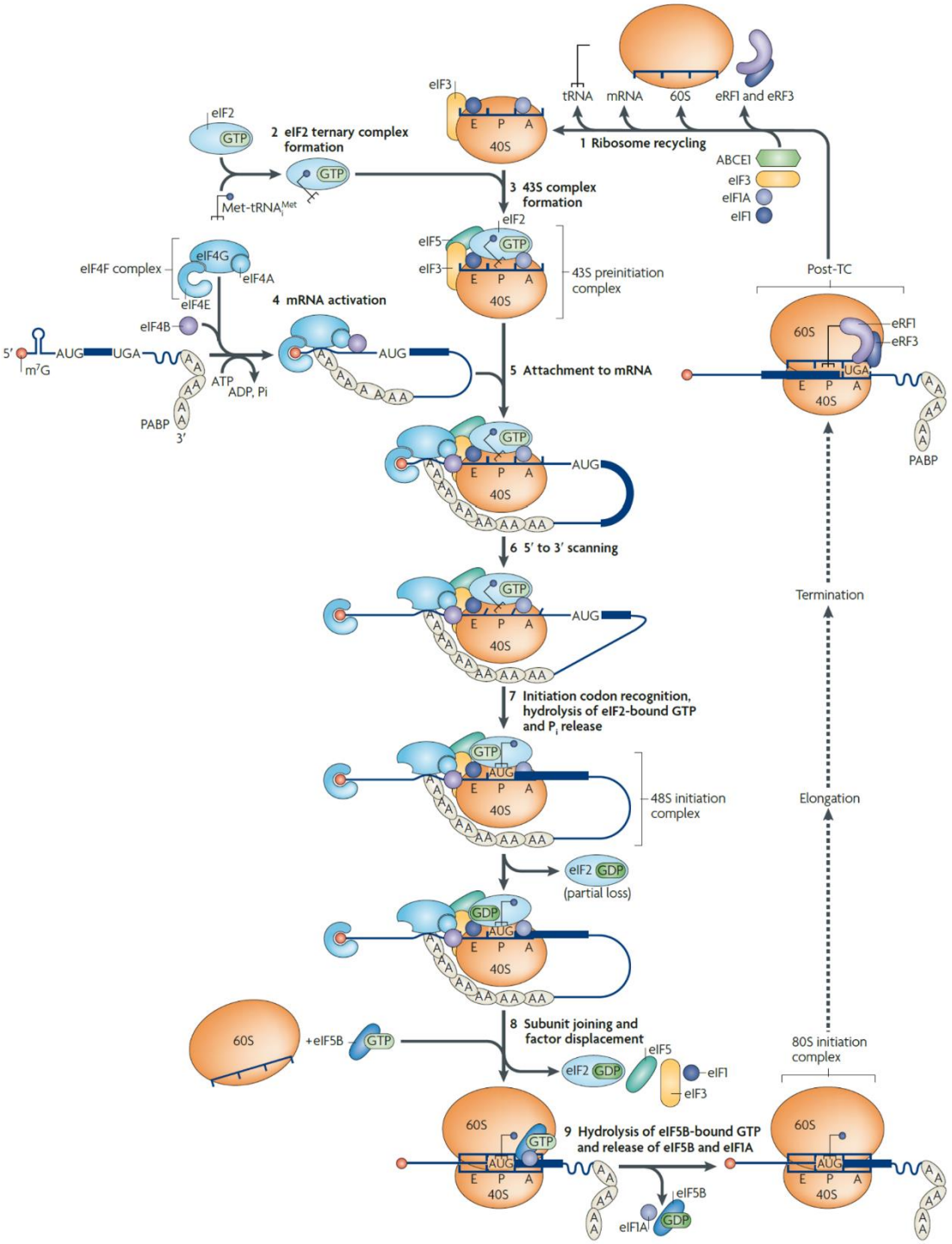

Figure 1 Schematic representation of the canonical pathway of eukaryotic translation initiation. (by Jackson & Hellen, 2010)

1.1.1 Non-canonical mechanisms

The cap-dependent translation mechanism or scanning model is the mechanism by which most mRNAs are translated into protein, but at least five other non-canonical mechanisms have been described: leaky scanning, termination-reinitiation, ribosomal shunting, translational readthrough, and internal initiation.

In the scanning mechanism, the protein synthesis begins at the first AUG codon after the 5'-UTR region. It may occur in the process known as leaky scanning, that the first AUG codon is skipped and the ribosome recognizes the second or third AUG downstream (Figure 2a). This mechanism is particularly used by viruses, where it presumably helps to save coding space.

In the termination-reinitiation mechanism, on the same mRNA molecule, a second ORF, following the stop codon of the first ORF, can be translated without dissociation of the 40S subunit of the ribosome. The translation starts from the first AUG encountered after the 5-UTR, it finishes at the stop codon and if an AUG is present in close proximity, the ribosome resumes translating a new protein (Figure 2b). The distance of the second start codon and particular sequences close to the stop codon of the first ORF can influence the frequency of this mechanism [4]**(Hinnebusch, 1990)**.

For ribosomal shunting, the 40S subunit binds the mRNA molecule at cap 5', but when it meets secondary RNA structures along the sequence, it skips the segment bypassing the hairpin loop and picking up again from a downstream start codon (Figure 2c). In this process sequences such as those placed near the hairpin loop and the start codon seems to play a crucial role. This mechanism is activated especially when many secondary structures composed the mRNA to the 5'-UTR [5]**(Yueh & Schneider, 2000)**.

With the translational readthrough mechanism, the UAG and UGA stop codons are translated as coding codons through particular tRNAs, avoiding the translation block and generally synthesizing a longer polypeptide.

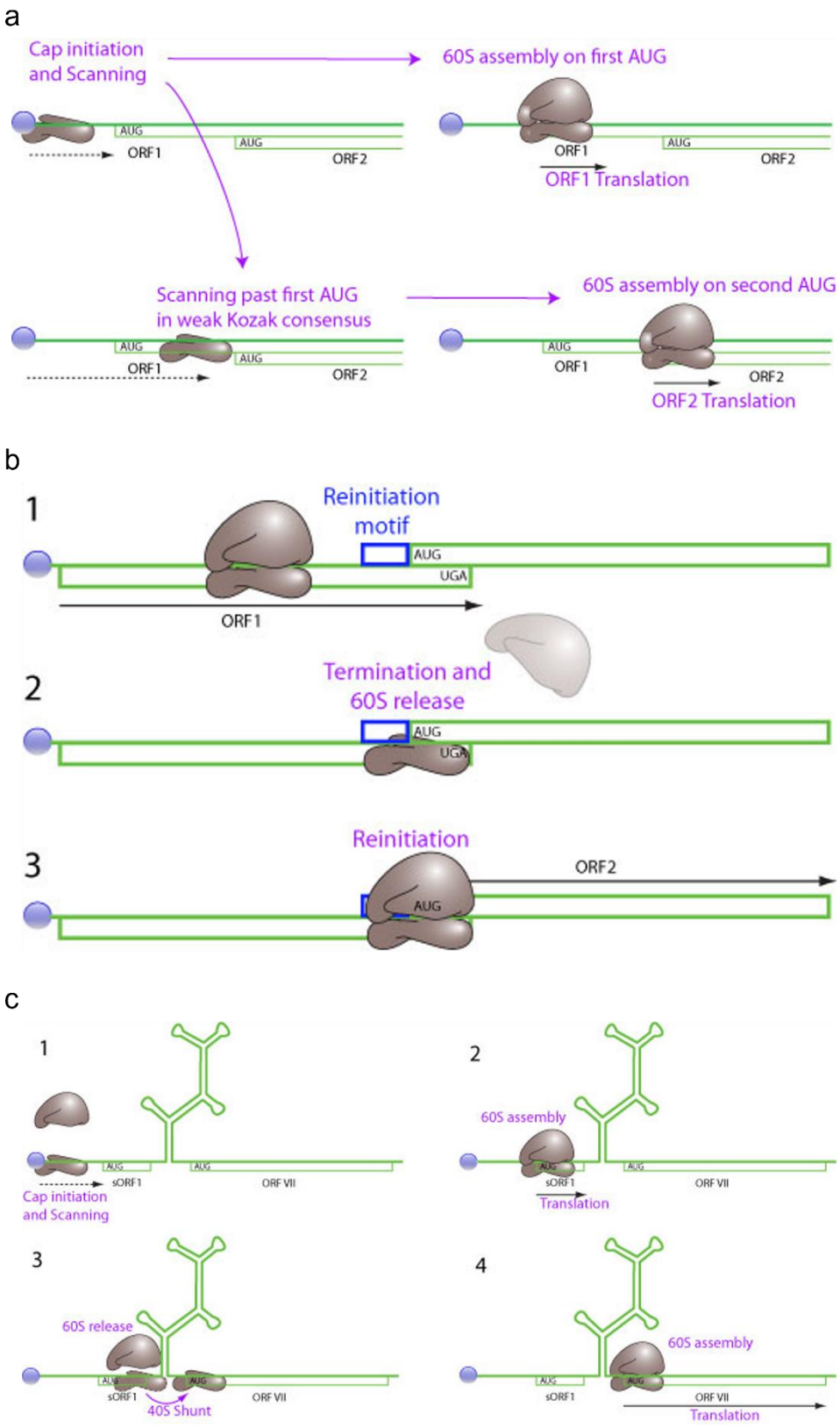

Figure 2 Graphic representation of the non-canonical mechanism of translation: a) leaky scanning, b) termination-reinitiation and c) ribosomal shunting. (by Expasy bioinformatics resource portal, Swiss Institute of Bioinformatics (SIB))

1.1.2 IRES and translation cap-independent

Recently it has been demonstrated that the presence of IRES sequences, which are common features of virus replication [6]**(Jackson & Kaminski, 1995)**, can mediate cap independent translation of eukaryotic RNAs [7]**(Hellen & Sarnow, 2001).**

The discovery of the process in the picornavirus, which bypassed cap recognition and allowed the 40S ribosomal subunit to be recruited directly in the vicinity of the start codon, was the first step in questioning the existence of only cap-dependent mechanism for translating mRNA into protein in the eukaryotes.

This process involves the presence of particular regions within the mRNA called Internal Ribosome Entry Site (IRES), a nucleotide sequence that allows the initiation of protein synthesis within the messenger RNA sequence.

This cap-independent translation is activated when cap-dependent initiation is impaired in pathological and stressful situations such as: hypoxia, nutrient limitation, cap impairment, or processes related to tumorigenesis such as angiogenesis; but it can also happen that it is induced in physiological conditions during mitosis, apoptosis and cell differentiation [2]**(Komar & Hatzoglou, 2011).**

Viral IRES are secondary or tertiary elaborated structures, which activate the translation process without the binding of the ribosome to the cap; the nucleotide sequence contains numerous non-conserved AUG codons upstream of the start codon, used as a barrier for ribosomes that use the scanning method**.** Unlike the viral, cellular IRES sequences are less known, because they are more heterogeneous in terms of sequence, size or even secondary and tertiary structure [7]**(Hellen & Sarnow, 2001)**.

The extremely variable conformation, the lack of precise structural motifs and clearly identifiable sequences have complicated the identification of IRES elements; they can also appear in the form of stem loops, pseudoknots or in alternative forms. The viral IRES sequences can be grouped into two categories, following the sequential and structural similarities:

- The first group identifies viruses containing an IRES sequence with an AUG triplet located towards the 3 'end of the sequence and 25 nucleotides

downstream of a tract rich in pyrimidines. Although not located at the 5' end, this triplet is bound directly by the ribosome without activating the scanning mechanism [8]**(Kaminski et al., 1990)**.

- In the second group, viral IRES have two AUG triplets spaced by 84 bases, responsible for the initiation of protein synthesis; in this case the mechanism is not perfectly known and it is still to understand how the ribosome binds, whether through a model of scanning or shunting of the subunits [9,10]**(Sangar et al., 1987, Belsham, 1992)**.

Most of the eukaryotic IRES are located within the 5'-UTR upstream of the start codon but they also may be located downstream the start codon or within the coding regions, resulting in the formation of truncated proteins [11]**(Komar et al., 2003)**.

The IRES of eukaryotic polycistronic mRNAs can induce formation of different proteins from a single mRNA sequence; sometimes they can have such large structures that they are divided into smaller elements in proximity to each other as if they were modules.

The mechanism of initiation of eukaryotic translation mediated by IRES is similar to the viral one, but the interaction between ribosomes and IRES sequence is not entirely clear. Some cellular IRES such as the derived from the homo-domain of the Gtx protein and the IRES of the human protooncogene IGF1R, appear to act through an interaction similar to the one which occurs during the prokaryotic translation process in the Shine-Dalgarno sequence between IRES and the 16S subunit of rRNA. IRES generally do not have a great need to recruit the canonical initiating factors, especially the members of the eIF4F complex, which normally are modified by phosphorylation or protein cleavage, which make them inflexible in the translation process [2]**(Komar & Hatzoglou, 2011)**.

In cases of extreme stressful situations, these eIFs factors are not minimally involved and there is a direct interaction of IRES with the ribosome [12]**(Baird et al., 2007)**; some studies have revealed that the IRES involved in the translation of c-myc and N-myc do not need either the eIF4E factor or the eIF4G factor but require interaction with initiating factors such as eIF4A and eIF3.

The eIF2 factor, the most important eukaryotic initiation factor, was also investigated to study its possible implication in the IRES-mediated pathway: some cellular IRES don't show sensitivity to the inhibition of protein synthesis caused by the

phosphorylation of the eIF2 factor, unlike what occurs in mRNAs without IRES. Phosphorylation of the α-subunit of eIF2 (eIF2α) is a common consequence under stressful conditions such as nutrient restriction, by reducing the activity of the ternary eIF2-GTP-Met-tRNAiMet complex, cap-dependent protein synthesis is inhibited: the fact that some IRES, both viral and cellular, are not sensitive to the inhibition of the ternary complex has suggested that they differ from each other in the recruitment of the different components necessary for the binding of the ribosome.

Others possible factors involved could be the eIF5B factor and ligatin: in this model, eIF5B allows the attack of Met-tRNAiMet and ligatin activates the translation process without the eIF2 factor or its other substitutes such as the MCT-1 oncogene and the density-regulated protein (DENR). Ligatin and MCT-1/DENR promote the attack of the ribosomal Met-tRNAiMet complex by initiating protein synthesis [2]**(Komar & Hatzoglou, 2011,** Figure 3**)**.

An IRES sequence may also require the engagement of non-canonical translation initiation factors called IRES trans-acting factors (ITAFs) [13]**(Fitzgerald & Semler, 2009)**, a heterogeneous group of nuclear ribonucleoproteins (HnRNPs) known as shuttles between the nucleus and the cytoplasm, which play numerous roles and participate in a variety of cellular activities such as mRNA splicing and its transport to the cytoplasm. The ITAFs increase the binding affinity between the IRES and the components of the translational apparatus, including the canonical initiating factors.

How they exactly act is not completely clear but, there are various hypotheses, including one saying that ITAFs remodel the structures of the IRES, modifying their conformation to allow an increase in affinity for the ribosomal components; another hypothesis is that they can build or abolish the bond between the mRNA sequence and the ribosome, modulating the action of canonical initiation factors; a third one argues that ITAFs take the place of eIFs by creating bridges themselves between the translational machinery and the nucleotide sequence [14]**(Lewis & Holcik, 2008)**.

In yeast has recently been discovered a new family of IRES characterized by an adenine-rich domain (A-rich), which efficiently activate cap-independent translation. The poly-A binding protein (PABP protein) interacts with the poly-A tract that precedes the AUG start codon and the factors eIF4G and eIF3, two very important scaffold proteins in the initiation of cap-dependent translation. In mammals, the interaction of the various proteins that take part in the IRES-mediated translation process with the non-canonical

factors ITAFs is not yet known, however, it is known that PABP interacts with some RNA binding proteins, including ITAFs, Unr and NSAP1, and these bonds help to build the missing bridges between RNA and ribosome.

Unlike the one found in yeast, the adenine-rich tract upstream of the start codon has a negative effect on the regulation of the activity of some eukaryotic IRES. An example is the mRNA of p27 (Kip1), an inhibitor of cyclin-dependent kinases, in which the ITAF Hur binds the A-rich region, inhibits the activation of IRES encoding p27 (Kip1), with consequent reduction of inhibitor expression and increase in tumor cell proliferation [15]**(Coleman & Miskimins, 2009)**.

Among the various explanations regarding the possible effects of the poly-adenine tract, the most accredited is the one affirming that it can activate or suppress the translation IRES-mediated by acting as a competitive target for canonical and non-canonical starting factors.

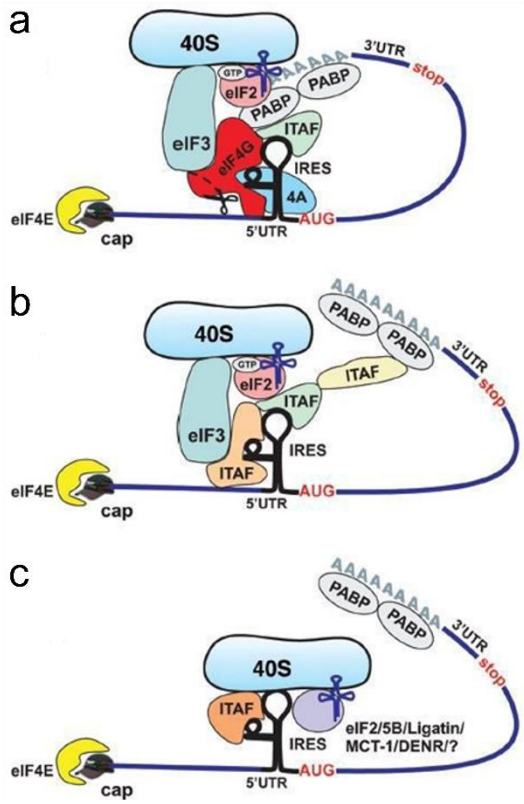

Figure 3 Hypothetical structure of IRES and interaction with canonical and non-canonical initiation factors in cellular translation IRES-mediated mechanism. (by Komar and Hatzoglou, 2011)

1.2 GPCRs

G protein-coupled receptors (GPCRs) are a large family of transmembrane receptors, consisting of a polypeptide chain forming seven transmembrane domains (TM domains I-VII) one extracellular N-terminal domain of variable length and an intracellular C-terminal one. The seven transmembrane regions are connected via three extracellular and three intracellular loops; the third of these cytoplasmic loops, together with the C-terminal domain, forms the G protein binding site.

Several endogenous ligands bind to these receptors (noradrenaline, dopamine, serotonin, LH, FSH, TSH, photons, angiotensin, substance P) with different binding manner based on the type of receptor [16](**Dorsam & Gutkind, 2007**). The binding site can be located in a transmembrane pocket (neurotransmitters and photons), on the extracellular surface of the receptor (cytokines and peptides) or even on the N-terminal domain of the receptor (glycoprotein hormones).

In the TM domains, there are highly conserved residues that increase towards the cytoplasmic side; the third loop can, instead, be very different both in terms of length and amino acid composition [17](**Clementi, 1996**).

The GPCRs are classified in 4 main classes according to the sequence, the structure, the length of the N-terminal domain, the localization of the binding site, the type of G protein they interact with:

- Class A, rhodopsin-like receptors, the most numerous class(representing approximately 80% of human GPCRs),which includes in addition to receptors for monoamines and neuropeptides, also many proteins involved in tumorigenesis.
- Class B, secretin-like receptors, which include the secretin receptors for glucagon and calcitonin.
- Class C, identified later than the others, which includes metabotropic glutamate receptors (mGlu) and calcium-sensitive receptors.
- Class D, groups the so-called Frizzled or adhesion receptors to which the lipoglycoproteins of the Wingless family (Wnt) bind.

G proteins have a heterotrimeric structure, the three subunits α, β and γ, are all anchored to the plasma membrane by means of a fatty acid chain. The α subunit binds guanine nucleotides, mostly GTP (guanosine triphosphate), and being endowed with intrinsic GTPase activity, catalyses the hydrolysis of GTP to GDP (guanosine diphosphate). The β and γ subunits are very hydrophobic and remain associated as a βγ complex to the cytoplasmic surface of the membrane. In the steady state, the G protein is in the trimeric form, associated neither with the receptor nor with intracellular effector molecules but with a molecule of GDP bound to the specific site of the α subunit. The conformational change induced by the ligand-receptor binding, activates the cytoplasmic domain of the receptor itself, which acquire an increasing affinity for the αβγ trimer. The trimer associated with the receptor causes the release of GDP, which is replaced with a molecule of GTP, leading to the release of α-GTP and the βγ complex. The α-GTP subunit and the βγ subunit both possess the ability to mediate the effects of the ligand on specific cellular effectors.

The activation cycle ends when the α subunit hydrolyzes GTP to GDP, leading to the new formation of the α-GDP complex and re-associating to the βγ complex, restoring the initial trimeric form.

A single GPCR can couple one or more Gα protein families, and each of these can activate or inhibit several downstream effectors in the signal pathway.

The classification of G proteins is based on the activity of the α subunit, allowing it to be divided into four families: Gαs, $G\alpha_{i/o}$, $G\alpha_{q/11}$ e $G\alpha_{12/13}$ (Figure 4).

The $G\alpha_s$ e $G\alpha_{i/o}$ subunits, respectively activate and inhibit the adenylate cyclase enzyme which catalyses the synthesis of cyclic AMP (cAMP) starting from ATP.

$G\alpha_{i/o}$ is more abundant in the nervous system; the $G_{i/1}$, $G_{i/2}$ e $G_{i/3}$ subunits mediate receptor-dependent inhibition of different isoforms of adenylate cyclase [18](**Wettschureck & Offermanns, 2005**).

The cAMP, a second messenger, has its main substrate in the cAMP-dependent protein kinase (PKA), which after activation acts by phosphorylating cytoplasmic substrates or activating nuclear transcription factors such as CREB (cAMP responding element binding protein) [19](**Rossi, 2005**).

$G\alpha_{q/11}$ family binds and activates the phospholipase C enzyme (PLC), which cleaves membrane phosphatidylinositol bisphosphate (PIP_2) into diacylglycerol (DAG)

and inositol triphosphate (IP_3), second messengers involved in the regulation of intracellular calcium levels.

$G\alpha_{12/13}$ subunits, often activated by $G\alpha_{q/11}$ coupled receptors, are ubiquitously expressed. Unlike the other families, the $G\alpha_{12/13}$ signaling pathway was difficult to identify, due to the lack of inhibitors of these proteins. Indirect studies with constitutively active mutant forms have shown that they can activate effectors such as phospholipase A2 (PLA2), tyrosine kinases and cadherins of class I and II [18](**Wettschureck & Offermanns, 2005**).

The other two subunits of G proteins, Gβ and Gγ act by activating different molecules, including phospholipases, ion channels, and lipid kinases that become activated in the signaling process.

In addition, the Gα and Gβγ subunits can control the activity of key intracellular signaling molecules, including some small GTP-binding proteins of the Ras families, members of the mitogen-activated protein kinase family (MAPK), serine-threonine kinases, including extracellular signal-regulated kinase (ERK), c-Jun N-terminal kinase (JNK), p38 and ERK5, all pathways that end with the activation of cell proliferation and growth processes [16](**Dorsam & Gutkind, 2007**).

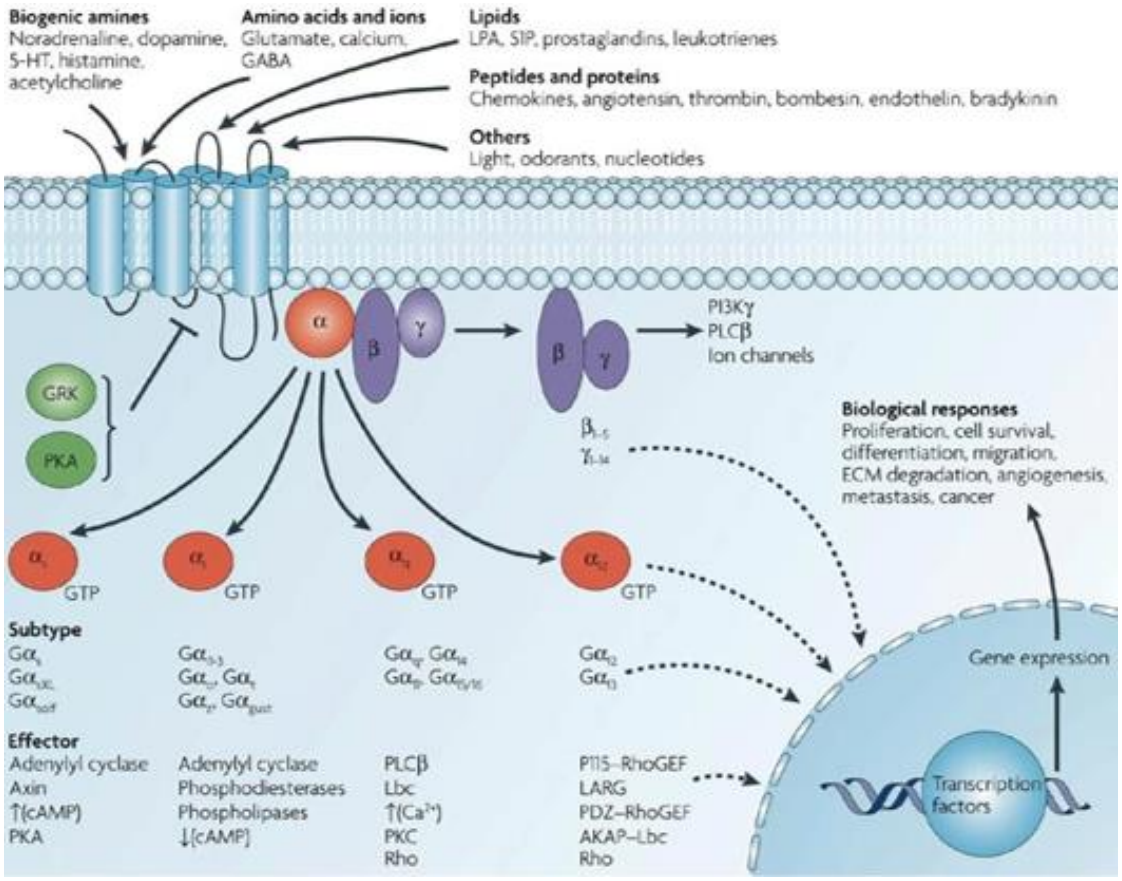

Figure 4 Ligand activation of G protein subunits with the relative signaling pathways and effector. (by Dorsam & Gutkind, 2007)

1.2.1 Muscarinic receptors

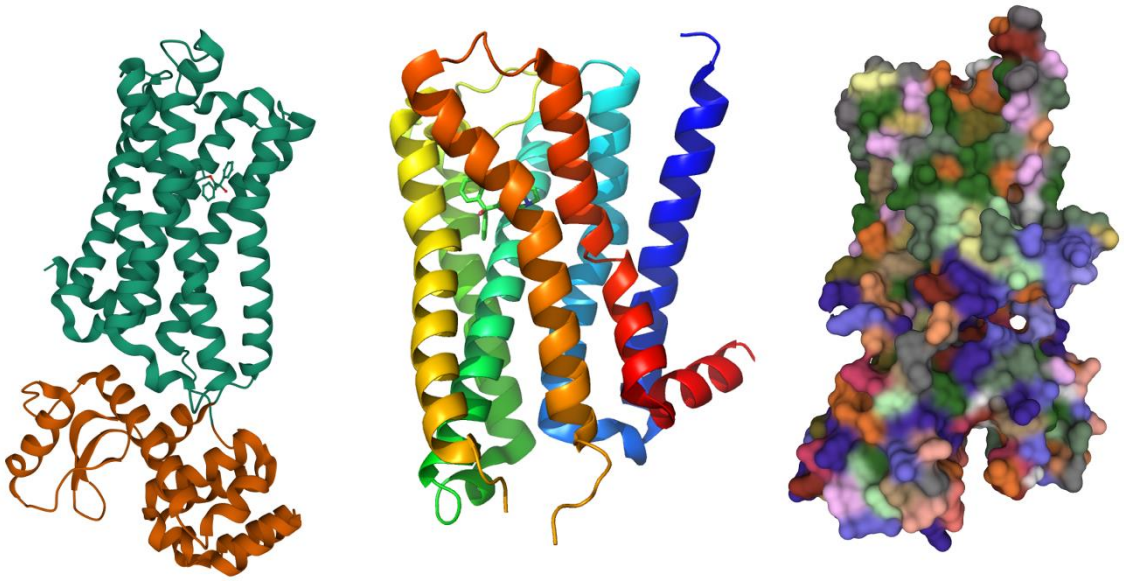

Figure 5 Structure of the M_2 receptor: on the left a representation of the polymer chain, in green the transmembrane region, the agonist is in the binding site, in orange the third cytoplasmic loop. In the middle detail of the TM segments in different colors from I to VII. On the right a representation of the molecular surface of the receptor, each color identifies different residues. (by rcsb.org)

Muscarinic cholinergic receptors are transmembrane metabotropic receptors, belonging to the family of G protein coupled receptors. The genes that code for the five muscarinic subtypes are called CHRM1, CHRM2, CHRM3, CHRM4 and CHRM5. They are found in different loci in the human genome and are highly compact as they do not contain introns; for this reason, the resulting gene products are highly homologues among the various species of mammals.

They are expressed in many organs and tissues, but each muscarinic receptor has a unique distribution in the central and peripheral nervous system, being expressed at both the pre- and postsynaptic level.

In tissues innervated by the parasympathetic nervous system, they mediate the slowdown of the heart rate, the stimulation of glandular secretion and the contraction of smooth muscle; in the sympathetic ganglia, they mediate the slow excitation triggered by acetylcholine and in the CNS, they modulate cortical activity, cognitive processes, and the activity of the extrapyramidal pathways.

Their endogenous ligand is the neurotransmitter acetylcholine (Ach). Ach exerts its physiological control through hormonal and neuronal mechanisms by acting on the five muscarinic receptor subtypes: M_1, M_2, M_3, M_4 and M_5, each of which can prevail over the others based on the anatomical site. All the five muscarinic receptors have a similar structure, with a high degree of homology especially for the seven transmembrane domains; differences are found in the intracytoplasmic portions, responsible for the interactions with the various signal transduction proteins.

The binding site is placed in a deep pocket on the extracellular side of the cell, where amino acid residues are highly conserved, one of the amino acids which acetylcholine comes in contact with is Asparagine 105 (Asp105) that is found in the transmembrane region III. Five residues Thr231, Thr234, Tyr148, Tyr506, Tyr529 and Tyr533 stabilize the binding of the neurotransmitter to the receptor [20]**(Jöhren & Höltje, 2002);** the activation by the Ach induces a conformational change of the TM domains III, V, VI, VII.

The M_1, M_3 and M_5 receptors are coupled to $G\alpha_q$ proteins that stimulate PLC, resulting in the formation of the second messengers DAG and IP_3 starting from the membrane phospholipid PIP_2. IP_3 is involved in signal transduction and spreading inside the cell, reaches and binds its receptor- a channel protein located on the surface of the endoplasmic reticulum- inducing its opening, and allowing the flow of calcium ions from the reticulum to the cytoplasm. Calcium can activate protein kinase C (PKC), a serine-threonine kinase that catalyzes the phosphorylation of other intracellular proteins involved in various functions such as DNA replication, synthesis and maturation of RNA, gene expression, nucleus-cytoplasmic transport.

Combining with calmodulin (CaM), calcium can activate cellular regulation which undergoes a conformational change from the inactive to the active state.

The Ca^{2+}/calmodulin complex can: activate a group of protein kinases that have as a target proteins that play a role in cellular metabolism, in protein synthesis and secretion and it can regulate the contraction of the striated muscles and the assembly of microtubules.

Both M_2 and M_4 receptors are coupled to $G\alpha_{i/o}$ proteins, and both appear to play a role in modulating hippocampal cholinergic function, as indicated by studies in which M_2 and M_4 were knocked out in mice. Other studies have shown that genetic variants of the M_2 receptor are found in various neurodegenerative diseases such as Alzheimer's disease or in depressive disorders.

The M_1 receptor outnumbers at the level of the autonomic ganglia and is present at the level of the CNS, where it is involved in the processes of memory and movement, in the salivary glands and in the stomach where it acts by stimulating secretion. M_1 receptor is also present at the post-synaptic level where it allows the initiation of the excitatory post-synaptic potential (EPSP), binding to the $G\alpha_q$ subunit. In addition to acetylcholine and carbachol agonists, other molecules acting as antagonists are scopolamine, dicycloverine and pirenzepine.

The muscarinic M_2 receptor is expressed in both the CNS and PNS, especially in the myocardium where when activated regulate the heart rate. The activation of this receptor by the ligand triggers a transduction of the signal that couples to Gαi protein, which inhibit the enzyme adenylate cyclase causing a decrease in the concentration of cAMP in the cell, resulting in the suppression of all cAMP-dependent cellular functions. The two βγ subunits induce the opening of potassium channels and in the heart, it means a bradycardic action, a reduction in the contractile force of the atrium and a reduction in atrio-ventricular conduction. The increase in the conductance of potassium ions counteracts the incoming current of sodium ions, typical of pacemaker cells. A state of hyperpolarization is thus induced at the level of the sinoatrial node responsible for cardiac changes such as the decrease in the force of contraction **[17](Clementi, 1996)**. In neurons, the βγ complex interferes with calcium channels voltage-dependent by blocking their flow, consequently, calcium ions cannot flow inside the cytoplasm and in this way the activation of calcium-dependent proteins is inhibited.

The M_3 receptor is involved in the contraction of smooth muscle, is responsible for the secretion of various exocrine and endocrine glands such as the salivary and stomach glands. It is prevalent in the eye, where it regulates the tension of the ciliary muscle by modulating accommodation and allowing close vision. In the CNS it is particularly present in the hippocampus, where it is involved in processes that regulate learning, as well as in the hypothalamus and in the dorsal vagal complex of the brainstem, areas that regulate insulin homeostasis. Furthermore, M_3 receptors appear to mediate the decrease in bone resorption driven by the PNS, allowing the formation of new bone tissue **[21](Wess et al., 2007)**. Is also widely expressed in the β cells of the pancreas, where it regulates glucose homeostasis by modulating insulin secretion; for this reason, it

represents an important target for understanding the underlying mechanisms of diabetes mellitus type 2 [22]**(Weston-Green et al., 2012)**. In vascular smooth muscle, the intracellular increase in calcium due to the activation of M_3, determines the CaM-dependent activation of the nitroxide-synthase enzyme, expressed at the endothelial level, which produces nitroxide, a gas with a vasodilatory action.

The M_4 muscarinic receptor, whose function is still under study today, is localized in the central nervous system, in particular in the striated nucleus and in the cortex and in smaller extent in the pancreas and heart [23]**(Peralta et al., 1987)**.

The M_5 receptor has been recently identified: it is expressed in restricted areas of the CNS, including the ventral tegmental area (VTA) and on the membrane of dopaminergic neurons of the substantia nigra, which regulate the release of dopamine at the striatal level [24]**(Eglen et al., 2001)**. It is also expressed at the peripheral level, more precisely at the level of the ciliary muscle cells of the iris, on the lymphocyte membrane and in the muscle cells of the esophagus. Its function in these sites is not yet fully clarified.

1.2.2 Alternative splicing and truncated receptors

In the human genome, genes are made up of different gene sequences, some coding, the exons, and others non-coding, the introns, interludes in the primary mRNA transcript (pre-mRNA) excise during the maturation process in an operation called alternative splicing. Some of them may remain in the sequence that will be translated into protein and others are cut by the spliceosomes.

Thus, a nucleotide sequence can give life to proteins of different nature called isoforms, as some introns can be kept in the mature mRNA, the exons excised, extended, or even skipped, giving life to various protein isoforms with similar or opposite functions to those. originals [25]**(Wise, 2012)**.

Because of post-translational modifications, alternative splicing and different G proteins or accessory proteins which they interact with, GPCRs also have a large number of isoforms that are widespread in various tissues depending on the receptor type. In this way the signaling and regulatory pathways and the pharmacological properties can be heterogeneous [25]**(Wise, 2012)**.

In particular, by alternative splicing it is possible to generate truncated receptors compared to the wild type one, with only some of the transmembrane domains of the receptor or receptors in which the C-terminal portion is completely missing; in the last case there is an alteration of the properties of the receptor at the level of traffic and coupling with the G protein.

During migration to the cell surface, GPCRs undergo post-translational modifications to become functional; in many cases the truncated form of the receptor retains the wild type inside the intracellular compartments, in the ER, preventing the accomplishment of the maturation process. This event can have relevant consequences since the biological response can be reduced [25]**(Wise, 2012)** and being involved in various pathologies, such as in nephrogenic (X-linked) diabetes insipidus, familial hypocalciuric hypercalcemia or deficit familial of glucocorticoids. In some circumstances, it has been shown that the truncated receptors, also remaining in the endoplasmic reticulum, have signaling activity. Studies on the β_2-adrenergic receptor has shown that during vesicular transport from the endoplasmic reticulum to the Golgi apparatus, GPCRs are "pre-associated" with G protein and with effector enzymes forming a signaling complex. An example is the truncated ghrelin receptor (GHS) which induces constitutive activation of extracellular signal-regulated kinases (ERK1/2) within the ER in HEK293 cells.

Under normal conditions, neurotransmitters and endogenous hormones do not bind to a truncated receptor, because its structure is not complete to recognize the ligands and because it is not expressed on the plasma membrane.

This testifies that the signal transduction pathways can be activated not only through exposure of the receptor on the cell surface, but also if it remains confined to the ER [25]**(Wise, 2012)**.

Other studies have highlighted the ability of the truncated forms of the receptors to interact with the missing domain to form a complete wild type protein, leading to the hypothesis that the GPCRs oligomerize through the exchange of fragments, thanks to the process called domain swapping, a mechanism known thanks to the use of two receptor chimera between the α_2-adrenergic receptor and muscarinic M_3 [26(]**Maggio et al., 1993a)**.

Chapter 2: IRES identification in the third cytoplasmic loop of M_2 receptor

2.1 M_2 wild type, mutants, and truncated forms

The analysis of the M_2 receptor structure led us to identify two functional segments: a N-terminal (TM I-V) and a C-terminal (TM VI-VII) (Figure 6); from ligand binding assays, some variants of the M_2 show K_d values for the N-Methylscopolamine ([^{3}H]NMS), an antagonist, and the IC_{50} values for the agonist carbachol, similar to those for the wild type M_2 receptor. In particular, these data were observed surprisingly for a mutant with a stop codon at position 228 (M_2Stop228, Figure 6); this mutant receptor produces an mRNA transcript of the same length as the wild type form, coding for a receptor functionally active as it inhibits adenylyl cyclase **[27](Maggio et al., 2016)** and increase ERK phosphorylation, even though the extent of response is lower than the wild type receptors.

When a stop codon is inserted upstream or downstream of position 228, no radioligand binding can be observed, as well as occurs with the M_2trunk(1-228), the first part of M_2stop228, until the stop 228, lacking the downstream sequence and with a receptor fragment with a stop codon in the i3 loop and devoid of the downstream sequence, called M_2trunk(1-283) (Figure 6). Both these constructs express only the TM I-V region of the M_2 but the co-transfection with a construct containing the TM VI-VII (M_2tail(281-466)) (Figure 6) restore binding and downstream signaling ability because there is the reconstitution of a functional full-length receptor at the cell membrane **[28](Maggio et al. 1993b)**: this is possible only if the C-terminal portion of the receptor is expressed despite the presence of stop codons in the i3 loop in the M_2stop228 mutant and the receptor sequence downstream of the stop codon, TM VI-VII is translated and interacts with the TM I-V segment of the M_2 receptor.

M_2 receptor mutant bearing the stop codon in TM V-VI, M_2stop400, doesn't show binding [^{3}H]NMS, restored by co-transfecting it with M_2tail(281-466), giving evidence of the interaction of that receptor fragment with the mutant stop mutant. **[29](Maggio et al., 1999)**.

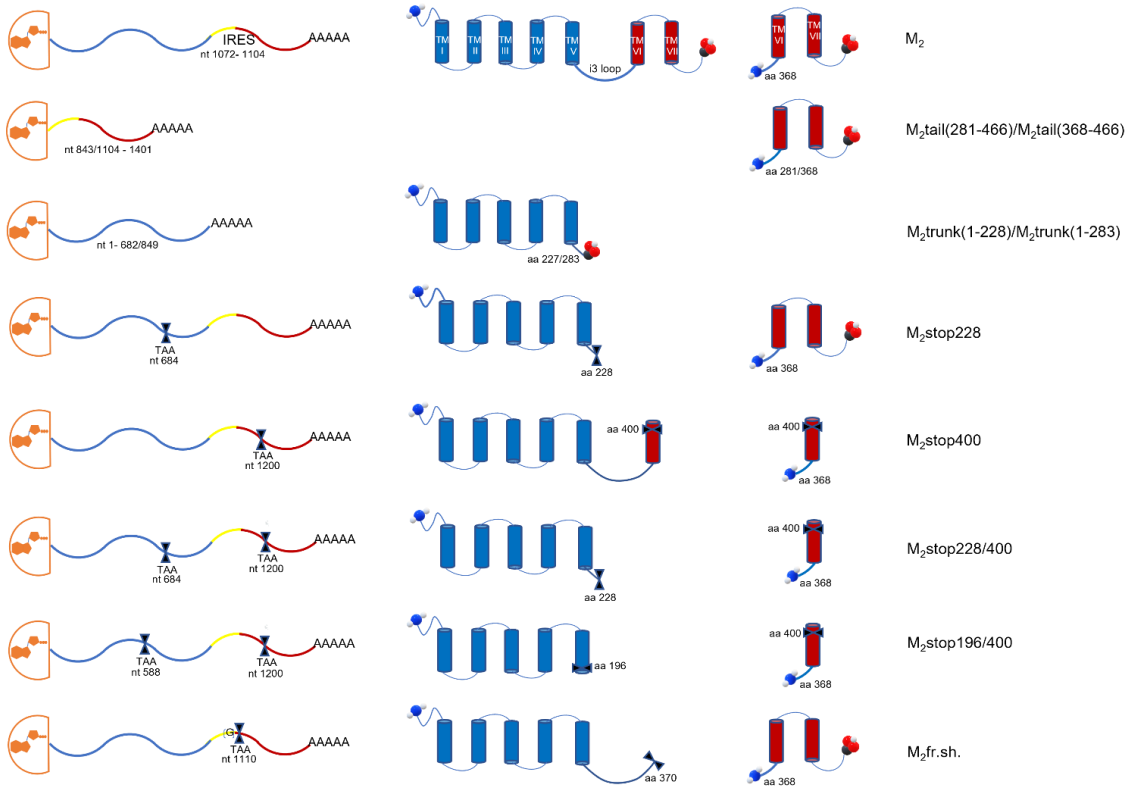

Figure 6 Representation of wild type muscarinic M_2 wild type receptor and derived mutants, the left structures indicate the mRNA products from each construct, the right one the expected protein product. TAA = Stop codon (by Petragnano et al., 2022, image created by Petragnano F.)

Also the receptor mutant containing two stop codons, M_2stop228/stop400 (Figure 6), when transfected alone in cells, didn't give evidence of capability of binding [^{3}H]NMS, but co-transfection with M_2tail(281-466) rescued the binding activity up to a value comparable to that observed after co-transfection of M_2trunk(1-283) with M_2tail(M281-466).

Unlike M_2stop228/stop400, co-transfection of M_2stop196/stop400 (Figure 6) with M_2trunk(1-283) or M_2tail(281-466), did not result in [^{3}H]NMS binding: this suggests that the rescue of these receptor mutants depends on the position of the stop codons and that the receptor can't be rescued if the stop codons are present both in TM V and VI, as in M_2stop196/stop400, that are the two segments that contain the third cytoplasmic loop.

Confirming the fact that in the M_2stop228 the C-terminal portion of the receptor is expressed despite the presence of stop codons in the i3 loop and the TM VI and VII are translated and interact with the TM I-V of the M_2 receptor, the enhanced green fluorescent protein (EGFP) has been fused at the C-terminus of some receptor mutants: cells expressing the M_2WT-EGFP displayed predominant plasma membrane localization, but

also cells expressing the M_2stop228-EGFP displayed intracellular green fluorescence, while cells expressing M_2stop400-EGFP do not show any fluorescent signal as well as the non-transfected control.

The fact that M_2stop228-EGFP shows green fluorescence is a strong evidence that the sequence downstream of the stop in position 228 is translated; to corroborate this evidence, another mutant has been used: the M_2fr.sh.-EGFP created by insertion of a single guanine (G) in the sequence of the M_2WT-EGFP, upstream of nucleotide 1102 that cause a change in the ORF and generates, following 2 amino acids, an in-frame stop codon (TAA) at position 370. But also in this case an EGFP signal has been found in transfected cells, even though the EGFP is now out of the ORF, supporting the presence of a cap-independent translation mechanism, starting from a methionine located between the position 228 and 400.

As suggested from this data and as we will demonstrate later, the starting point is the third in-frame methionine of the i3 loop, Met368.

2.1.1 Excluding other possible mechanisms

Assumed that for binding activity to occur the carboxyl-terminal part of the M_2stop228 construct has to be translated, to exclude other possible mechanism, the possibility of the presence of alternative splicing that can remove the stop codon has been verified; the mRNA extracted from cells transfected with M_2WT and M_2stop228 for the reverse transcription, amplified by PCR reaction, showed a single band comparable in size to both M_2WT and M_2stop228 receptor mRNAs, as well as it was for the M_2 cDNA control (Figure 7), whose amplification was carried out with the same antisense oligos used for reverse transcription, together with a sense oligo directed against nucleotides at the 5' end of the M_2 open reading frame.

Stop codon suppression or translational read-through occur when a stop codon is interpreted as a sense codon encoding a standard amino acid **[30](Schueren et al., 2014)**. The insertion of four bases AATT downstream the stop codon 228 creates a frameshift in the construct M_2stop228/fr.sh., that was used to verify the possibility that the stop codon has been read as a sense codon, but also in this case the frameshift doesn't alter [^{3}H]NMS

binding activity of the mutant that essentially retains the B_{max} values of 47 ρmol/mg of protein.

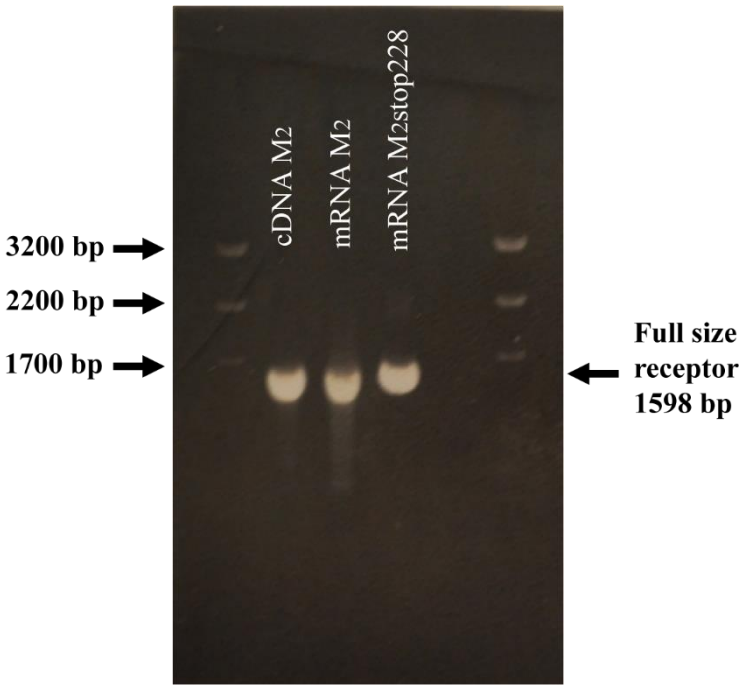

Figure 7 The image shows mRNAs extracted from COS-7 cells, proving a lack of alternative splicing in in both M_2 wild type and M_2stop228, as inferred from the single band of 1401 bp corresponding to the full-size receptor, running at the same level of the band amplified directly from the M_2 pcD plasmid. (by Petragnano et al., 2022)

As described above, termination re-initiation allows ribosomes to reach and initiate translation at downstream second AUG codon when the first AUG resides in a suboptimal context. This is likely to occur when the first AUG codon is at a short distance by an in-frame terminator codon and post-termination ribosomes resume scanning. Re-initiation is thus strictly connected to the length of the first ORF, so the farther the ORF the more re-initiation probability decrease, and to the nucleotide distance of the termination codon from the subsequent AUG initiation codon **[31](Kozak, 2001)**.

M_2stop228 mRNA is far from complying with both these conditions, as the first ORF is 684 nucleotides long and the following first in-frame AUG is 57 nucleotides far from the artificial stop codon. However, in spite of these adverse conditions, the carboxyl terminal could still be translated by a termination re-initiation mechanism. So a palindromic sequence was inserted 15 nucleotides downstream of the stop codon, that forms a hairpin structure with a ΔG of −64 kcal/mol when transcribed into mRNA,that is a value high enough to block ribosome scanning **[31,32](Kozak 2001,1989)**. The insertion

of the hairpin reduced slightly the [^{3}H]NMS binding activity of the receptor, without abolishing it, attaining a B_{max} value of 37 ρmol/mg protein.

In this way the possibility of read-through [30,33] **(Schueren et al., 2014; Loughran et al., 2014)** and termination-reinitiation was assessed, and the evidence confirms that these are not the mechanisms that account for the binding of M_2stop228.

The only explanation left for the translation of the carboxyl terminal was the presence of a mechanism enabling a cap-independent initiation of protein synthesis, most probably an internal ribosomal entry site (IRES) positioned downstream of the artificial stop codon 228 and preceding the third in-frame methionine (codon 368) of the i3 loop [6,7] **(Jackson & Kaminski, 1995; Hellen & Sarnow, 2001)**.

2.1.2 M368: the starting point of IRES-mediated translation

To figure out which of the three start codons of the i3 loop was responsible for the translation of the M_2stop228 c-terminus fragment, all the possible start codons have been mutated into an additional Stop codon beyond that in position 228.

Thus, these three new mutants were created: M_2stop228/stop248, M_2stop228/stop296 and M_2stop228/stop368, the first two are still able to bind [^{3}H]NMS with B_{maxs} of 49 fmol/mg and 38 fmol/mg of protein, respectively, while the third one lost completely the [^{3}H]NMS binding ability. It is rescued when it is co-transfected together with the M_2tail(281-466) construct.

This radio-ligand binding data, together with the results from fluorescence microscopy, proof that Met368 is the site for the cap-independent initiation of translation of the C-terminal domain.

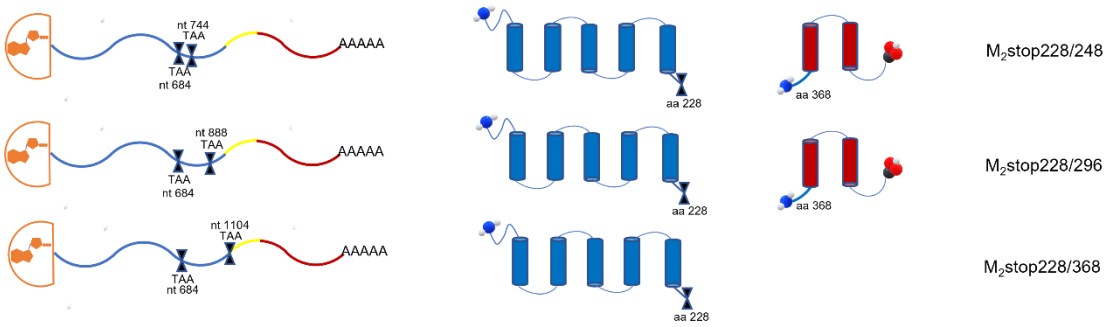

Figure 8 Representation of the double stop mutants derived from the wild type receptor, used for individuating the methionine responsible for the start of IRES dependent translation, the mRNA products for each construct and the expected protein products. (by Petragnano et al., 2022, image created by Petragnano F.)

2.2 Use of bicistronic constructs to mark out IRES sequence

To verify the presence of the IRES, a plasmid with the sequence from nucleotide 685 (a.a. 228) to nucleotide 1101 (a.a. 368) of the i3 loop of M_2 was created and inserted between two fluorescent proteins; the first one, Sirius protein -an emitting blue light protein located upstream the sequence-is expected to be translated according to the classical cap-dependent mechanism, while the second one, EGFP protein-a green fluorescent protein-is translated by the IRES mechanism supposed to be present in the inserted sequence, being the gene for the EGFP downstream the sequence itself.

This construct was named Sirius-M_2i3(417n)-EGFP and different type of cells transfected with it were positive for both blue and green fluorescence.

The bicistronic plasmid was modified with the insertion of a hairpin loop after the stop codon of the Sirius protein -Sirius-H-M_2i3(417n)-EGFP- to exclude again read-through and termination-reinitiation mechanisms and the result was only a slight reduction of the EGFP fluorescence, 85 ± 8% of the value measured for the Sirius-M_2i3(417n)-EGFP plasmid; quite the opposite the Sirius-Hairpin-EGFP plasmid, where only the hairpin was left, abolished green light emittance completely, reducing the relative fluorescence to a level comparable to that of the control plasmid bearing only the Sirius protein (Figure 9). This made it possible to conclude that the M_2i3 loop is essential for EGFP to be expressed and that the presence of an IRES within the sequence is required to control its expression.

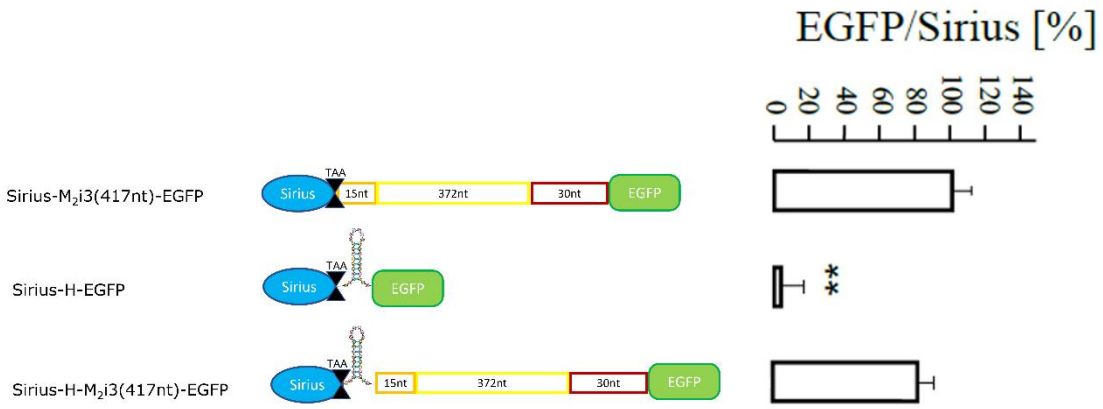

Figure 9 Representation of the bicistronic constructs Sirius-M_2i3(417n)-EGFP, Sirius-Hairpin-EGFP and Sirius-H-M_2i3(417n)-EGFP with the relative ratio EGFP/Sirius. (by Petragnano et al., 2022)

Thanks to the comparison between all the i3 loop sequence of all the five muscarinic receptors (Figure 10), it was possible to define and limit the IRES sequence within the M_2i3 loop; only the last portion of the M_2i3 loop, more precisely the 30 nucleotides from 1072 to 1101, clearly shows several conserved nucleotide residues, corresponding to regions adjacent to the second in frame ATG in M_1, the fourth in M_3 and M_4 and first in M_5.

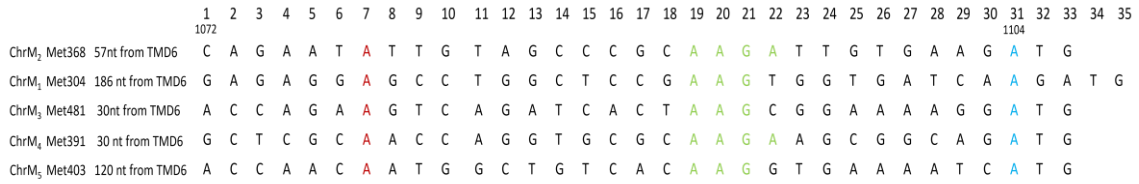

Figure 10 Alignment of five Muscarinic receptors; the conserved and common residues are highlighted with different colors following the different position. (by Petragnano et al., 2022)

Thus, the M_2i3 loop was divided into three nucleotide sequences 685-699 (15nt), 685-1071 (387nt) and 685-699/1072-1101 (15/30nt), and inserted downstream of the hairpin loop in three different plasmids: Sirius-H-M_2i3(15n)-GFP, Sirius-H-M_2i3(387n)-GFP and Sirius-H-M_2i3(15n/30n)-GFP (Figure 11).

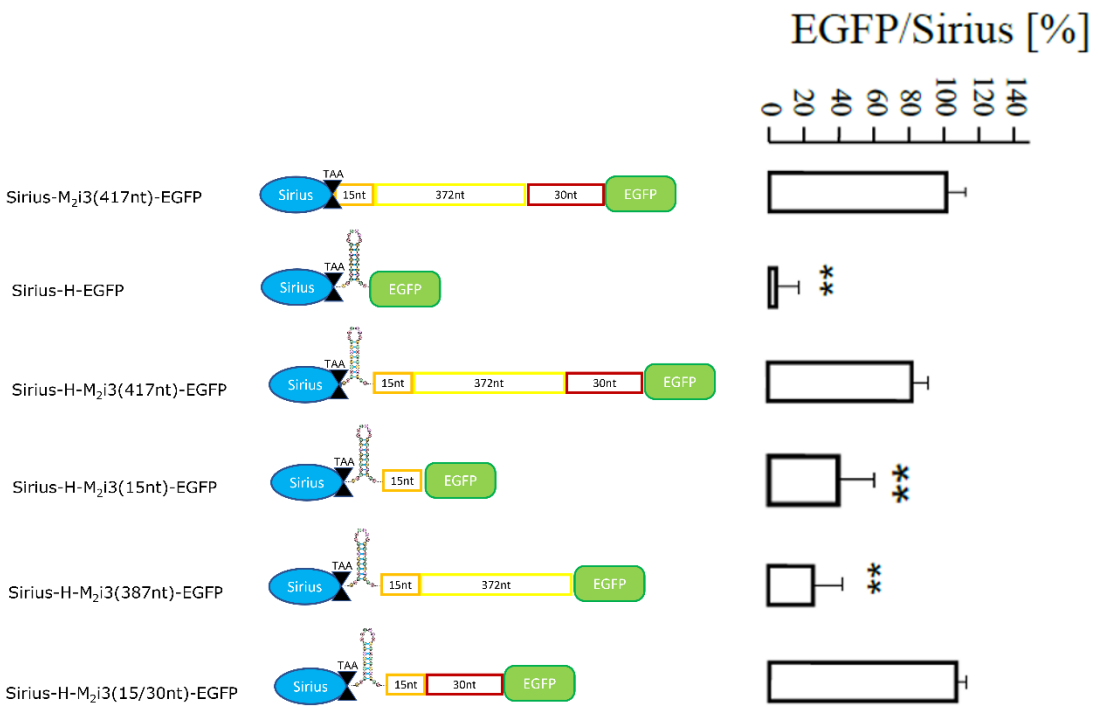

Figure 11 Bicistronic plasmids reporting the three segments of M_2i3 loop IRES and comparison of the relative fluorescence. (by Petragnano et al., 2022)

Comparing their EGFP fluorescence activity with that of Sirius-H-M_2i3(417n)-GFP (Figure 11), we can see that it was completely lost upon insertion of the first 15 nucleotides 685-699 of the i3 loop after the hairpin, retained partially (27 ± 13%) by the 387 nucleotides (685-1071) and it was recovered when the last portion 685-699/1072-1101 was inserted into the plasmid after the hairpin (110 ±5%).

Putting together the previous data of the complete abolishment of the binding ability after the mutation of the Met368 with these data, it's possible to conclude that the IRES is located in a region of the i3 loop sequence immediately upstream of the third methionine 368.

To determine which are the most important conserved residues for the recruitment of the ribosome, the IRES sequence has been mutated following the results below obtained by the sequence alignment of the 33 nucleotides (Figure 10), from 1072 to 1104 of the M_2i3 loop, adjacent to the in frame ATGs of the five muscarinic receptors:

- an A in position 1078.
- three nucleotides AAG in position1090-1092, four nucleotide AAGA 1090-1093 considering the two most related muscarinic M_2 and M_4 receptors.

The position of the ATG was conserved in four out of five muscarinic receptors.

Replacing nucleotide A1078 with T, Sirius-H-M_2i3(15n/30n)Mut#1-GFP, the EGFP fluorescence intensity compared to Sirius-H-M_2i3(15n/30n)-EGFP is split in half; mutation of the four nucleotides AAGA1090-1093 with TTTT, Sirius-H-M_2i3(15n/30n)Mut#2-EGFP, clearly decreased EGFP expression, retaining only a fluorescence of 24 ± 14% compared to Sirius-H-M_2i3(15n/30n)-EGFP (Figure 12).

The residues AAGA that affected more dramatically EGFP expression, were altered and mutated in a T sequence comprised between nucleotides 1083 and 1101, Sirius-H-M_2i3(15n/30n)Mut#5-EGFP, and then inserted again in their original position in the T altering sequence, Sirius-H-M_2i3(15n/30n)Mut#6-EGFP: comparing them only 12.3 ± 10.3% of the green fluorescence originally present in Sirius-H-M_2i3(15n/30n)-EGFP was retained in the first mutant while it could be recovered up to 118 ± 7% in the second one (Figure 12).

Also, random mutations of other non-conserved purine nucleotides were placed, as control experiment, respectively Sirius-H-M_2i3(15n/30n)Mut#3-EGFP and Sirius-H-

M_2i3(15n/30n)Mut#4-EGFP, and they did not show to alter significantly EGFP expression (Figure 12).

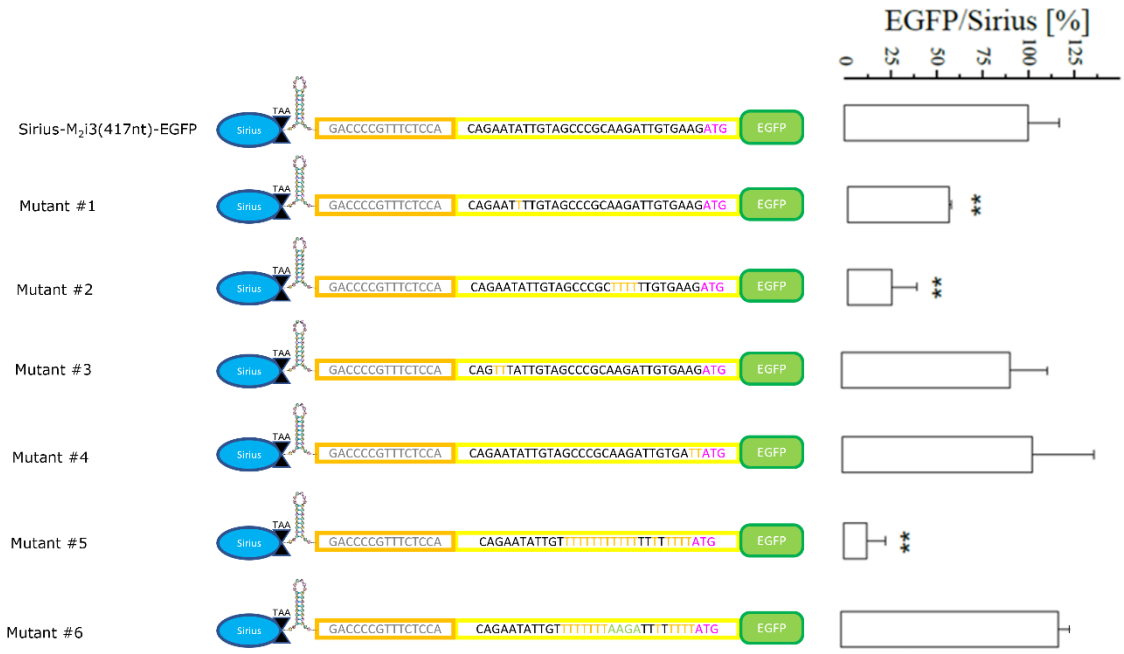

Figure 12 Mutation of conserved residues in the sequence of 30 nucleotides important for the recruitment of ribosome, compared on the relative fluorescence ratio. (by Petragnano et al., 2022)

All these data together underline that expression of the carboxyl terminal domain of the M_2stop228 receptor is made possible thanks to an IRES sequence located in the N-terminal of the M_2i3 loop that recruits the ribosome.

2.2.1 Common sequence in GPCRs

As we previously showed by alignment of the 34 nucleotides, from 1072 to 1105 of the M_2i3 loop, several nucleotide residues are conserved corresponding regions of all four muscarinic receptors. Extending the alignment to the other amine receptors, with at least one methionine in the i3 loop looking at the methionine with the nearest AAGA sequence or an analogous sequence containing at least three purines, it appeared that some purine residues are still conserved even among these receptors.

If there were more than one AAGA or analogous sequence, it was chosen the one that allowed the best match with the muscarinic receptors. The sequences were then aligned by centring them on the AAGA or analogous sequence and it appeared that some purine residues were still conserved even among these receptors.

The frequency of the four nucleotides was calculated and all the A's and G's were mutated into T's that pulled together scored higher than 65%.

Aminergic Receptors

Figure 13 Alignment of amine receptor: the already fixed residues are highlighted with green color; in red are reported other purine residues in another position, repeated frequently in the receptor's sequences; in blue are the pyrimidine residues common in all the sequences.

By comparison of the short sequence of i3 loop in different species for the M_2 (Figure 14), M_3 (Figure 15) and D_2 (Figure 16) receptors, a sort of selection for purine bases in the sequence is dominantly important for the IRES mechanism; the D_2 is one of the no muscarinic receptor with more similarity in the sequence.

```
Human          TGGAGGTAGTGGGGTCTTCAGGTCAGAATGGAGATGAAAAGCAGAATATTGTAGCCCGCAAGATTGTGAAGATG
Rat            TAGAACTAGTTGGGTCGTCGGGTCAGAGTGGGGATGAAAAGCAGAACGTTGTAGCCCGCAAAATCGTGAAGATG
Mouse          TAGAACTAGTTGGATCGTCAGGTCAGAATGGGGATGAAAAGCAGAACATTGTAGCCCGCAAAATTGTGAAGATG
Pig            TGGAGCTTGTTGGTTCTTCAGGTCAGAATGGAGATGAAAAACAGAACATTGTCGCTCGCAAGATTGTGAAGATG
Chicken        ACACTACAGTGGAGATTGTAGGCACCAATGGGGATGAGAAGCAGAACAGTGTAGCCCGGAAAATAGTCAAGATG
Bovine         TGGAGCTAGTTGGTTCTTCAGGTCAGAATGGAGATGAAAAACAGAACATCGTTGCTCGCAAGATTGTGAAAATG
Poec.Prolifica(fish) CATCAAATGCCACAGTCGAGATTGTGCCAAGCACAGAACGTCAGAACCACGTGGCGAGGAAGATCGTGAAGATG
Chimpanzee     TGGAGGTAGTGGGGTCTTCAGGTCAGAATGGAGATGAAAAGCAGAATATTGTAGCCCGCAAGATTGTGAAGATG
Drosophila     CGGGTGTAACACCACCGGTGCCACTGGAAAGGATTGAGGAGCGAGAAACCTCGGACAGTAATACCAACAAGATG
Cat            TGGAGCTAGTTGGTTCTGCAGGTCAGAACGGAGACGAAAAACAGAACATCGTCGCTCGTAAGATTGTGAAGATG
Zebrafish      CTTCAAATGCGACGGTGGAGATCGTGCCGGCAGTGGAAAGGCAGAACCACGTGGCGAGAAAGATCGTGAAGATG
GuineaPig      TGGAGTTAGTTGGGTCTTCGGGTCAGAATGGAGATGAAAAACAGAATATTGTGGCCCGCAAGATTGTGAAGATG
Ornithorhyn.   CGGAAGTCGCGGGGTCCCGGGGCCAGAACGGGGACGACAGGCAAAACGTAGTGGCCCGCAAGATCGTCAAGATG
Gorilla        TGGAGGTAGTGGGGTCTTCAGGTCAGAATGGAGATGAAAAGCAGAATATTGTAGCCCGCAAGATTGTGAAGATG
Opossum        TGGAGATTGTTGGTCCTCCAGGACAGAATGGGGATGATAAACAGAATATTGTTGCCCGCAAGATTGTGAAGATG
Am.Chameleon   TGGAGATTGTAGGCCCCGATGAACAAAATGGAGATGAGAAGCAGAATGTTGTAGCACGTAAGATTGTCAAGATG
Dog            TGGAACTAGTTGGTTCTGCAGGTCAGAACGGAGATGAAAAACAGAACATTGTAGCTCGCAAGATTGTGAAGATG
GiantPanda     TGGAGCTCGTTGGTTCAGCAGGTCAGAACGGAGATGAAAAGCAGAACATTGTGGCTCGCAAGATTGTGAAGATG
Orangutan      TGGAGGTAGTGGGGTCTTCAGGTCAGAATGGAGATGAAAAGCAGAATATTGTAGCCCGCAAGATTGTGAAGATG
Ch.S.Turtle    TGGAGATTGTAGGTACTAATGGCCAAAATGGGGATGAAAAGCAAAACACTGTGGCACGTAAAATTGTCAAGATG
S.-E.Galago    TGGAGCTAGTTGGGTCTTCAGGCCAGAATGGGGATGAAAAGCAGAACATTGTAGCCCGTAAGATTGTGAAGATG
Squirrel       TGGAGCTAGTTGGGTCTTCTGGTCAGAACGGAGAAGAAAAACAGAACATTGTAGCCCGTAAGATTGTGAAGATG
Sheep          TGGAGCTAGTTGGTTCTTCAGGTCAGAATGGAGATGAAAAACAGAACATCGTTGCTCGCAAGATTGTGAAAATG
Bonobo         TGGAGGTAGTGGGGTCTTCAGGTCAGAATGGAGATGAAAAGCAGAATATTGTAGCCCGCAAGATTGTGAAGATG
Goat           TGGAGCTAGTTGGTTCTTCAGGTCAGAATGGAGATGAAAAACAGAACATCGTTGCTCGCAAGATTGTGAAAATG
Af.Elephant    TGGAGCTAATTGCTTCTGCAGGTCAGAATGGAGACGAAAAGCAGAACATCGTAGCCCGCAAGATTGTGAAGATG
Marmoset       TGGAGGTAGTGGGGTCTTCAGGTCAGAACGGAGATGAAAAGCAGAACATTGTAGCCCGCAAGATTGTGAAGATG
SperWhale      TGGAGCTAGTTGGTTCTTCAGGTCAGAATGGAAATGAAAAACAGAACATTGTTGCTCGCAAGATTGTAAAGATG
Rabbit         TGGAGCTAGTTGGGTCTTCAGGTCAGAATGGAGATGAGAAACAGAACATTGTAGCCCGCAAAATTGTGAAGATG
T.Killifish    CCTCGAACGCCACCGTCGAGATTGTCCCGAGCGCGGAGCGGCAGAACCACGTTGCAAGAAAGATTGTGAAGATG
T.E.Snake      TGGAGATTGTTGCCACGGATGGACAAAATGGGGAGGAGAAGCAGAACATTGTAGCGCGTAAGATTGTCAAGATG
```

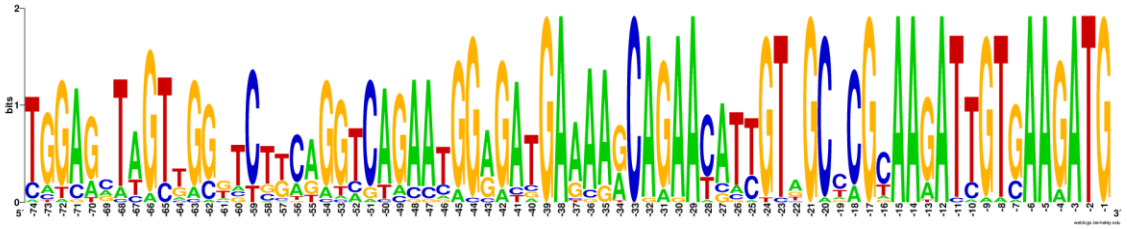

Figure 14 The upper part of the figure shows the comparison of the short sequence of i3 loop in different species of the M_2 receptor; in the lower part there is a graph showing how a sort of selection for purine bases in the sequence is dominantly important for the IRES mechanism. (Alignment and image by Petragnano F.)

```
Human              CCTTCAAGGAAGCCACTCTGGCCAAGAGGTTTGCTCTGAAGACCAGAAGTCAGATCACTAAGCGGAAAAGGATG
Rat                CCTTCAAGGAGGCCACGCTGGCTAAGAGGTTTGCTCTCAAGACCAGAAGTCAGATCACCAAGCGGAAGAGGATG
Mouse              CCTTCAAAGAAGCCACGCTGGCTAAGAGGTTTGCTCTCAAGACCAGAAGTCAGATCACCAAGCGGAAAAGGATG
Zebrafish          CTTTCAAAGAGGCAGCTTTAGCAAAACGTTTTGCAGCTCGCGCAAGGACACAAATCACCAAGCGCAAGCGCATG
Pig                CCTTTAAGGAAGCTACTCTGGCCAAGAGGTTTGCTCTGAAGACCAGAAGTCAGATCACCAAGCGGAAACGGATG
Bovine             CCTTTAAGGAAGCTACACTGGCCAAGAGGTTTGCTCTGAAGACCAGAAGCCAGATCACTAAGCGGAAACGGATG
Chicken            CCTTCAAGGAAGCAACTCTGGCAAAAAAATTTGCCTTGAAGACCAGAAGTCAAATCACAAAGCGAAAACGAATG
Chimpanzee         CCTTCAAGGAAGCCACTCTGGCCAAGAGGTTTGCTCTGAAGACCAGAAGTCAGATCACTAAGCGGAAAAGGATG
Orangutan          CCTTCAAGGAAGCCACTCTGGCCAAGAGGTTTGCTCTGAAGACCAGAAGTCAGATCACTAAGCGGAAAAGGATG
Gorilla            CCTTCAAGGAAGCCACTCTGGCCAAGAGGTTTGCTCTGAAGACCAGAAGTCAGATCACTAAGCGGAAAAGGATG
Rhesus macaque     CCTTCAAGGAAGCCACTCTGGCCAAGAGGTTTGCTCTGAAGACCAGAAGTCAGATCACTAAGCGGAAAAGGATG
Giant Panda        CCTTCAAGGAAGCCACTCTGGCCAAGAGGTTTGCCCTGAAGACCCGAAGCCAGATCACCAAGCGGAAGCGGATG
Chin. Alligator    CGTTTAAGGAAGCCACTCTGGCAAAAAAGTTTGCCTTGAAGACCAGAAGTCAGATCACCAAGCGAAAACGAATG
Northern mallard   CCTTCAAGGAGGCAACCCTGGCAAAAAAGTTTGCCTTGAAAACCAGAAGTCAGATCACAAAACGAAAACGAATG
Americ.chameleon   CATTCAAGGAAGCCACCCTGGCCAAGAAGTTTGCCTTGAAGACAAGAAGTCAAATCACCAAACGGAAACGAATG
Minke whale        CCTTTAAGGAAGCTACTCTGGCCAAGAGGTTTGCTCTGAAGACCAGAAGCCAGATCACTAAGCGGAAACGGATG
Austrof.limnaeus   TGCACTGGCCAAACGCTTTGCTCTGAAAGCCAAAACAGAGATGAACAAGCGCAAAAATGAAAAGAAGGCTAATG
Dog                CCTTCAAGGAAGCCACCCTGGCCAAGAGATTTGCTCTCAAGACCAGAAGTCAGATCACCAAGCGGAAACGGATG
Goat               CCTTCAAGGAAGCTACACTGGCCAAGAGGTTTGCTTTGAAGACCAGAAGCCAGATCACTAAGCGGAAACGGATG
Guinea pig         CTTTCAAGGAAGCCACACTGGCCAAGAGGTTTGCTCTGAAGACCAGAAGTCAGATCACAAAGCGGAAGAGGATG
C.cap.imitator     CCTTCAAAGAAGCCACTCTGGCCAAGAGGTTTGCTCTGAAGACCAGAAGTCAGATCACTAAGCGGAAAAGGATG
Green monkey       CCTTCAAGGAAGCCACTCTGGCCAAGAGGTTTGCTCTGAAGACCAGAAGTCAGATCACTAAGCGGAAAAGGATG
Angolan colobus    CCTTCAAGGAAGCCACTCTGGCCAAGAGGTTTGCTCTGAAGACCAGAAGTCAGATCACTAAGCGGAAAAGGATG
Rock dove          CCTTCAAGGAAGCAACCCTGGCAAAAAAGTTTGCCGTGAAGACCAGAAGTCAGATCACAAAGCGAAAACGAATG
Beluga whale       CCTTTAAGGAAGCTACTCTGGCCAAGAGGTTTGCTCTGAAGACCAGAAGCCAGATCACTAAGCGGAAACGGATG
Kangaroo rat       CCTTCAAGGAAGCCACGCTGGCCAAGAGATTTGCTCTGAAGACCCGAAGTCAGATCACCAAGAGAAAGAGGATG
Horse              CCTTCAAGGAGGCCACTCTGGCCAAGAGATTTGCTCTGAAGACCAGAAGTCAGATCACTAAGCGGAAACGGATG
Europ.hedgehog     CCTTCAAGGAAGCAACGCTGGCCAAGAGGTTTGCTCTGAAGACCAGAAGTCAGATCACAAAGCGTAAACGGATG
Cat                CCTTCAAGGAAGCCACTCTGGCCAAGAGGTTTGCTCTGAAGACCAGAAGTCAGATCACCAAGCGGAAGCGGATG
Tortoise           CCTTCAAGGAAGCAACCCTGGCCAAAAAGTTTGCCTTGAAGACCAGAAGTCAGATCACCAAGCGAAAACGAATG
African elephant   CCTTCAAAGAAGCGACTCTGGCCAAGAGGTTCGCTCTGAAGACCAGGAGTCAGATCACTAAACGGAAAAGAATG
Wild turkey        CCTTCAAGGAAGCAACTCTGGCAAAAAAATTTGCCTTGAAGACCAGAAGTCAAATCACAAAGCGAAAACGAATG
Mustela furo       CCTTCAAGGAGGCCACTCTGGCCAAGAGGTTTGCTCTGAAGACCCGAAGCCAAATCACCAAGCGGAAGCGGATG
Little br.bat      CCTCCAAGGAGGCCACTCTGGCCAAGAGGTTTGCCCTGAAGACCCGGAGCCAGATCACGAAGCGGAAGCGGATG
```

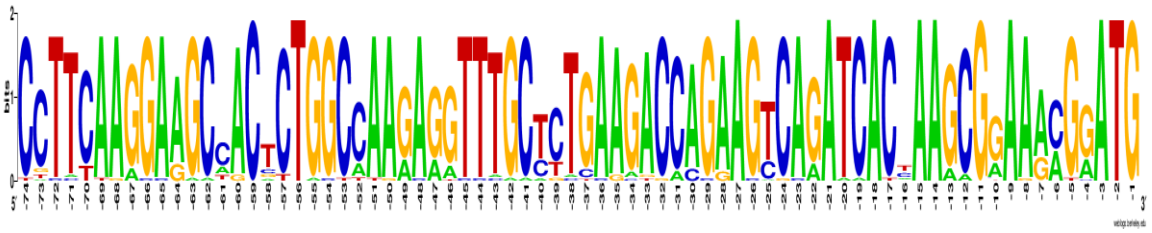

Figure 15 The upper part of the figure shows the comparison of the short sequence of i3 loop in different species of the M_3 receptor; in the lower part there is a graph showing how a sort of selection for purine bases in the sequence is dominantly important for the IRES mechanism. (Alignment and image by Petragnano F.)

Human	CCGCCAAACCAGAGAAGAATGGGCATGCCAAAGACCACCCCAAGATTGCCAAGATCTTTGAGATCCAGACCATG
Rat	CCAAACCAGAGAAGAATGGGCACGCCAAGATTGTCAATCCCAGGATTGCCAAGTTCTTTGAGATCCAGACCATG
Mouse	CCAAACCAGAAAAGAATGGGCATGCCAAGATTGTCAATCCCAGGATTGCCAAGTTCTTTGAGATCCAGACCATG
Mustela furo	CCGTCAAACCAGAGAAGAATGGGCATGCCAAAGACCACCCCAAGATTGCCAAGATCTTTGAGATCCAGTCCATG
Bos taurus	CCAAACCAGAGAAGAACGGGCATGCCAAGACCGTCAATCCCAAGATTGCCAAGATCTTTGAGATCCAGTCCATG
Dog	CCGCCAAACCAGAGAAGAATGGGCATGCCAAAGACCACCCCAAGATTGCCAAGATCTTTGAGATCCAGTCCATG
Chicken	CTGGGAAAGTAGAGAAGAATGGACATGCCAAAGAAAACCTACACACAGCCAAGGTCTTTGAGATCCAGTCCATG
Guinea pig	CTGCCAAGCCAGAGAAGAACGGGCACGCCAAAGACCACCCCAAGATTGCCAAGATCTTTGAGATCCAGTCCATG
Whiteearmarmoset	CCGCCAAACCAGAGAAGAACGGGCATGCCAGAAACCACCCCAGGATTGCCAAGTTCTTTGAGATCCAGACCATG
Chimpanzee	CCGCCAAACCAGAGAAGAATGGGCATGCCAAAGACCACCCCAAGATTGCCAAGATCTTTGAGATCCAGACCATG
Pig	CTGCCAGACCAGAGAAGAACGGACACGCCAAAGATCACCCCAAGATTGCCAAGATCTTTGAGATCCAGTCCATG
Amer. Chameleon	CACTTCAAGTCGCAAAGAACGGGCACACAACAGACAACCCCAAAACAGCCAAGGCCTTTGAGATCCAAACCATG
Horse	CTGCCAAACCAGAGAAGAACGGGCATGCCAAAGACCACCCCAAGATTGCCAAGATCTTTGAGATCCAGTCCATG
Opossum	TAAAGCCAGAGAAGAATGGGCATGCCAAAGGCCACCACCCCAGGTCTGCCAAAGTCTTTGAGATCCAGTCTATG
Swan goose	CTGGGAAACTGGAGAAGAATGGACATGCCAAAGAAAACCCCCCACACAGCCAAGGTCTTTGAGATCCAGTCTATG
Rhesus macaque	CCGCCAAACCAGAGAAGAACGGGCATGCCAAAAACCACCCCAAGATTGCCAAGATATTTGAGATCCAGACCATG
Kangaroo rat	CTGCCAAACCAGAGAAGAACGGGCATGCCAAAGACCACCCCAAGATTGCCAAGATCTTTGAGATCCAGTCCATG
Prairie vole	CCAAGCCAGAGAAGAATGGGCATGCCAGGATTATCAACCCCAGGATTGCCAAGATCTTTGAGATCCAGACCATG
Sumatran orangutan	CCGCCAAACCAGAGAAGAATGGGCATGCCAAAGACCACCCCAAGATTGCCAAGATCTTTGAGATCCAGACCATG
Small-eared galago	CTGCCAAACCAGAGAAGAATGGGCACGCCAGAGACCACCACAGGATTGCCAAGTTCTTTGAGATCCAGACCATG
Sheep	CCGCCAAGCCAGAGAAGAACGGGCATGCCAAAGACCACCCCAAGATTGCCAAGATCTTTGAGATCCAGTCCATG
Bolivian squirrel monkey	CCGCCAAACCAGAGAAGAACGGGCATGCCAGAAACCACCCCAGGATTGCCAAGTTCTTTGAGATCCAGACCATG
Sperm whale	CTGCCAAACCAGAGAAGAACGGACATGCCAAAGACCACCCCAAGATTGCCAAGATCTTTGAGATCCAGTCCATG
Tasmanian devil	CCATGAAGCCAGAAAAGAATGGGCATGCCAAAGGTCACCCCAGGTCTGCCAAAGCCTTTGAGATCCAGTCTATG
white-cheeked gibbon	CCGCCAAACCAGAGAAGAATGGGCATGCCAAAGGCCACCCCAAGATTGCCAAGATCTTTGAGATCCAGACCATG
Green monkey	CCGCCAAACCAGAGAAGAATGGGCATGCCAAAAACCACCCCAAGATTGCCAAGATCTTTGAGATCCAGACCATG
Red fox	CCGCCAAACCAGAGAAGAATGGGCATGCCAAAGACCACCCCAAGATTGCCAAGATCTTTGAGATCCAGTCCATG
Polar bear	CCGCCAAACCAGAGAAGAATGGGCACGCCAAAGACCACCCCAAGATTGCCAAGATCTTCGAGATCCAGTCCATG
Giant panda	CCGCCAAACCAGAGAAGAATGGGCACGCCAAAGACCACCCCAAGATTGCCAAGATCTTCGAGATCCAGTCCATG
Amer. black bear	CCGCCAAACCAGAGAAGAATGGGCACGCCAAAGACCACCCCAAGATTGCCAAGATCTTCGAGATCCAGTCCATG
Philip. tarsier	CCGCCAAACCAGAGAAGAATGGGCACGCCAAAGACCACCCCAAGATTGCCAAGATCTTTGAGATCCAGACCATG
Common wombat	CCATGAAGCCAGAGAAGAATGGGCATGCCAAAGGTCACCCCAGGTCTGCCAAAGTCTTTGAGATCCAGTCTATG
Crab-eating macaque	CCGCCAAACCAGAGAAGAACGGGCATGCCAAAAACCACCCCAAGATTGCCAAGATCTTTGAGATCCAGACCATG
Rabbit	CTGCCAAACCGGAGAAGAATGGGCACGCCAAAGACCACCCCAAGATTGCCAAGATCTTTGAGATCCAGACCATG
Naked mole rat	CTGCTAAGCCAGAAAAGAATGGGCATGCCAAAGACCACCCCAAGATTGCCAAGATCTTTGAGATCCAGTCTATG
Squirrel	CCGCCAAACCAGAGAAGAATGGGCATGCCAAAGACCACCCCAAGATTGCCAAGATCTTTGAGATACAGTCCATG
Golden hamster	CCAAACCAGAGAAAAATGGGCATGCCAAGATTGCCAACCCCAAGATTGCCAAGATCTTTGAGATCCAGACCATG
Northern mallard	CTGGGAAACTAGAGAAGAACGGACATGCCAAAGAAAACCCCCACACCGCCAAGGTCTTCGAGATCCAGTCTATG
Wild turkey	CTGGGAAAGTAGAGAAGAATGGACATGCCAAAGAAAATCTGCACACAGCCAAGGTCTTTGAGATCCAGTCCATG
Afric. Elephant	CTGCCAAACCAGAGAAGAATGGGCATGCCAAAGACCACCCCAAGATTGCCAAGATCTTTGAGATCCAGTCCATG
West. Gorilla	CTGCCAAACCAGAGAAGAATGGGCATGCCAAAGACCACCCCAAGATTGCCAAGATCTTTGAGATCCAGACCATG

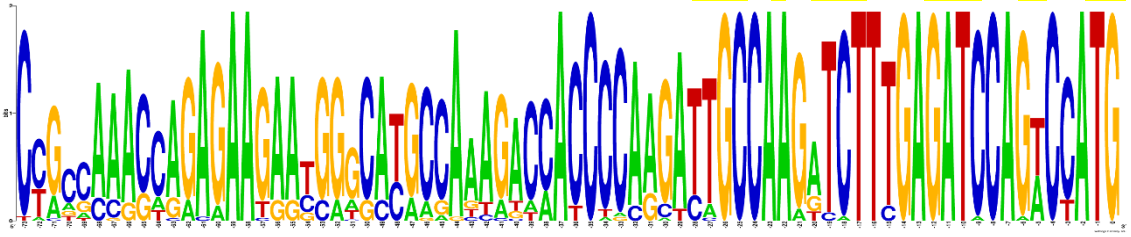

Figure 16 The upper part of the figure shows the ccomparison of the short sequence of i3 loop in different species of the D_2 receptor; in the lower part there is a graph showing how a sort of selection for purine bases in the sequence is dominantly important for the IRES mechanism. (Alignment and image Petragnano F.)

Chapter 3: Localization of C-terminal fragment in the cells

3.1 Study of the behaviour of the tail fragment

At this point we have established and asserted two fundamental points about how the expression of the M_2 carboxyl terminal domain occurs:

- it is regulated by an IRES,
- its translation starts at Met368.

It was important to clarify the possible role and behavior of this fragment and to do it, we used fluorescence microscopy assay, in collaboration with the AG Lohse group of the Max Delbrück Center in Berlin; the usual localization of the M_2 receptor is the cell membrane, and it was easily confirmed by transfecting cells with the WT receptor labelled at the C-terminus with the red fluorescent protein EGFP; when the M_2WT-EGFP was expressed and the cells were co-stained with a conventional mitochondrial stain -Mitotracker Deep Red- a faint EGFP signal was also observed within the cells (Figure 17a), although the expression of the full-length receptor masks this effect.

Surprisingly the M_2tail(368-466)-EGFP transfected alone showed a mitochondrial localization; so using a co-staining with Mitotracker (Figure 17c) and by co-expressing M_2tail(368-466)-EGFP with Tom20-mCherry (Figure 17b) -a fluorescently labelled construct of a fundamental component of the TOM (translocase of outer membrane), receptor complex responsible for the recognition and translocation of cytosolically synthesized mitochondrial preproteins- we were able to demonstrate green fluorescence signal from mitochondria.

Even more surprising was the co-localization of M_2mRuby2 signal with the M_2tail(368-466)-EGFP when co-expressed in HEK-293 cells (Figure 17d), strongly contrasting to the canonical cellular localization of the M_2 receptor, while weak expression of M_2tail(368-466)-EGFP was observed on the plasma membrane, as confirmed by the fluorescence correlation and cross correlation spectroscopy experiments aimed at assessing the potential interaction with the full-length receptor.

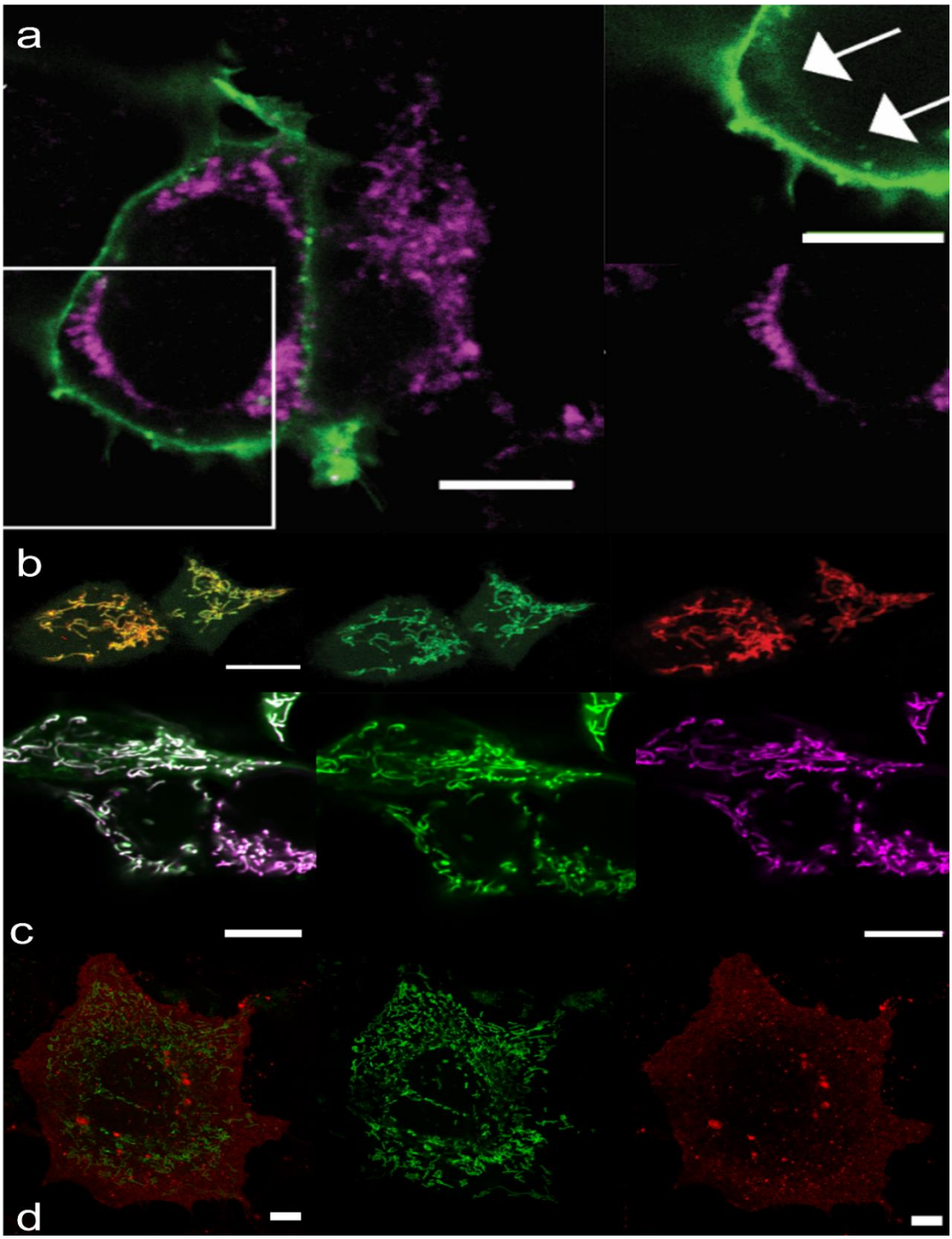

Figure 17 The panel (a) shows a merge of the co-staining between M_2WT-EGFP (green) and Mitotracker Deep Red (magenta), the right part of the panel shows the detail of two different signals; the panel (b) is a confocal image displaying the co-localization of M_2tail(368-466)-EGFP co-expressed with the outer mitochondrial membrane marker Tom20-mCherry (left part), in the middle the single image of the green signal from M_2tail(368-466)-EGFP alone and the right part is the Tom20-mCherry; panel (c) illustrates respectively the merge (left part) for the co-localization of M_2tail(368-466)-EGFP together with the Mitotracker in HEK293 cells, and the different channels of the two fluorescent signal (green in the middle and magenta in the right part); the panel (d) in the bottom of the figure displays co-expression of M_2tail(368-466)-EGFP and wild type M_2-mRuby2 (left part) in HEK293 and the separate spectral channels M_2tail(368-466)-EGFP in the middle and M_2-mRuby2 in the right part. (by Petragnano et al., 2022,)

Unexpectedly co-expression of M_2stop228 with M_2tail(368-466)-EGFP exhibits a modest localization on the cell membrane, suggesting a chaperoning effect of the N-terminal of M_2, explaining the binding data observed through the M_2stop228 and M_2trunk(1-228)/M_2tail(368-466) co-transfection in the cells.

Mitochondrial signal was also observed when HEK cells were transfected with M_2fr.sh-EGFP; this construct has a frame shift created inserting a G base upstream the third in-frame methionine of the third loop (M368) -nucleotide 1102- that leads to a stop codon after 2 amino acids. Expression of the C-terminal fragment in mitochondria indicates that, also in the presence of the frame shift, translation occurs anyway, and this provides additional evidence about the role played by IRES.

To discard any possible bias due to the fluorescent tag and related to the mitochondrial localization, constructs such as M_2-mRuby2, M_2fr.sh-mRuby2, M_2tail(368-466)-mRuby2, and M_2tail(368-466)-tdTomato -a tandem-dimer red fluorescent protein- , were used to transfect the cells, and a they displayed mitochondrial signal, too.

New data of this relevance, should be also verified to exclude the possibility that the above observations could be due to overexpression; thanks again to the collaboration with the AG Lohse group of the Max Delbrück Center in Berlin, we used a strategy involving the use of particular constructs, one of them is M_2-mRuby2-STOP-M_2-i3-tail-EGFP (Figure 18), where the expression of the tail of the M_2 receptor is under the control of IRES, not of a viral promote and the resulting peptide concentration in the transfected cells should be maintained within levels compatible with the physiological production. The plasmid includes the full wild type M_2 receptor labelled with mRuby2, followed by the stop codon of mRuby2 fused to the C-terminal part of the M_2 receptor starting at 229 position (nucleotide 685) of the i3 loop labelled with EGFP sequence. High EGFP expression of the M_2tail(368-466)-EGFP (green) after the STOP codon as expected, was clear evidence that the in vivo production of the tail was due to the role played by IRES within the i3 loop; furthermore M_2-mRuby2 localizes correctly and predominantly to the cell plasma membrane, but also inside the cells, due to a cap dependent M_2-mRuby2 and IRES-driven M_2tail(368-466)-mRuby2, both derived from the M_2-mRuby2 gene (Figure 18). The same results were repeated with COS-7.

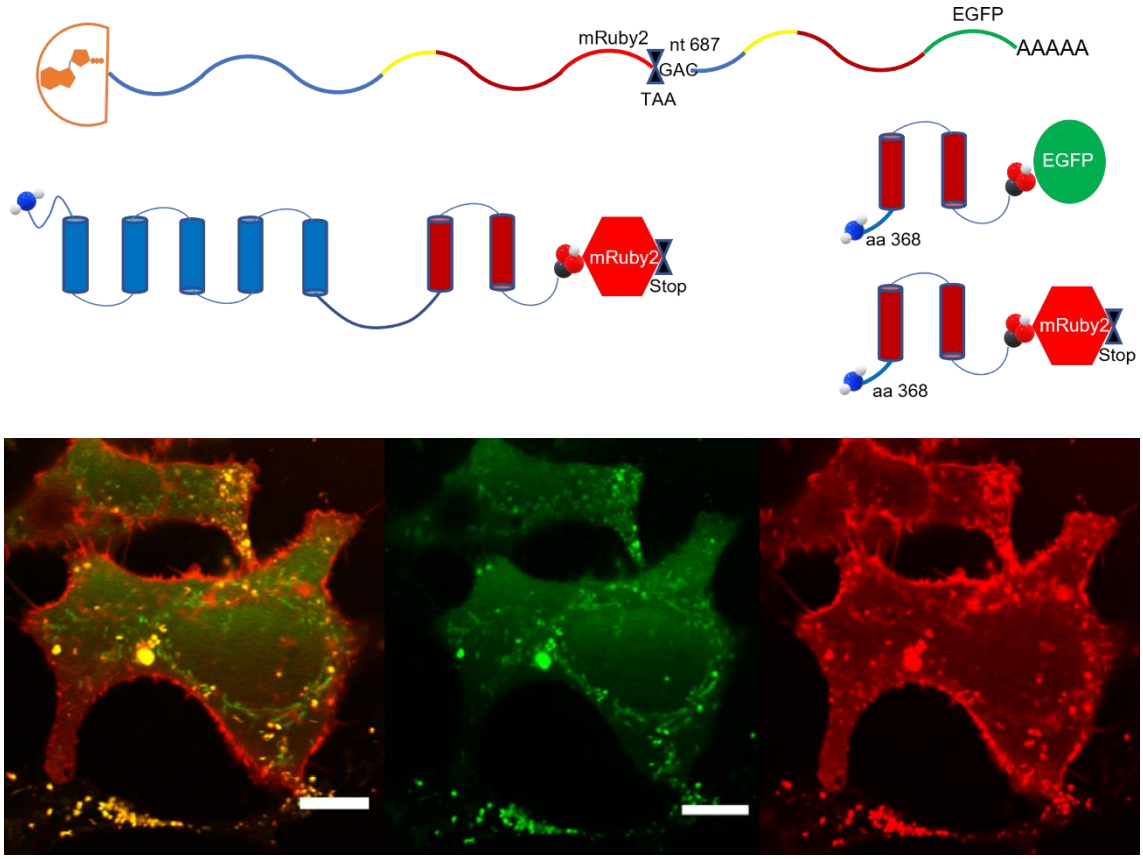

Figure 18 Representation of M_2-mRuby2-STOP-M_2-i3-tail-EGFP construct, with the mRNA and the relative protein products; the image below illustrates co-expression of M_2tail(368-466)-EGFP and wild type M_2-mRuby2 in HEK cells with the separate spectral channels in the middle (green for M_2tail(368-466)-EGFP) and in the right part (red for M_2-mRuby2). While M_2-mRuby2 emits a fluorescent signal in the cell plasma membrane, M2-tail (368-466) -EGFP instead in cell mitochondria. Expression of the M_2tail(368-466)-EGFP (green) after the STOP codon: 1) is an indicator of the endogenous IRES activity and 2) excludes that the mitochondrial localization of the M_2-tail(368-466)-EGFP construct depends on its overexpression. (by Petragnano et al., 2022)

3.2 Research within the mitochondrial compartment

The discovery of this new localization of the tail, prompted us to investigate its exact location inside the mitochondria; a big step in this direction was the analysis of the import process in the mitochondria, made possible thanks to a kinetic assay that take advantage of the co-localization strategy already used in another experiment:
a time course for the localization of the green signal of the fluorescent protein has been performed transfecting cells with M_2tail(368-466)-EGFP and staining them with mitotracker; therefore it has been possible to see the kinetics pattern of M_2tail, that was what we expected for a protein imported into mitochondria: preliminary expression in the endoplasmic reticulum (ER) after 5h, with increasing merging of the two signal from 6 to 9h post transfection; this is an indication that the tail fragment at the beginning follows the same trafficking pathway of the full length receptor and then head towards the mitochondria.

This data was corroborated by an in vitro assay with isolated mitochondria from S. cerevisiae: mitochondria incubated with ^{35}S-labelled full length muscarinic M_2 receptor or M_2tail(368-466), were monitored to assess import proteins and from 5 up to 30 minutes a clear mitochondrial import has been detected and this import seems to be unrelated with the transporters outer membrane Tom5, Tom6, Tom7 and Tom70. From extraction with carbonate, in the pellet was found most of the M_2tail(368-466) and blue native analysis suggests that it is not imported as a monomer but rather it is part of a bigger complex of 180 kDa about. These two results indicate that M_2tail(368-466) is integrated inside one of the mitochondrial membranes and forms a complex with native mitochondrial proteins. Furthermore, the full-length receptor turns out not to be imported into mitochondria.

Following the knowledge about a possible association of the tail with the mitochondrial membranes, the only thing left to discern was which of the outer or inner membrane it was; fluorescence microscopy, first helps to indicate mitochondria as a new cell compartment for the tail, but it lacks sufficient resolution to provide information about the localization of it within the organelle; cell expressing M_2stop228/c-myc receptor were examined after immune-gold labelling by electron microscopy (Figure 19),

to have a more accurate insight, thanks to another collaboration with the Section of Electron Microscopy of the Great Equipment Center of Tuscia University in Viterbo.

In high magnification of portion of the cell cytoplasm, a total number of 236 gold particles in 40 mitochondria from 19 sections were detected, samples prepared for Immune Electron Microscopy weren't post-fixed with osmium tetroxide, because cell membranes cannot be envisioned as clearly as in normal ultrastructural analysis, and the cristae can only be distinguished as translucent tubular areas in an electrondense matrix. Nevertheless, gold particles appear associated with the mitochondrial cristae or their lumen or with mitochondrial matrix (Figure 19).

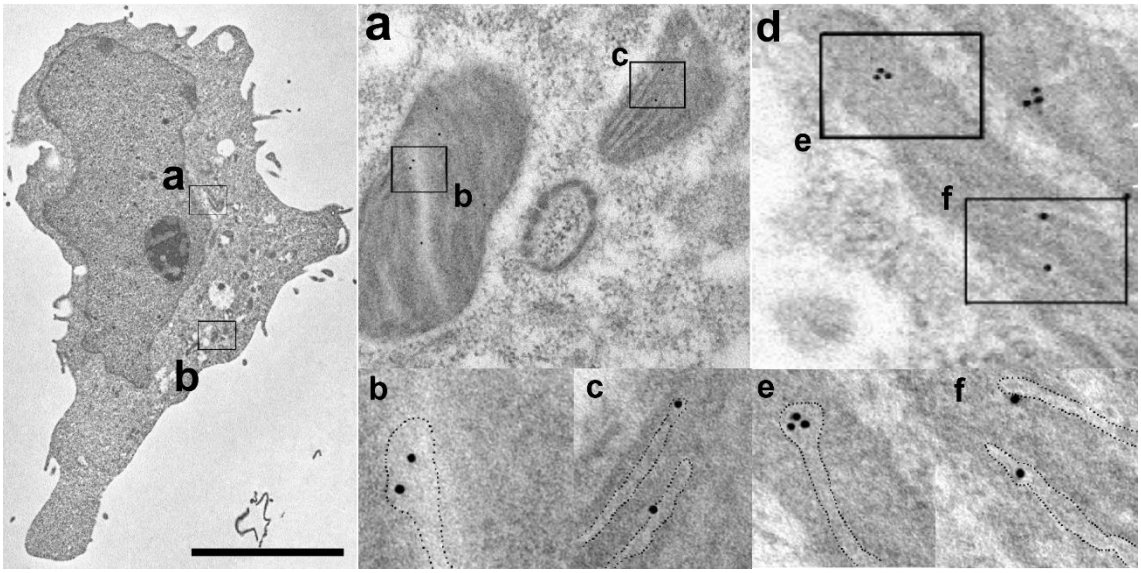

Figure 19 TEM micrograph of COS-7 cells examined by electron microscopy with immune-gold particles, observed in mitochondria, where they appeared localized either to the mitochondrial matrix or to the lumen of the cristae highlighted by the dotted line. (by Petragnano et al., 2022)

To help shed some light on the question, a self-complementing split GFP protein assay was performed . This assay is used to analyse protein-protein interactions and it is based on the split into two parts of the sequence of GFP, consist of eleven b-strand: GFP1-10 and GFP11, with GFP11 being a short, 16 amino acid peptide and the GFP1-10 fragment, which contains the three residues that constitute the GFP chromophore, that is nonfluorescent by itself because chromophore maturation requires the conserved residue located on GFP11. These reporter proteins are fused with interacting proteins and ,only upon interaction of these proteins, the fragments of the GFP are brought into proximity

and thus they are able to complement reconstituting GFP, that becomes fluorescent after the chromophore maturation reaction is completed.

HEK293 cells were transfected with two plasmids: first with mito-GFP1-10, in which the cytochrome c oxidase subunit 8 (COX8A) is fused to the N-terminal of the GFP fragment containing the 10 beta strands and then M_2tail(368-466)-GFP11, in which the short 16 amino acid peptide of GFP is fused at the C-terminus of tail (Figure 20a).

COX8A is subunit 8A of the human mitochondrial respiratory chain enzyme complex cytochrome c oxidase important for the efficacy of complex IV, a large integral membrane protein, the last enzyme in the respiratory electron transport chain of cells located in the inner mitochondrial membrane.

The presence of green fluorescence signal due the successful recombination of the two parts of GFP has been seen within the mitochondrial matrix (Figure 20a).

Applying the same strategy to the full length M_2 receptor by generating the M_2-GFP11 construct, the green signal from the recombined GFP was still visible in the mitochondria (Figure 20b).

The assay has been performed also with another mitochondrial protein to test the result found previously; the second mitochondria-derived activator of caspases (SMAC) protein was also fused to the N-terminal of the GFP1-10 fragment: SMAC is a mitochondrial protein, normally localized in the mitochondrial intermembrane space, that promotes cytochrome c and TNF receptor-dependent activation of apoptosis by inhibiting the effect of inhibitor of apoptosis proteins (IAP), that negatively regulate apoptosis. Co-transfection of SMAC-GFP1-10 and M_2tail(368-466)-GFP11, gives no green signal or mitochondrial co-localization (Figure 20c).

All together, these data are a strong evidence that the receptor fragment is imported into the mitochondria and that it is not just adhering to the outer mitochondrial membrane, but rather the M_2 tail fragment is localized in the inner mitochondrial membrane, with its own C-terminal domain facing the matrix.

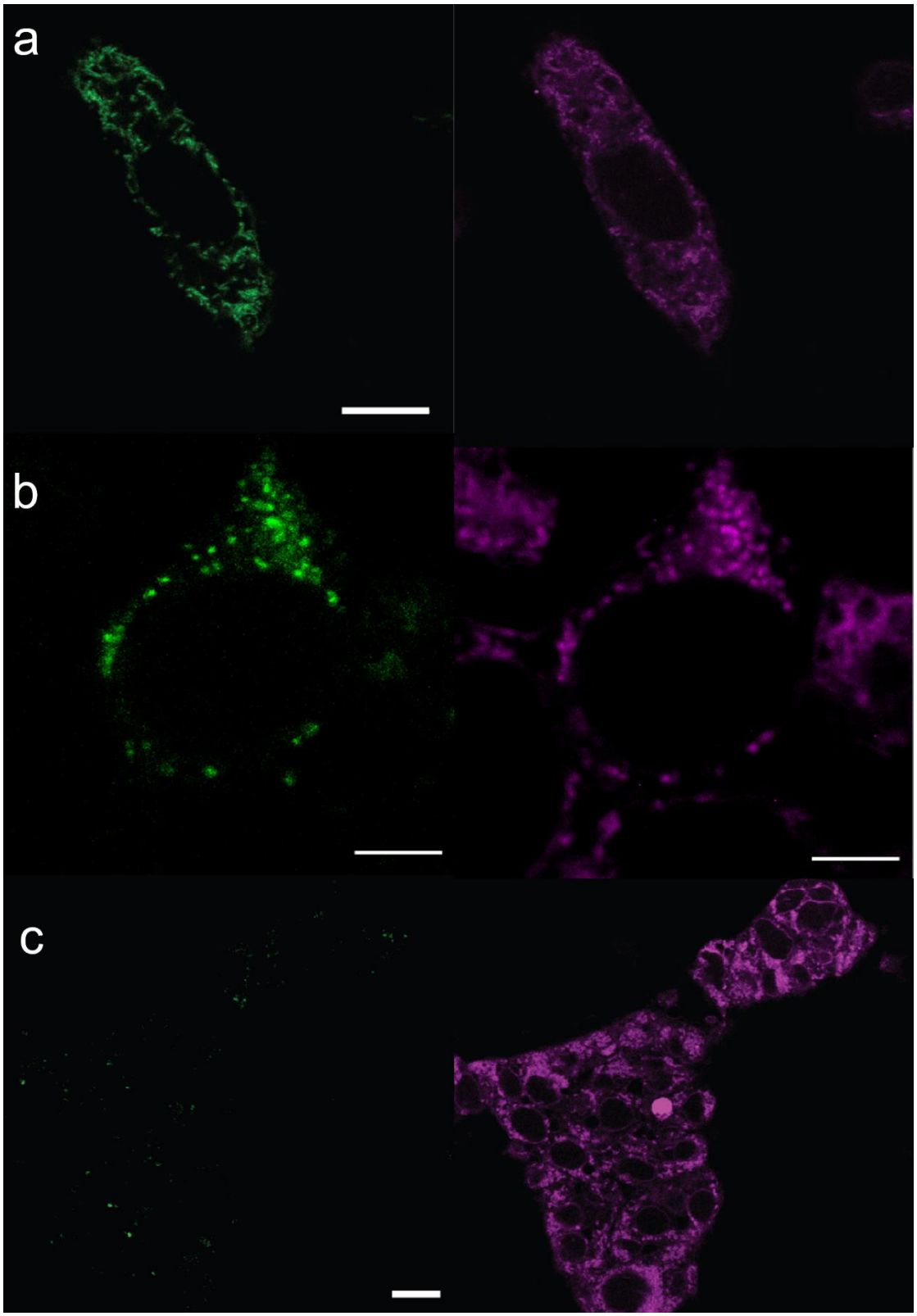

Figure 20 Confocal micrographs showing cellular localization of split GFP constructs in HEK293 cells co-transfected with (a) M_2tail(368-466)-GFP11 and mito-GFP1-10, (b) M_2-GFP11 and pmito-GFP1-10 (c) M_2tail(368-466)-GFP11 and SMAC-GFP1-10 on the left, and Mitotracker deep red (magenta) on the right. (by Petragnano et al., 2022)

Chapter 4: Proteomic analysis of M_2 tail fragment

4.1 Western blot characterization of tail fragment

At this point, by collecting all the data obtained from the binding assays and microscopy, the further step is to carry out a proteomic analysis of our receptor of interest and its C-terminal fragment.

Many of the M_2 receptor mutants already used before have been tagged with a myc-tag (EQKLISEEDL), a small protein with a very low molecular weight that should not affect any of the features of our target; all sequences were subcloned in a bicistronic vector backbone, allowing also the expression of the red fluorescent protein mRuby2 as a fluorescent reporter, that helps to check comparable expression levels; both COS-7 and HEK293 were transiently transfected and the whole cells lysates were resolved by SDS-PAGE.

As shown in the Figure 21, we used the M_2WT-myc, M_2tail(368-466)-myc, M_2stop400 and the M_2M368A-myc, the latter is a new mutant of the M_2 receptor with the third in frame methionine mutated to an alanine, that should affect the cap-independent translation, also helping us to detect our tail band more accurately on the membrane.

According to the amino acid sequence, the expected molecular weight for the full-length receptor was, at least, inclusive of the myc tag, ~50 kDa [34]**(Park & Wells, 2003)** and for the C-terminal fragment ~15 kDa. The lane for the M_2WT-myc clearly shows strong bands from ~52 kDa to ~75 kDa in the upper part and the lower band pair also at ~20 and ~15 kDa. The heavier bands represent the full-length receptor correspond to the glycosylated and non-glycosylated M_2 receptor proteins (Figure 21), the lower ones presumably represent the tail bands, with the difference between the two explained by the presence of post-translational modifications and protein processing that might derive from mitochondrial processing [35]**(Taylor et al., 2001)**; these bands first define the pattern expected for the M_2 carboxyl terminal fragment starting at the third in-frame methionine (Met368).

The lane for M_2tail(368-466)-myc clearly displays only the same lower molecular weight bands already seen for M_2WT-myc, giving greater certainty about the pattern

expected for the tail fragment. In the lane of M_2M368A-myc is still possible to see the same bands in the upper part of the lane as for the M_2-WT with the with the disappearance of the ~20 kDa band that is a further proof of a cap-independent translation process (Figure 21).

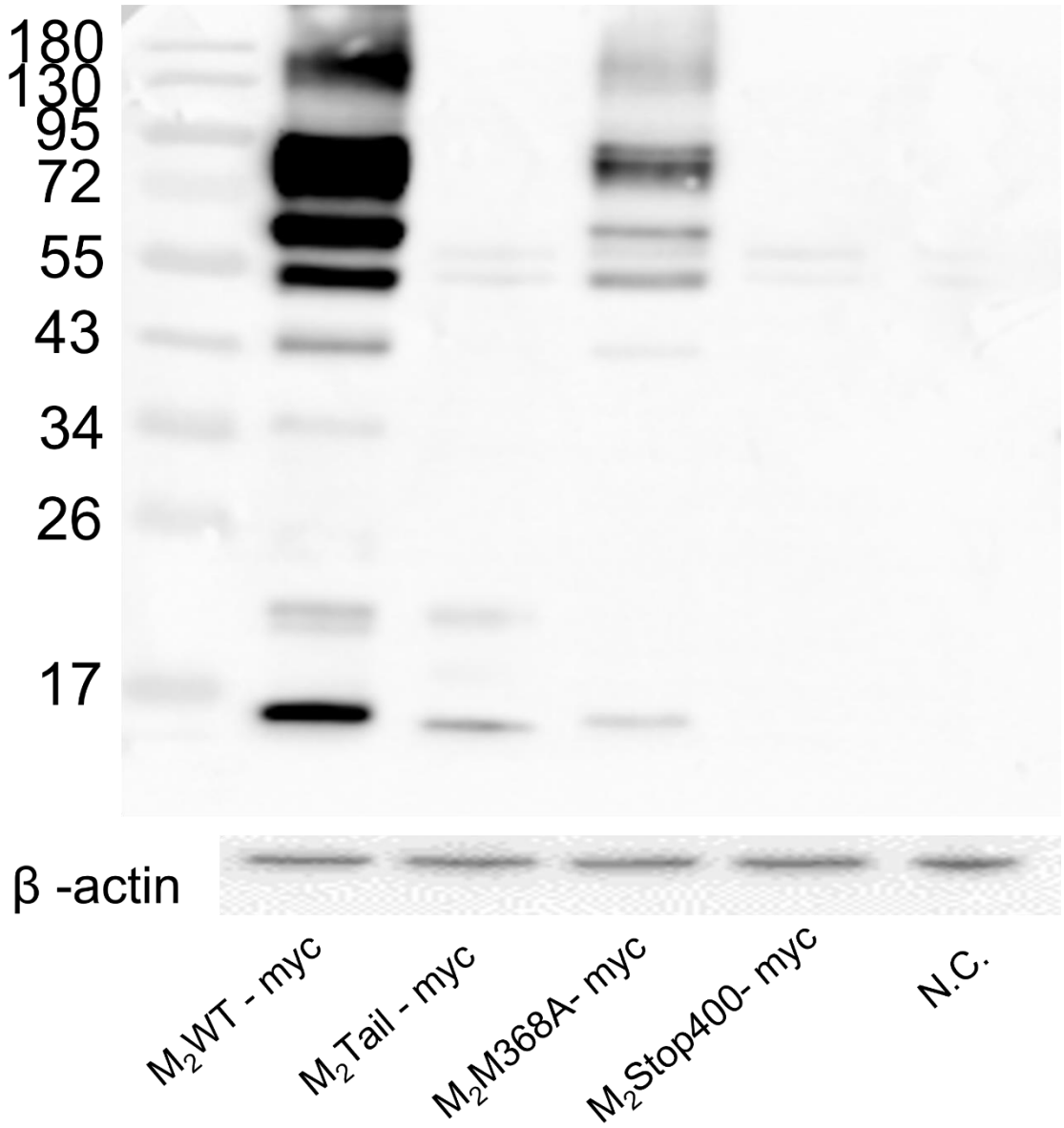

Figure 21 Western blot of whole cell lysates of Hek transfected with the constructs fused with the myc-tag and the untransfected cells (N.C. = negative control). (by Petragnano et al., 2022, western blot performed by Petragnano F.)

In addition, as expected, the M_2stop400-myc did not display any specific band (Figure 21) justified by the stop codon presence in the mutant and also the negative control shows no band detectable giving confidence about the specificity of the detected band; moreover the absence of any band for the M_2stop400-myc excludes the possibility of a downstream cap-independent translation site yielding a fragment originating from the next in frame methionine.

4.1.1 Tail fragment in mitochondrial fraction of cells lysates

After having primarily established the molecular weight of our target and to better assess the migration pattern of the tail fragment inside the mitochondria, we obtained protein extracts from purified mitochondria of HEK293 cells transfected with myc-tagged M_2WT, M_2tail(368-466) and M_2M368A.

We used an extraction protocol that is able to separate three different fractions from each sample: cytosolic, microsomal and mitochondrial; cells are suspended in lysis buffer, which selectively disrupts the plasma membrane without solubilizing it, resulting in the isolation of cytosolic proteins. Plasma membranes and compartmentalized organelles, such as nuclei, mitochondria, and the endoplasmic reticulum (ER), remain intact and are pelleted by centrifugation and then resuspended in a disruption buffer and recentrifuged to push down nuclei, cell debris and unbroken cells in order to collect the supernatant which contains mitochondria and the microsomal fraction; the supernatant is centrifuged again to separate mitochondria from the remaining part.

As shown in the figure, we observed the same pattern already seen in the whole cells lysate samples, at least for the microsomal fraction; surprisingly in the last f obtained fraction, the mitochondrial one, is possible to see the pattern of tail bands only in the M_2WT-myc and M_2tail(368-466)-myc.

The lanes for negative control and M_2M368A-myc are completely clear and the last construct confirm that the third in frame methionine M368, in the i3 loop of the M_2 receptor, is necessary for the C-terminal fragment production and its localization in the mitochondria.

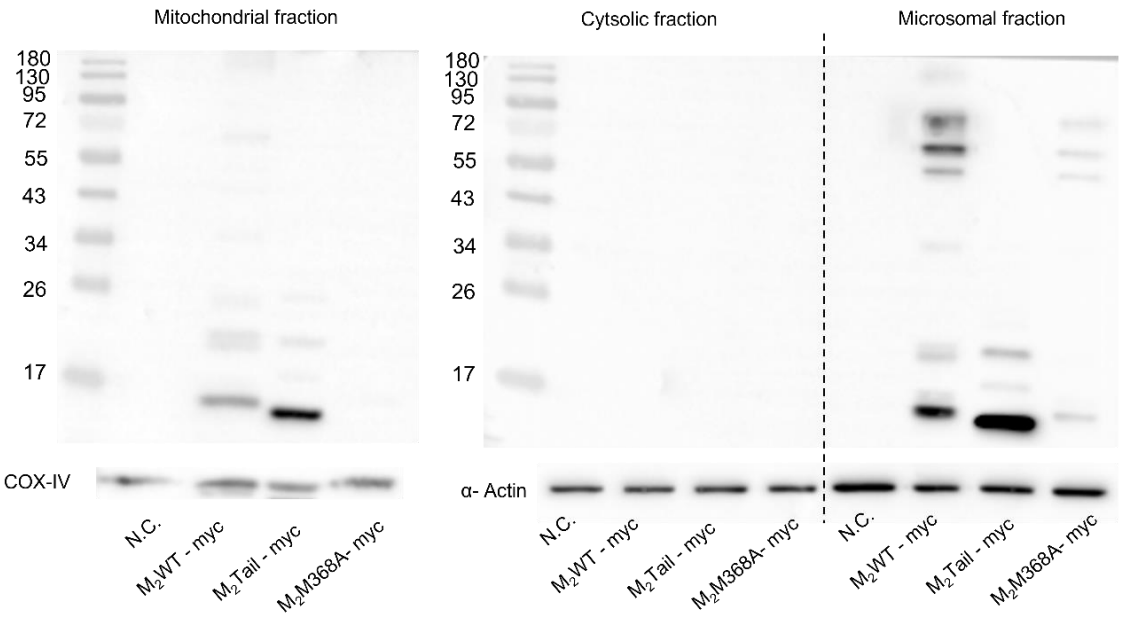

Figure 22 Western blot of the three fractions obtained through the purification from lysates of HEK293 transfected with myc-tagged constructs and the untransfected cells (N.C. = negative control): mitochondrial, cytosolic and microsomal fractions. (by Petragnano et al., 2022, western blot performed by Petragnano F.)

4.1.2 Evaluation of possible alteration due to ubiquitination

To determine the cause of the different size in the tail band, we examined the possibility that the C-terminal domain of the muscarinic receptor directed to the mitochondria, could undergo some post-translational modification; one of the hypothesis was about ubiquitin conjugation.

The ubiquitin-proteasome system (UPS) could play a dual role in mitochondrial protein import, ubiquitination contributes by unlocking blocked import channels, but deubiquitination can also directly promote the import process.

So we decided to test what could happen blocking the ubiquitination with TAK-243 (MLN7243) a potent inhibitor of the ubiquitin activating enzyme (UAE), whose treatment causes depletion of cellular ubiquitin conjugates. TAK-243 inhibits UAE from transferring ubiquitin to an E2 enzyme and shows equally potent inhibition of the two E1 enzymes capable of activating ubiquitin

- UBA6: activates ubiquitin by first adenylating its C-terminal glycine residue with ATP, and thereafter linking this residue to the side chain of a cysteine residue in E1, yielding a ubiquitin-E1 thioester and free AMP. Specific for ubiquitin, does not activate ubiquitin-like peptides.
- UAE (E1 enzymes): E1 enzyme binds ATP-Mg^{2+} and ubiquitin and catalyses ubiquitin C-terminal acyl adenylation. A catalytic cysteine on the E1 enzyme attacks the ubiquitin-AMP complex through acyl substitution, simultaneously creating a thioester bond and an AMP leaving group. In the end the E1-ubiquitin complex transfer ubiquitin to an E2 enzyme through a transthioesterification reaction, in which an E2 catalytic cysteine attacks the backside of the E1-ubiquitin complex.

So we tested this molecule with the HEK cells transfected with M_2WT-myc and M_2tail(368-466)-myc , and as shown in the western blot figure, we didn't see any evident change in the molecular weight of the two bands (~20/~15 kDa) neither on the level of expression. The negative control doesn't show any band or alteration due to the compound.

This does not completely exclude the possibility of ubiquitination since conjugation of Ub to the ε-amino group of lysine residues is the most common form of ubiquitination, but other acceptor residues such as Thr, Ser, Cys, and the α-amino group of substrate N-termini have been identified and represent noncanonical ubiquitination targets. From literature we know that N-terminal ubiquitinated proteins do not significantly accumulate upon proteasome inhibition, suggesting that N-terminal ubiquitination might have additional roles beyond promoting proteasome-mediated degradation [36]**(Davies et al, 2021**).

4.2 Western blot characterization of tail fragment endogenously expressed

To investigate the endogenous expression of the C-terminal fragment, in physiological settings at levels compatible only with the activity of the endogenous IRES sequence, we have identified a transgenic animal carrying a knock-in of the fluorescent protein td-tomato at the c-terminus of the M_2 gene, driven by the endogenous M_2 muscarinic acetylcholine receptor promoter/enhancer sequences.

The Chrm2-tdT-D mice (also called Chrm2-tdT-Δ or Chrm2-tdT-Δneo) were obtained from 'The Jackson Laboratory'. They are heterozygous (HT) animals that have a tdTomato sequence replacing the endogenous translational STOP codon in the M_2 muscarinic acetylcholine receptor locus (Chrm2) on chromosome 6.

The use of a transgene tag is explained, since antibody are notoriously ineffective against the M_2 receptor or c-terminus of the M_2 receptor, also antibodies directed against the M_2i3 loop work well, but they would be useless in this context because the epitope is external to the C-terminal fragment. On the other hand, the tdTomato fluorescent protein can be targeted by a specific polyclonal antibody.

We first analysed whole tissue lysates from the heart and spleen: in the heart they are known to express high levels of the M_2 receptor, whereas the spleen was used as a negative control, as no expression of the M_2 receptor is reported in the proteomics databases.

Performing the western blot, we detected in the lane of the heart from the HT mice a band at ~130 kDa and a band at ~75 kDa, not visible in the lane of the WT mouse's heart (Figure 23). They presumably represent respectively the full-length receptor-tdTomato fusion band, with ~75 kDa contributed by the receptor and ~55 kDa that is the molecular weight of tdTomato, and the tail fragment, ~20 kDa plus the molecular weight of tdTomato. This data match correctly with what we observed previously.

Moreover, the lane for spleen samples, both HT and WT, are lacking any kind of bands ascribable to the M_2 or the tail fragment.

Important results were acquired from purified mitochondria from the mouse's heart and spleen processed with the same protocol used for the mitochondrial purification

from cell lysates. To have a better comparison of our target we performed the same protocol also on cells transfected with M_2tail(368-466)-tdTomato and negative control cells (Figure 23).

A band at ~75 kDa, matching the molecular weight of the M_2 C-terminal domain, was visible in the HT heart lane showing also the same fingerprint associated with the M_2 C-terminal fragment, by purifying mitochondria from HEK cells expressing the construct M_2tail(368-466)-tdTomato.

Nothing comparable can be seen in the WT heart lane, in both HT and WT spleen, as well as in the untransfected cells extract.

Cytosolic and microsomal fraction show a ~75 kDa protein band matching closely the bands observed in mitochondria from mouse tissues, in addition to lower molecular weight bands most likely arising from the degradation of the tdTomato tag.

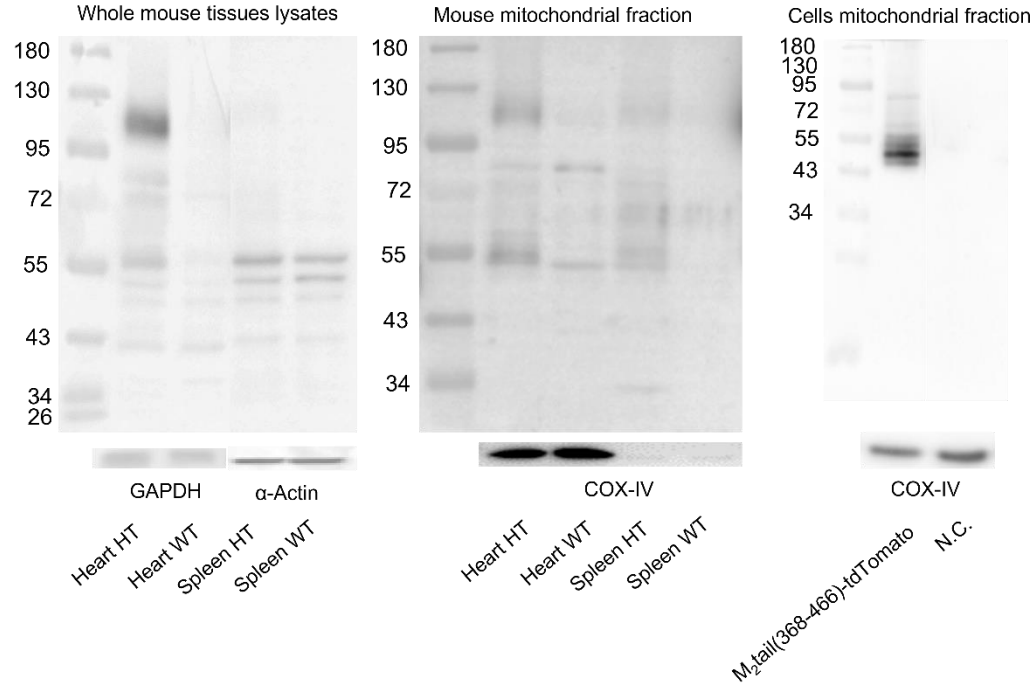

Figure 23 Western blots: on the left lysates of mouse's hearts and spleens, showing bands at ~130 kDa and a band at ~75 kDa relative to the protein target tagged with the tdTomato; in the middle immunoblot of the mitochondrial purified fraction of the mouse's hearts and spleens that present the same pattern seen in the mouse tissues lysates; on the right immunoblot of lysates from cells untransfected (N.C. = negative control) and transfected with the M2tail(368-466)-tdTomato used to compare the pattern between the mouse's tissues and cells for the tail. (by Petragnano et al., 2022, western blot performed by Petragnano F.)

Chapter 5: Role and influence of M_2 tail fragment

5.1 Functional consequences of the localization of the C-terminal fragment in the mitochondria

At this point we have identified an IRES in the i3 loop of the M_2 receptor, characterized how expression of the M_2 carboxyl terminal domain is molecularly regulated and pinpointed the molecular weight of the tail and claimed that it is imported into the mitochondria. Now we want to investigate which kind of role it can have in the cells and how it can influence the mitochondrial activity.

The main functions of mitochondria concern the metabolism of energy substances and the production of energy during cellular function and include:

- β-oxidation, an oxidation process involving fatty acids to form Acetyl-CoA molecules that will enter the Krebs cycle. During oxidation, electrons are donated to the nicotinamide adenine dinucleotide (NAD) and flavin adenine dinucleotide (FAD) co-enzymes.

- The Krebs cycle or citric acid cycle is a metabolic process which, through a series of 8 reactions, allows the complete oxidation of organic substrates. The molecules entering the Krebs cycle are Acetyl-CoA (which are formed during the degradation of carbohydrates, lipids, amino acids), which at the end of the cycle are oxidized to carbon dioxide (CO_2). During the cycle, there is the direct production of GTP (phosphorylation at the substrate level) and of high energy electrons sent to the electron transport chain through the soluble transporters NAD and FAD.

- oxidative phosphorylation, the system by which the molecules of ATP, the energy source used by cellular processes, are produced. The high-energy electrons, coming from the metabolic pathways, are transferred to the electron transport chain complexes present on the mitochondrial crests, releasing energy with each transfer from one complex to another. The released energy is exploited to pump protons (H^+) against the gradient from the mitochondrial matrix to the intermembrane space. After passing through the transport chain, the electrons are in a lower energy state and a mole of oxygen is released, which combining with 2 electrons and 2 protons are reduced to water (H_2O).

Finally, the protons accumulated return accumulated in the intermembrane space in the matrix, this time in favour of the gradient, crossing the channel of the membrane enzyme ATP-synthase, which exploiting the energy of the passage of the protons is able to synthesize molecules of ATP.

We wondered if its location could be somehow connected to an action on the cell economy, more probably on the energy metabolism of the cell. To prove it, we measured the extent of oxygen consumption in COS-7 cells expressing M_2WT, M_2stop228, M_2trunk(1-228), and M_2tail(368-466), with the Clarke electrode (Figure 24a), a polarographic method, which allows to conduct quantitative analyses by measuring the flowing current in an electrochemical cell during an electrolysis reaction. This is based on Clark electrodes, which measure the concentration of oxygen dissolved in solution by amperometric, that is at determined potential, inserted in a chamber with a volume equal to 2 mL maintained under continuous stirring at a constant temperature of 37°C [37]**(Zhang et al., 2012)**.

What we observed is that COS-7 cells transfected with M_2stop228 and M_2tail(368-466) show an appreciable decrease of oxygen consumption rate compared to mock transfected cells and the wild-type M_2 receptor and the M_2trunk(1-228) fragment (Figure 24a).

To better understand what the lower oxygen consumption was due to, we sifted through the hypothesis that O_2 depletion was coupled oxidative phosphorylation, so we added theoligomycin -an ATP synthase inhibitor- to the culture medium during the oxygen consumption measurement.

Oligomycin inhibits oxidative phosphorylation and all the ATP-dependent processes occurring on the coupling membrane of mitochondria, by blocking the proton channel (F_0 subunit) of ATP synthase, which is necessary for oxidative phosphorylation of ADP to ATP. The inhibition of ATP synthesis by oligomycin greatly reduces electron flow through the electron transport chain, giving rise to an accumulation of protons outside the mitochondrion because the proton pumping system is still intact, but the proton channel is blocked.

The oligomycin optimal concentration was determined experimentally at 17 nM and was added to the culture medium: the oligomycin addition caused the O_2 consumption rate to consistently decrease not only in control samples, proving that the oxygen consumption rate was coupled oxidative phosphorylation, with an average value of 44.9

± 6.3%, but also in cells transfected with M_2 and M_2trunk(1-228), while it only slightly reduced oxygen consumption rate in cells transfected with M_2stop228 and M_2tail(368-466), suggesting that C-terminal suppresses the portion of the oxygen consumption rate that is coupled to the oxidative phosphorylation.

To confirm the results with the Clarke electrode, a similar experiment to measure metabolic functions has been repeated with a Seahorse assay using COS-7 cells transfected with M_2WT-EGFP, M_2tail(368-466)-EGFP or the EGFP as a control, in starvation-stress conditions (Figure 24b). The EGFP constructs were used to help in normalizing the expression of the protein to the amount of fluorescent protein.

This experiment has been performed by the Centre for Translational Pharmacology, Institute of Molecular, Cell and Systems Biology, College of Medical, Veterinary and Life Sciences, University of Glasgow, UK.

Sea horse is a living cell assay that allows to keep track of OCR in real time, adding four modulators of respiration during the assay to reveal the key parameters of mitochondrial function: oligomycin, carbonyl cyanide-4 (trifluoromethoxy) phenylhydrazone (FCCP), rotenone and antimycin, in this order.

Oligomycin is injected first in the assay following basal measurements and its impacts on the cells decreases electron flow through the electron transport chain, resulting in a reduction in mitochondrial respiration, is linked to cellular ATP production. Carbonyl cyanide-4 (trifluoromethoxy) phenylhydrazone (FCCP), the second modulator, is an uncoupling compound that collapses the proton gradient and disrupts the mitochondrial membrane potential, inhibiting electron flow through the ETC and oxygen consumption reaches the maximum by complex IV. The FCCP-stimulated OCR is used to calculate the difference between maximal respiration and basal respiration as a measure of the ability of the cell to respond to increased energy demand or under stress.

The third injection is a combination of rotenone, a complex I inhibitor, and antimycin A, a complex III inhibitor, that shuts down mitochondrial respiration and permit the calculation of non-mitochondrial respiration driven by processes outside the mitochondria.

With Seahorse we noticed a significant decrease of oxygen consumption in M_2WT-EGFP and greater with M_2tail(368-466)-EGFP, while a prominent difference wasn’t seen in untransfected control or cells transfected with EGFP (Figure 24b).

Notably, in this assay, the wild type M_2 receptor inhibits O_2 consumption more than with the Clarke electrode; this is probably because in the assay with the Clarke electrode cells were not starved, then the cap dependent translation is prevailing.

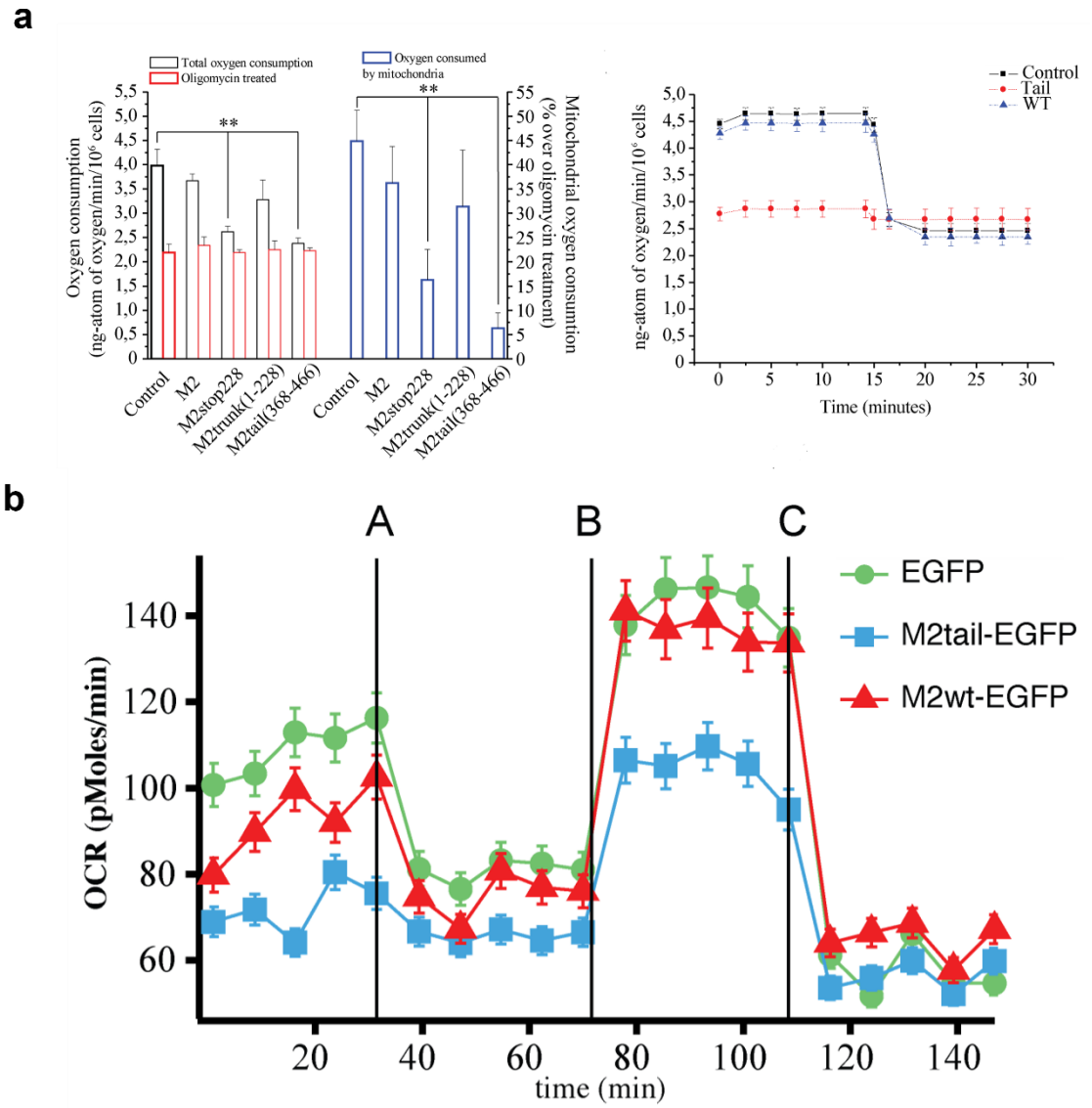

Figure 24 Graphs oxygen consumption measured by a Clark type electrode based-polarographic method (a) Oxygen consumption in the absence and presence of oligomycin is represented by black and red bars, respectively, the blue bars represent the percentage mitochondrial oxygen consumption (total minus oligomycin treated) in cells transfected with each construct. On the right representative experiment showing the time course of inhibition of oxygen consumption by M_2tail(368-466), compared to the same experiments performed in control cells and cells transfected with the M_2 wild type construct, upon addition of oligomycin.

(b) Graph representing experiment of Seahorse assay showing the time course of inhibition of oxygen consumption by M_2tail(368-466)-EGFP and wild type M_2-EGFP, compared to the same experiments performed in control cells transfected with EGFP. (by Petragnano et al., 2022)

5.2 Effects on ROS production

ROS are highly reactive oxygen bearing molecules, describing the chemical species formed upon incomplete reduction of molecular oxygen, superoxide radical anion ($O_2^{\cdot -}$), hydrogen peroxide (H_2O_2), and hydroxyl radicals ($OH^{\cdot}$), and singlet oxygen ($^1O_2$). ROS are implicated in oxidative damage inflicted on fatty acids, DNA and proteins as well as other cellular components, oxidizing and modifying them and invalidating their original functions. ROS overproduction is associated among other things with numerous disorders: the oxidative stress caused by the imbalance between the excessive formation of ROS and poor antioxidant defenses is connected to many pathologies including age-related disorders, cancer, cardiovascular, inflammatory, and neurodegenerative diseases such as Parkinson's and Alzheimer's diseases but, at the opposite, rising evidence suggests that ROS might have a beneficial physiological role as messengers in cellular signaling. As second messengers they are important for the expression of several transcription factors and other signal transduction molecules such as heat shock-inducing factor and nuclear factor and participate in the regulation of cell adhesion, redox-mediated amplification of the immune response and programmed cell death.

Mitochondria represent one of the major sources of intracellular ROS production that takes place in the electron-transport chain at Complex I (NADH dehydrogenase) and at Complex III (ubiquinone–cytochrome c reductase) upon one electron transfer to oxygen.

If the mitochondrial localization can affect the oxygen consumption, maybe this can reflects consequences also on the ROS production so, performing a single cell assay, the measurements of ROS production show a strong decrease within and in proximity of mitochondria expressing a high level of the M_2 tail fragment; these data were obtained by confocal microscopy on HEK-293 cells transfected with M_2tail(368-466)-EGFP and stained with Cell Rox Deep Red (Figure 25), a fluorogenic probes non-fluorescent or very weakly fluorescent while in a reduced state and upon oxidation it exhibits a strong fluorogenic signal, specific for reactive oxygen species. Analyzing the level of expression of ROS marker it has been possible to disclose an inverse correlation between the amount of M_2tail abundance (green fluorescence) and the amount of ROS production (red fluorescence). Relationship between green versus red fluorescence intensities measured from regions of the mitochondrial network were divided in four groups as a function of the amplitude of Cell Rox Deep Red signal 0-2.5, 2.5-5, 5-7.5 and 7.5-10 intensity counts.

These experiments demonstrate that the receptor fragment has a relevant role in the cell balance.

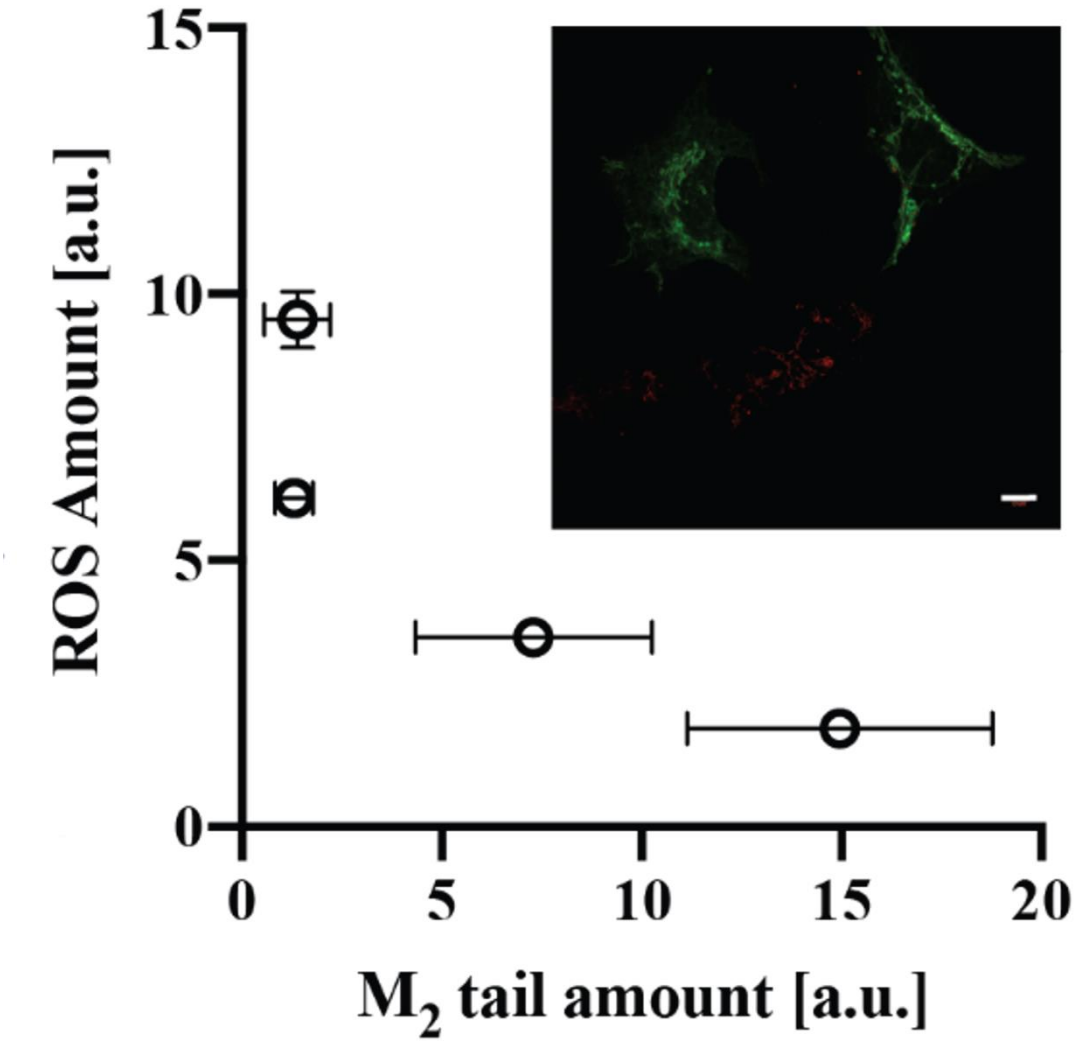

Figure 25 Graph of the relationship between green (M_2tail expression) vs. red (amount of ROS produced) fluorescence intensities measured from regions of the mitochondrial network. The data were binned in four groups as a function of the amplitude of Cell Rox Deep Red signal (0-2.5, 2.5-5. 5-7.5 and 7.5-10 intensity counts). (by Petragnano et al., 2022)

5.3 Effect of stress on tail fragment production and localization

Cells respond to stress stimuli by changing gene expression [38]**(Holcik & Sonenberg, 2005)** and stressed cells attenuate the translational activity phosphorylating the initiation factor eIF2α but, if the translation is activated by IRES eIF2α, phosphorylation can turn out insensitive to some mRNA and their expression can increase rather than reduce [39]**(Thakor & Holcik, 2012)**; so a question arises about the effect of stress on the level of expression of the C-terminal fragment.

COS-7 cells transfected with the Sirius-M_2i3(417n)-GFP have been stressed by starvation for 3 hours by replacing the culture medium with a physiological saline solution, both PBS and HBSS were used (Figure 26a). The green fluorescent protein expression was monitored for 3h and it gradually increased, compared to the basal level observed, up to 1.4 times for HBSS starvation and 3.5 times for PBS; this represents a confirm that GFP expression is driven by the IRES sequence inserted in the M_2i3 loop, and so it counts for the tail of the M_2 receptor, and its translation is upregulated in response to stress conditions such as cell starvation.

A similar experiment was reproduced on single cells: a time course of single HEK cell followed through confocal microscope expressing the Sirius-M_2i3(417n)-EGFP construct compared with that in basal conditions, gave us data that put in a graph together with the average EGFP and Sirius fluorescence intensity values measured from single cells, comparing basal and 3h HBSS starvation conditions, displayed an increase of the average EGFP/Sirius ratio upon HBSS starvation in cells (Figure 26b).

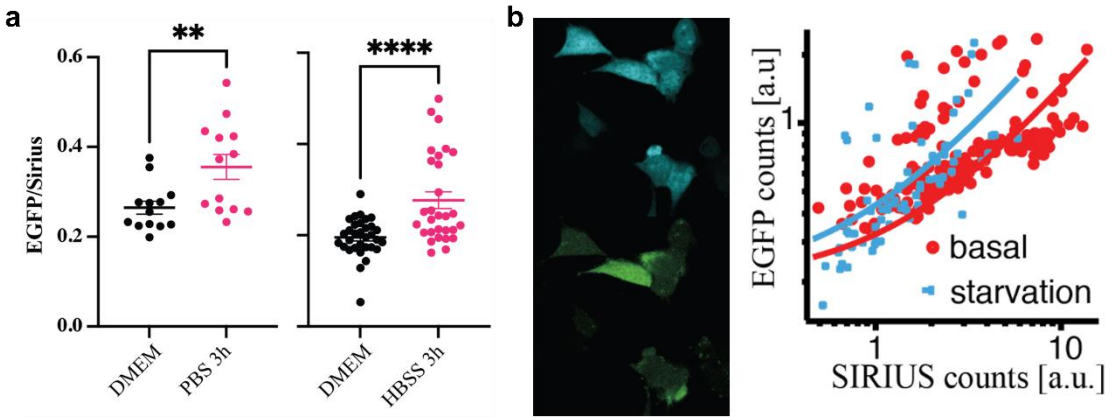

Figure 26 (a) Measurement of the increase of EGFP fluorescence relative to Sirius in COS-7 cells transfected with the bicistronic Sirius-M2i3(417n)-EGFP plasmid and starved for three hours respectively in PBS (left graph) and HBSS (right graph). **(b)** Representative single cell confocal and DIC micrographs of HEK293 cells expressing the Sirius-M2i3(417n)-EGFP construct in basal conditions, together with scatter plot of the average EGFP and Sirius fluorescence intensity values measured from single cells in the basal (red dots) and 3h HBSS starvation (blue dots) conditions. (by Petragnano et al., 2022)

But a further proof of this effect is given also by looking at the relative intensity of the M_2 C-terminal fragment band with respect to the full-length receptor band, upon serum starvation of cells in western blot from whole cell lysates of HEK293 cells transfected with the M_2WT-myc receptor, subject to increasing hours of serum starvation up to a maximum of 6h or 12h (Figure 27). The ratio between the lower bands representing the tail(368-466) and the full-length receptor, shows an increasing expression up to 50% of the basal level of the two smaller bands.

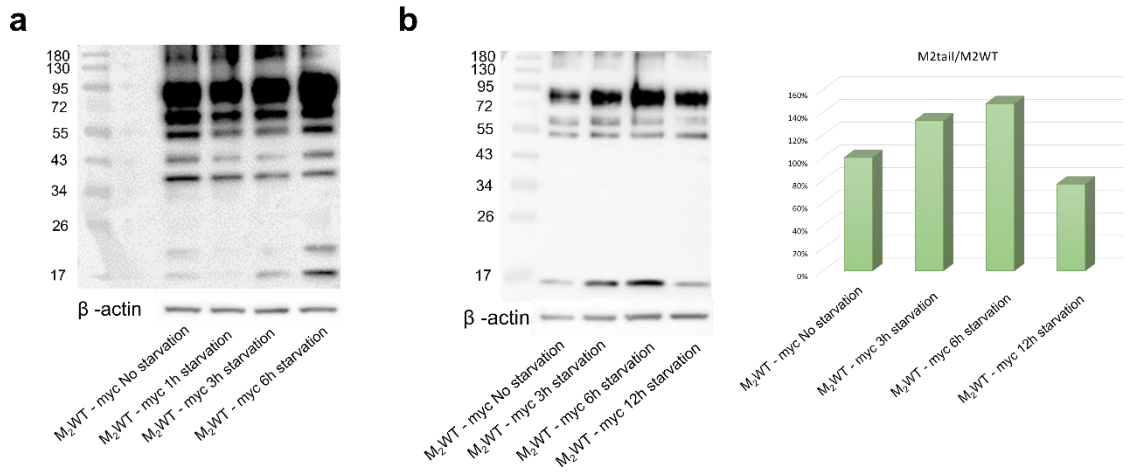

Figure 27 (a) Immunoblot of the M_2WT-myc in cells transfected and underwent to a serum starvation time course in PBS at increasing time of exposure to 1 up to 6h; (b) image of the western blot of a second experiment of a time course of serum starvation in PBS to 3h up to 12h of cells transfected with M_2WT-myc and the graph of the relative ratio between tail(368-466) and the full-length receptor. (western blot performed by Petragnano F.)

We decided to adopt the previously used strategy to prove that the tail of the M_2 receptor expression is under the control of the IRES: using the construct M_2-mRuby2-STOP-M_2-i3-tail-EGFP and study the expression of M_2tail(368-466)-mRuby2 originated from the M_2-mRuby2 part of the construct and of M_2tail(368-466)-EGFP originated as a single segment of the M_2-i3-tail-EGFP part.

Transfecting HEK cells and exposing them to a stress by serum starvation stimulus for 2h and incubated in HBSS buffer, staining them with mitochondrial staining it was possible to see that mitochondrial localization of the IRES mediated C-terminal fragment is enhanced upon cellular stress, because there is a notable increased localization of the EGFP labelled portion to the mitochondria. It's clearly possible to notice mitochondrial localization of the M_2tail(368-466)-EGFP and M_2tail(368-466)-mRuby2, while the M_2-mRuby2 signal is restricted to the cell membrane without EGFP signal (Figure 28 a-e).

To further validate this observation, we repeated the same experiment with the M_2(M368A)-mRuby2-STOP-M_2-i3-tail-EGFP construct, analogous of M_2-mRuby2-STOP-M_2-i3-tail-EGFP, with the third in-frame methionine of the i3-loop of the M_2 muscarinic mutated to alanine (M368A); when transfected, in the cells can be detected mRuby2 staining along the plasma membrane, but expression of M_2tail(368-466)-mRuby2 is not observed and therefore no red signal is visible in mitochondria, but M_2tail(368-466)-EGFP is still observed within mitochondria, thus corroborating the hypothesis that, under these conditions, the IRES driven translation of M_2tail(368-466)-mRuby2 is suppressed (Figure 28 f-l).

With this data, we can affirm that the IRES mediated C-terminal fragment localization to the mitochondria in cells expressing the mega construct M_2-mRuby2-STOP-M_2-i3-tail-EGFP was enhanced upon cell starvation, and greatly reduced in the presence of the mutation of the Met368.

To highlight the role of the stress in the expression of the M_2, we have recourse to the GFP complementation assay, transfecting cells sequentially first Mito-GFP1-10 and after 24h M_2-GFP11, subjecting the cells at 6h of starvation with HBSS.

A mainly mitochondrial green fluorescence signal of the complemented GFP due to IRES mediated translation of the M_2tail(368-466) fragment was observed; this data is exactly in agreement with the mitochondrial localization of the IRES mediated C-terminal fragment expressed in the construct M_2-mRuby2-STOP-M_2-i3-tail-EGFP, under starvation condition.

This is also supported by the lack of complementation of M_2tail(368-466)-GFP11 with SMAC-GFP1-10 **[40](Newman et al., 2016)**. Confocal imaging gives the idea of the drastic change of expression under starvation.

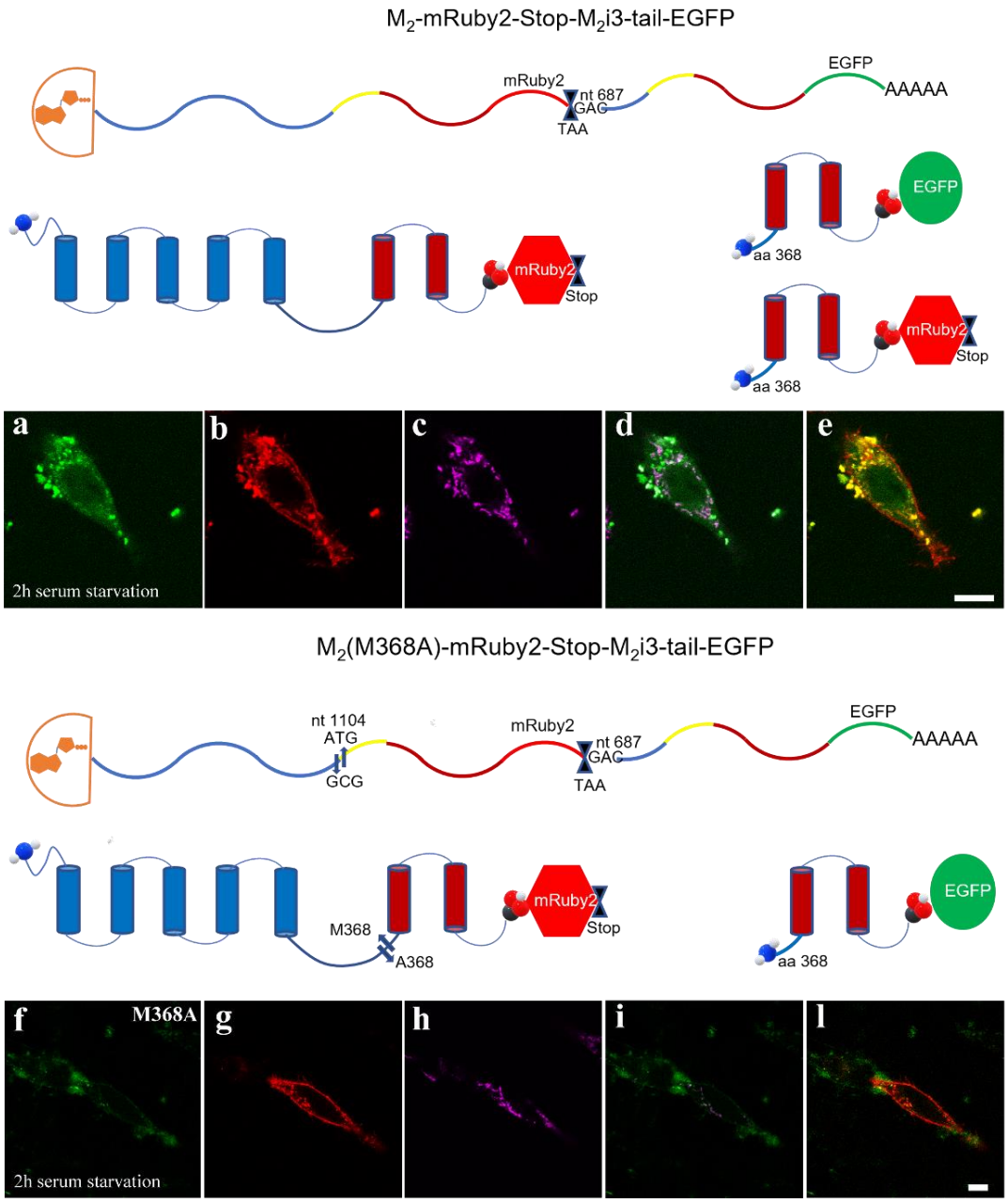

Figure 28 M_2-mRuby2-STOP-M_2-i3-tail-EGFP display increased localization of the EGFP labelled portion to the mitochondria, upon serum starvation for 2 hours and incubation of the cells in HBSS buffer, in presence of Mitotracker: (a) is IRES-driven M_2tail(368-466)-EGFP, (b) cap dependent M_2-mRuby2+IRES-driven M_2tail(368-466)-mRuby2, both derived from the M_2-mRuby2 gene, (c) Mitotracker Deep Red, (d) merge of Mitotracker Deep Red and EGFP, (e) merge between GFP and mRuby2. Localization of the mutant construct M_2(M368A)-mRuby2-STOP-M_2-i3-tail-EGFP after 2 hours incubation in HBSS buffer: (f) is IRES-driven M_2tail(368-466)-EGFP showing again localization of the EGFP to the mitochondria, (g) cap dependent M_2-mRuby2 but is not visible the IRES-driven M_2tail(368-466)-mRuby2 because the mutation M368A (h) Mitotracker Deep Red, (i) merge of Mitotracker Deep Red and EGFP, (l) merge between GFP and mRuby2. Above each series of images are shown representation of the two constructs used for the experiments, the mRNA products from each construct at the top, the expected protein products at the bottom. TAA = Stop codon . (by Petragnano et al., 2022)

5.4 Tail influence on mitochondrial morphology

After the discovery of the important role of the stress condition on the localization of C-terminal fragment, we decided in addition, to evaluate the mitochondrial network organisation after serum starvation, to check any adversely affect the morphology of the mitochondria in cells transfected with M_2tail(368-466)-EGFP; confocal microscopy show that when stained with Mitotracker and after 2h of serum starvation mitochondrial network result intact.

Apoptosis is the programmed cell death, which implies cell changes morphology, including cell shrinkage, nuclear fragmentation, chromatin condensation and DNA fragmentation and death. Apoptosis can start through two pathways:

- the intrinsic pathway, in which the cell kills itself because cell stress, is also called the mitochondrial pathway and mitochondria are essential to cellular life. Apoptotic proteins that target mitochondria may cause mitochondrial swelling through the formation of membrane pores, or they may increase the permeability of their membrane and cause apoptotic effectors to leak out.
- the extrinsic pathway in which the cell kills itself because of signals from other cells, can be initiated by two modulator the TNF (tumor necrosis factor) mediated pathway or the Fas (First apoptosis signal)-Fas ligand-mediated pathway, both involving receptors of the TNF receptor (TNFR) family coupled extrinsic signals.

The convergence of the extrinsic and intrinsic pathways occurs at the proteolytic activation of caspase 3, that once activated, induce a series of irreversible events that lead to the death of the cell.

When apoptosis occur, cytochrome c is released from mitochondria through the actions of the proteins Bax and Bak and once it is released, it binds to apoptotic protease activating factor–1 (Apaf-1) and ATP, which then bind to pro-caspase-9 to create a protein complex known as an apoptosome, that cleaves the pro-caspase-9 to its active form of caspase-9, which cleaves and activates pro-caspase-3 into the effector caspase-3. The caspase-3 protein is a member of the cysteine-aspartic acid protease (caspase) family, the zymogen feature, caspase-3 zymogen has virtually no activity until it is cleaved by an initiator caspase, is important because if unregulated, its activity would kill cells

indiscriminately; the sequential activation of caspases, dimerization to form the active enzyme plays a central role in cell apoptosis. This protein cleaves and activates caspases 6 and 7 that continue the signal cascade.

Thus a cell apoptosis assay, based on the detection of activated caspase-3 **[41](Bonfili et al., 2017)** were performed on M_2WT, M_2tail(368-466), M_2Stop228 and M_2Stop400, to assess fragmentation of the mitochondrial network and cell apoptosis. But the cells transfected with these construct did not display any differences on the level of the full-length caspase-3; overexposing the gel a weak band corresponding to a tiny amount of activated caspase-3 is detectable in most of the of the lane except for M_2WT and negative control ones, indicating that the expression of M_2tail(368-466) in mitochondria, in agreement with the confocal images, doesn't damage the organelle.

5.5 Influence of the C-terminal fragment localization on cell metabolism

After establishing the effects on the mitochondria by the tail fragment, it was obvious to investigate any kind of effect on the cell metabolism: the first step was to assess the cell growth and viability of the cells transfected with M_2WT, M_2tail(368-466) and M_2M368A, compared to untransfected control.

To exclude that the growth or the proliferation could be influenced by the conventional signaling pathway of the receptor, we decided to incubate the cells with a saturating concentration atropine: it is a competitive antagonist of the actions of acetylcholine and other muscarinic agonists and competes for a common binding site on all muscarinic receptor family.

To also exclude that the difference in proliferation rate could be due to differences in the expression of the constructs transfection, efficiency was monitored thanks to the mRuby2 fluorescent reporter within a bicistronic cassette within each vector. Cells were exposed throughout to 100 nM atropine and counted at 24h and 72h after transfection in a type of time course to check the immediate and long-term effect on the growth (Figure 30).

Data from the count, show how transfection of HEK cells with the wild type M_2 receptor and the tail fragment reduced cell growth compared to the control, while cells

transfected with the mutant M_2M368A, that do not express the M_2 C-terminal fragment, displayed a significantly higher growth almost comparable to the untransfected control.

These result matches with a similar experiment repeated on COS-7 cells 48 hours after transfection.

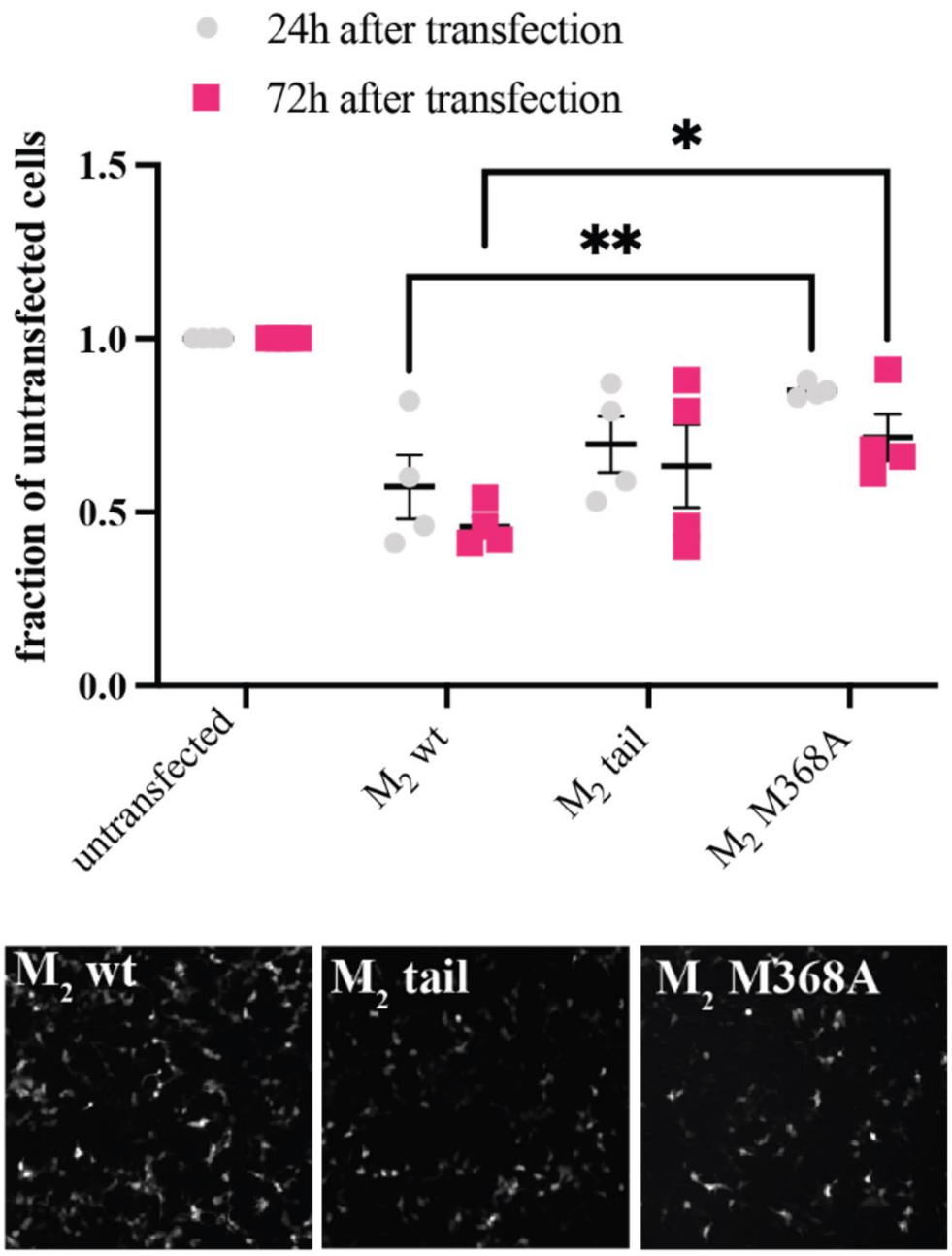

Figure 30 Cell viability assay performed on cells transfected with M_2, M_2tail(368-466) and M_2(M368A), compared to an untransfected control. Below the chart, there are the images of the cells used to assess transfection efficiency monitoring the mRuby2 fluorescent reporter within a bicistronic cassette within each vector. (by Petragnano et al., 2022, viability assay performed by Petragnano F.)

5.5.1 Use of hiPSCs line for the study of the growth and oxygen consumption

A mutant line of hiPSC has been cloned from human induced pluripotent stem cell (hiPSC) line BIHi005-A to generate an isogenic iPSC clone (BIHi005-A-1206 39) with M368A mutation **[42](Richardson et al., 2016)**. A small guide RNA (sgRNA), 5`-AGTCATCTTCACAATCTTGC-3`, directed to the M_2 gene close to the mutation site to be corrected were designed and synthesized and the donor ssODN template was designed to convert the ATG to GCT, 5´-AAAAGTGACTCATGTACCCCAACTAATACCACCGTGGAGGTAGTGGGGTCTTCAGGTCAGAATGGAGATGAAAAGCAGAATATTGTAGCCC**GCAAGATTGTGAAGGCTACTAAGC**AGCCTGCAAAA-3´. Cell suspension containing Cas9 RNPs and ssODN cells were electroporated and the bulk population has been sequenced, the single cell cloning of the genome edited cell pool was performed **[43](Vallone et al., 2020)** and then screened and the positive confirmed clones were banked and characterized for pluripotency and karyotype stability **[44](Metzler et al., 2020)**.

So an engineered human induced pluripotent stem cell (hiPSC) line was created, with both alleles of the M_2 gene carrying the M_2M368A mutation, that represents a model as close as possible to a physiological model and label-free, characterized by the removal of the production of the tail fragment with a mitochondrial localization. Compared to the WT line the M_2M368A hiPSCs seems to show a little change in the phenotype,it appears to be a little bit elongated; we also know from literature that M_2 receptor not only has been found to be expressed in PSCs lines, but it also has shown to have a role in stem cell differentiation **[45,46](Ishizuka et al. 2018, Hoogduijn, Cheng & Genever 2009)** so we decided to perform our experiment as already done previously, with a saturating concentration of atropine, to block any possible activity of the receptor and its signaling pathway.

We used this cell line first to evaluate the proliferation and compare the resulting data with those obtained with the cells overexpressing our constructs, shown above, so after seeding the cells they were counted after 24 and 72h and we found a significant increase in the proliferation of the M_2M368A clone, exactly as seen in the cells overexpressing the M_2WT and its mutant (Figure 31); so once again we demonstrated that impairing the production of the C-terminal fragment and as a consequence abolishing the

translocation into the mitochondria, we eliminate the effect of the tail on the cell metabolism and growth.

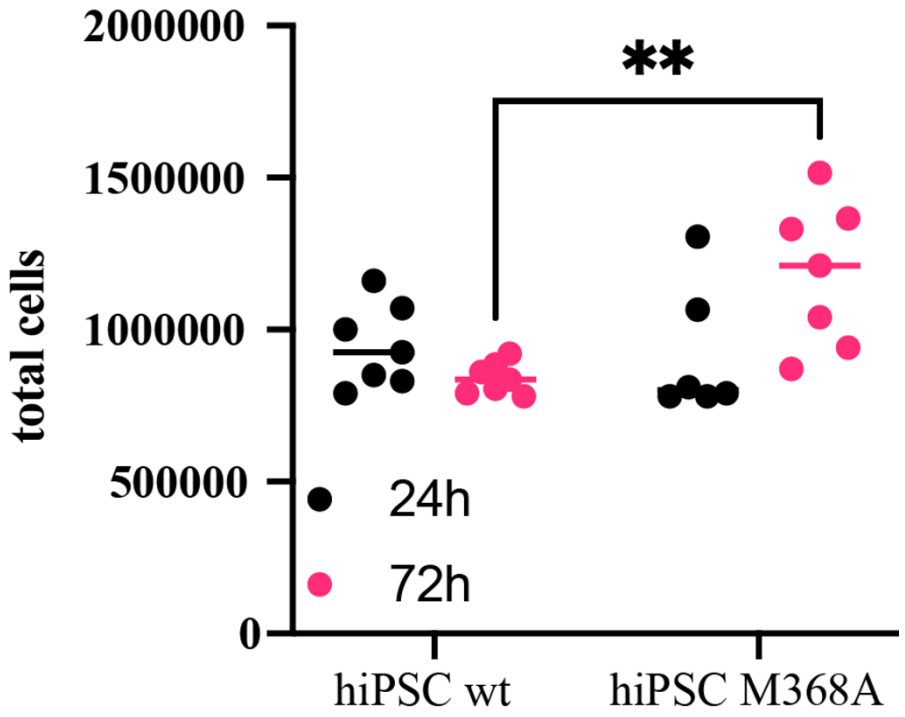

Figure 31 Cell proliferation assay performed for WT hiPSCs and M368A hiPSCs. (by Petragnano et al., 2022, cell proliferation assay performed by Petragnano F.)

Another supporting result has been achieved differentiating wild type and M_2M368A hiPSCs upon exposure for seven days to DMEM-F12 medium.

The hiPSCs and differentiated hiPSCs were used to perform an extracellular oxygen consumption assays, together with untransfected cells and HEK overexpressing the wild type M_2 receptor and the mutant M_2M368A as compared (Figure 32): the Extracellular O_2 Consumption Assay provides a direct, real-time measurement of extracellular oxygen consumption rate (OCR) to analyze cellular respiration and mitochondrial function, relying on the ability of oxygen to quench the excited state of an extracellular O_2 consumption reagent present in the kit. As the test cells used for the test respire, oxygen is depleted in the surrounding environment, which is detected as a consequent increase in phosphorescence signal and the addition of a mineral oil limits back diffusion of ambient oxygen.

The M_2M368A cells, hiPSC and transfected HEK display after 60 minutes of incubation, an accelerated oxygen consumption rate (Figure 32), and this effect increase for the hiPSC as the cell progressively differentiates and on the other hand, we observed a reduced oxygen consumption of the M_2WT receptor compared to untransfected cells, in line with what we observed in the previous experiment performed for the assessment of cell starvation stress effect above.

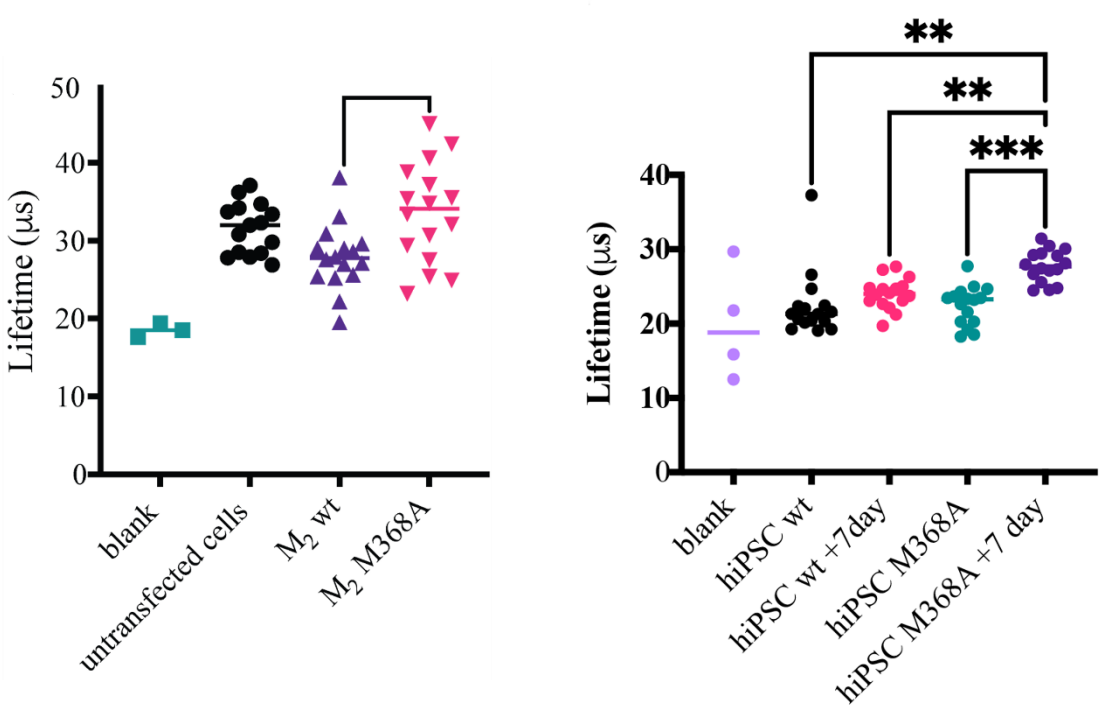

Figure 32 Extracellular oxygen consumption assay: on the left chart of HEK293 cells transfected with the indicated M_2 receptor and M_2M368A using a fluorogenic dye quenched by oxygen. Blank indicates the dye lifetime measured in wells containing the dye, but no cells. On the right the chart of the same extracellular oxygen consumption assay, performed on WT and M368A hiPSCs, prior to and after 7 days. (by Petragnano et al., 2022, oxygen consumption assay performed by Petragnano F.)

Chapter 6: Discussion and conclusions

It is well known that GPCRs are subject to interindividual variability due to mRNA alternative splicing, which leads to different isoforms through the recombination of exons, which may present distinct signaling and localization properties [47]**(Marti-Solano et al., 2020)**. Receptor variants with different functional and localization properties may occur due to other processes, for example, small open reading frames (smORFs), also within lncRNAs (long noncoding RNAs), are an important class of genes that often present mitochondrial localization [48]**(van Heesch et al. 2019)**.

In this thesis, we present data showing the presence of an IRES sequence in the third intracytoplasmic loop of the M_2 muscarinic receptor, which drives expression of a membrane receptor fragment composed of the last two transmembrane regions, VI and VII; IRES are particular regions of the mRNA that are able to recruit ribosome in a cap-independent manner, close to an internal AUG codon and in particular in the M_2 receptor, that plays a fundamental role regulating the expression levels and function of its C-terminal domain. [1,6-7,13]**(Petragnano et al., 2022**, **Jackson & Kaminski 1995, Hellen & Sarnow 2001, Fitzgerald & Semler 2009)**.

Indeed when the muscarinic receptors express only the first five TM regions, they are not able to bind their ligands and run their signaling pathway, but these abilities are completely recovered when it is possible to express the two missing TM regions, suggesting that N- and C-terminal receptor portions behave as autonomous folding units capable of reconstituting a physiologically active receptor [28]**(Maggio et al., 1993b)**, as demonstrated by the M2Stop228 receptor. This mutant with a stop codon at the N-terminal end of the i3 is still functionally active, but a stop codon inserted in the TM V or VI, see the double stop codon or the M2stop400, induce the loss of activity: the carboxyl terminal part of the receptor has to be translated for the receptor to bind its ligands.

Evidence of the involvement of IRES sequences in regulating M_2 GPCR expression, prompt us to exclude alternative mechanism:

- introducing 4 bases downstream of the stop codon (M_2stop228/fr.sh.), a shift in the main reading frame is created, without effect for the receptor expression, effectively excluding the possibility of Stop codon suppression or translational read-through [30]**(Schueren et al., 2014)**.

- a palindromic sequence, long 42 nucleotides, was inserted in the M2stop228 construct following the artificial termination codon to form a hairpin structure in the mRNA, that should block ribosome scanning [32]**(Kozak, 1989)**. The observation that this sequence did not block the receptor expression, can be taken as a reliable indication that the mechanism of termination re-initiation is not responsible for the translation of the carboxyl terminal part of M_2stop228 receptors.
- if the carboxyl terminal domain should be translated by differential RNA splicing, then the stop codon within the i3 loop would also have to be removed without altering TM regions V and VI, restoring the correct reading frame and creating a difference in the DNA size, but the observation that only a single band of the expected size can be detected by reverse transcription PCR assays for both M_2 and M_2stop228 mRNAs or cDNA samples, indicates that the M_2 carboxyl terminal domain is not translated through this mechanism.

This is evidence that expression of the carboxyl terminal domain must be mediated by an IRES sequence.

To determine which of the three in-frame AUG following the artificial stop codon at position 228 may act as the initiation codon for the IRES mediated translation of the C-terminal M_2 domain, three additional mutants have been generated with one of the three in-frame AUG codons replaced by stop codons leading us to affirm that the third AUG codon, in position 368 is crucial for tail expression: only replacing it the [^{3}H]NMS binding of M_2stop228 is abolished whereas mutating the AUG248 or AUG296 codons the receptor expression is only slightly reduced. But these data do not rule out the possibility that multiple AUG codons could still be utilized to initiate translation.

The use of a bicistronic constructs carrying two reporter proteins, Sirius and GFP, proved to be useful to demonstrate the IRES involvement: a part of the i3 loop from a.a. 228 to a.a. 368 was inserted between the ORFs of the two fluorescent proteins and transfected in different cell line COS-7, SHSY-5Y, CHO and HeLa where both proteins could be clearly detected by fluorescence microscopy; although the number of GFP labelled cells was slightly less than Sirius labelled cells, this can be easily explained by the results of the starvation experiments, that highlighted how protein expression driven

by IRES increases in such condition [38]**(Holcik and Sonenberg, 2005)**, and so is for the GFP fluorescence that tends to increase under stressful conditions when the expression is under control of IRES, as in the bicistronic construct.

A preliminary analysis of the i3 loop sequence of the M_2 taking as fulcrum the AUG codon 1104, displays a moderately conserved nucleotide pattern and mostly comprised of purines. In other muscarinic receptors, this i3 loop sequence falls close to the last in-frame AUG for three of them, M_1, M_3 and M_4, whereas it falls close to the penultimate AUG in M_5.

Aligning sequences of all amine receptors we found that this motif is abundantly conserved, so we split the sequence of the M_2 i3 loop, 417 nucleotides long, in two regions: one with the first 387 nucleotides of the i3 loop and the other with the remaining 30 nucleotides comprising the conserved bases, and we inserted them separately in a bicistronic vector: the construct with the sequence of 387 nucleotides exhibited low GFP fluorescence; the construct containing only the last 30 nucleotides preceding AUG instead, greatly enhanced the GFP fluorescence, suggesting that this short stretch of nucleotides is enough to work as an IRES; the same thing occurred when a hairpin loop was inserted upstream of the i3 loop into the bicistronic plasmid, proving again that this is important for the IRES mechanism. Short IRES are not an exception in eukaryotic cells as, for example, a only 9 nucleotide segment long within the mRNA that operate as an internal ribosome entry site in the homeodomain protein Gtx [49]**(Chappell et al., 2000)**.

Mutating most of the IRES conserved A,G residues of the 30 nucleotide stretch in T, GFP fluorescence was significantly reduced, in particular this happened when nucleotide A at position 7, Sirius-H-M_2i3(15n/30n)Mut#1-GFP, or even more severely when the tetranucleotide AAGA, starting at position 19, M_2i3(15n/30n)Mut#2-EGFP, were both mutated. Replacing the last 20 nucleotides of this 30-nucleotide segment with T, GFP fluorescence was almost abolished, but it was completely restored reintroducing AAGA tetranucleotide at position 19. These data indicate that these conserved residues play a pivotal role in recruiting ribosomes on mRNA.

An important part of this thesis has been investigating the role that C-terminal fragment could play in the regulation of the wild type receptor activity, so we tagged M_2tail(368-466) with the GFP and tested it by fluorescence microscopy; to our surprise the green fluorescence of the M_2tail(368-466)-EGFP construct was expressed mostly in mitochondria, unlike the M_2 that is sorted to plasmatic membrane. Mitochondrial

localization was markedly visible when we have overexpressed the C-terminal fragment M_2tail(368-466), but it could be clearly detected also when the C-terminal fragment was expressed under the control of the IRES sequence of the full-length receptor.

To discard the possibility that the mitochondrial localization could be a result of the overexpression of the M_2tail(368-466)-EGFP construct, transfection experiments were repeated with a bicistronic construct M_2-mRuby2-STOP-M_2-i3-tail-EGFP; with this construct the M_2tail(368-466)-EGFP is expressed only by IRES translation, simulating a physiological expression, and the fluorescence although slightly reduced, is still confined to mitochondria, confirming its location as a physiological phenomenon and not as artifact. Fluorescence confinement to mitochondria could not still be observed with the wild type M_2EGFP receptor, when we substitute methionine 368 with an alanine in the sequence of the wild type receptor, that we identified as the starting point of the IRES-mediated translation, as we also noticed in mitochondria purified from HEK293, because this mutation implicates a lack of expression of the C-terminal fragment and confinement to mitochondria, thus providing other evidence to the notion that the third methionine acts as the start site of the IRES driven translation, which instead is preserved with a single amino acid insertion that causes a frame shift after a stop codon.

The mitochondrial localization of the M_2tail(368-466) raises the question of how this fact is related to the [^{3}H]NMS binding of the M_2stop228 and how the two peptides are physiologically associated: previously it has been shown that the N-terminal fragment of the muscarinic M_3 receptor may reach the plasma membrane when truncated in correspondence of the three internal and external loops **[50](Schöneberg et al., 1995)**; this could shed light on a possible chaperone effect that the truncated part of the M_2stop228 receptor exerts on the C-terminal M_2 fragment by attracting it to the plasma membrane, competing with its mitochondrial sorting, proving also consistent with the observation noticed in both co-transfected cells with M_2stop228 and M_2tail(368-466)-EGFP, in which part of the green fluorescence appeared limited to the membrane.

It is well known that specific sequence elements define protein targeting in many eukaryotic cells for mitochondrial import, these sequences are recognized by mitochondrial receptors, among which there is the Tom20, located on the outer mitochondrial membrane **[51](Stojanovski et al., 2012)**. Two distinct mitochondrial targeting signals are recognized: a non-cleavable internal import signals and a classical amino-terminal cleavable pre-sequences **[52](Vögtle et al., 2009),** that most frequently

work as import signals forming charged amphipathic α-helices rich in positively charged amino acids as arginine and lysine; once inside the organelle, these pre-sequences are cleaved by the mitochondrial processing peptidase (MPP) to release the mature protein [53]**(Taylor et al., 2001)**.

The mitochondrial localization of the M_2C-terminal fragment, and in particular its preferential clustering on the internal matrix or cristae, that was proved by immune electron microscopy, may be related to the high hydrophobicity of the M_2 fragment, as it contains only the last two trans-membrane regions of the receptor rich of arginine and lysine amino acids, specially the N-terminal of the M_2tail(368-466), from methionine 368 to the beginning of TM VI: they amount to eight amino acids in a stretch of twenty that result in a structural motif which assimilates the N-terminal of the M_2tail(368-466) to those mitochondrial targeted proteins that express a cleavable pre-sequence.

A further step could be a deep analysis to verify whether this stretch of amino acids does indeed act as a real pre-sequence and eventually to determine which part of it works as a cleaving site in mitochondria, but our data, from live cell import kinetics as well as from in-vitro import into isolated mitochondria, support the notion that the fragment becomes rapidly imported into mitochondria following translation in the cytosol.

Furthermore, fluorescence complementation assays suggest that the M_2 C-terminal fragment predominantly resides in the inner mitochondrial membrane, with its own C-terminal domain exposed towards the matrix.

Peptides translated from the M_2 mutant mRNAs that initiates with the third AUG (codon 368) could be expected to have a molecular weight of about 15 kDa by western blots. This esteem is consistent with what we obtained both in the immune-blotting assay from whole cell lysate carried out with myc-C-terminal labelled M_2 transfected cell and protein extracts from knock-in mice heart and spleen, carrying a tdTomato tag at the C-terminal of M_2 receptor and under the control of the endogenous promoter/enhancer sequences; even though additional band at 20 kDa was also detected, these results are still in line with the expectation that partial translation of the carboxyl-terminal segment occurs in native M_2 receptors under physiological conditions. Moreover the fragment is found predominantly in a carbonate-insoluble fraction, i.e. a membrane, where it appears to form a high molecular weight complex of ~180 kDa with other mitochondrial proteins.

Another important passage for the study of the C-terminal fragment was to verify its role related to the new localization.

The M_2tail(368-466) fragment translated by IRES is inactive and previous experiment showed that the C-terminal fragment of the M_2, as well as the M_3 tail, are not functional in the cell when transfected alone [28]**(Maggio et al. 1993b)**; in the past years, growing evidence has accumulated indicating that GPCRs can be functional also at other cellular locations, associated with their canonical trafficking pathways such as sorting vesicles and endosomes [54]**(Weinberg & Puthenveedu 2019)**, but also to non-canonical locations, such as the nucleus, the nuclear membrane, the Golgi apparatus and the mitochondria: G-proteins as $G\alpha_i$ [55]**(Lyssand & Bajjalieh, 2007)** and $G\beta_2$ [56]**(Zhang et al., 2010)** have been found in mitochondria, where it has been shown to regulate mitochondrial fusion via mitofusin binding; also a few GPCRs, have been found in this organelle, even though it is the full receptor protein to be sorted out in the mitochondria; mitochondrial localized GPCRs have been shown to specifically affect the organelle function, ranging from oxygen consumption rates to Ca^{2+} handling and even to apoptosis: serotonin $5HTR_{3/4}$ [57]**(Wang et al., 2016)** exerted the opposite effects on the mitochondrial respiration: 5-HTR_3 increased RCR (respiration control ratio), but 5-HTR_4 reduced RCR, moreover, activation of 5-HTR_3 and 5-HTR_4 both significantly inhibited the opening of mPTP (mitochondrial permeability transition pore); activation of the melatonin MT_1 receptors by a mitochondrial melatonin pool can affect the cytochrome C release [58,59]**(Wang et al., 2011; Suofu et al., 2017)**; the CB_1R on the outer mitochondrial membranes affects cyclic AMP concentration, protein kinase A activity, complex I enzymatic activity and respiration in neuronal mitochondria [60]**(Benárd et al 2012)**. Anyway, this means that probably mitochondria provide an adequate context for canonical GPCRs signalling.

The specific localization of these receptors appears to go in accordance with a specific function and the M_2tail(368-466) expression driven by an IRES, suggests that it might have a physiological role and the connection with stressful conditions is in line with this hypothesis, as indicated by the increase of fluorescence of the Sirius-M_2i3(417n)-GFP and M_2-mRuby2-STOP- M_2-i3-tail-EGFP constructs related to the increase in the expression of the M_2 C-terminal fragment.

Since mitochondria are the kingpin of regulation of cellular energy homeostasis, where oxidative phosphorylation occurs, the C-terminal fragment must have an effect on the their metabolism and consequently on the cellular physiology: we have demonstrated this with the measure of the oxygen consumption in cells, COS-7, transfected with

M_2stop228 and M_2tail(368-466), which show a reduction of the consumption, but an interesting particular was that the addition of the ATP synthase inhibitor, oligomycin, only slightly reduced the extent of oxygen consumption in cell transfected with M_2tail, pointing out how the effect of the C-terminal fragment can be due to a real confinement to mitochondria and correlate to a mimic action like that of an uncoupling agent; this acts by increasing the permeability of the membrane to H^+ ions and dissipating the proton gradient. At the moment the exact mechanism by which M_2tail(368-466) reduce oxygen consumption in mitochondria is unclear, but for sure it will be a matter of study.

Although the relationship between rate of oxygen consumption and ROS production is not yet completely understood, the general opinion is that a low ATP synthesis in mitochondria correlates significantly with a decrease in ROS production **[61](Murphy, 2009)**, so we have checked this in cells transfected with the M_2tail(368-466) fragment and what we observed was a drastic reduction in the production of reactive oxygen species: ROS are implicated in the pathogenesis of several diseases **[62](Guo et al., 2013)**, thus in our opinion an increased expression of this fragment in mitochondria, as it occurs under stressful conditions, might have a protective role in cells that express muscarinic M_2 receptor.

In addition to these direct effects on mitochondrial functionality, proliferation assays have shown that the C-terminal fragment, both expressed by the wild type receptor and by the M_2tail(368-466)-myc constructs, influence cell proliferation by inducing a decrease; this is an effect that disappears again when the gene sequence carries the M368A mutation.

This data were confirmed in physiological label-free conditions, by genetically editing human induced pluripotent stem cells in order to induce the M368A mutation in the gene of the M_2 receptor: this clone compared to the normal counterpart, increase oxygen consumption and cell proliferation corroborates our hypothesis that the M_2 C-terminal fragment upon reaching the mitochondria can exert its effects on cell metabolism, that is still confirmed when the cells were undirectedly differentiated, an observation consistent with the shift of the cell phenotype towards oxidative phosphorylation **[63](Zhang et al., 2012)**.

With this study, we can assert that the C-terminal-M_2 fragment is not a waste product of the M_2 receptor translation, but a functional protein with a clear effect on mitochondria respiration, nevertheless many aspects remain unclear and should be

explored deeply: how is the fragment targeted to mitochondria and how does it reduce oxygen consumption; if the tail have a role to play in human physiology and pathology, since ROS production is implicated in the pathogenesis of several diseases [62]**(Guo et al., 2013);** how we can regulate its expression by drugs inasmuch the increased mitochondrial localization of the M_2 C-terminal fragment, occurring under integrated stress response, might have protective effects; eventually, if this behaviour of the M_2 receptor may be adopted by other GPCRs indicating a common trait of this receptor family, since the mechanism of IRES-dependent modulation of translation and consequent non canonical targeting of translation products, may provide another means of a generic cellular response to overcome different types of stress by modulating the mitochondrial proteome and adjusting the mitochondrial bioenergetic state.

Chapter 7: Materials and methods

7.1.1 Cell culture and transfection

COS-7 cells (from American Type Culture Collection) were grown at 5% CO_2 and 37°C, in high glucose DMEM supplemented with 10% FBS, 2 mM L-glutamine, 50 IU/mL penicillin, and 50 mg/mL streptomycin, and non-essential amino acids. HeLa cells (from American Type Culture Collection) were cultured in the same medium, but with the double amount of L-glutamine. SHSY-5Y cells were cultured in RPMI medium supplemented with 10% FBS, 2 mM L-glutamine, 50 IU/mL penicillin, and 50 mg/mL streptomycin. Media and reagents used for cell cultures were from Euroclone, PAN Biotech, Biochrome and Sigma-Aldrich.

HEK293 cells (ECACC 96121229 from Sigma-Aldrich Chemie GmbH) were cultured in DMEM (Dulbecco's modified Eagle's medium PAN biotech, Aidenbach, Germany), supplemented with 4.5 g/L glucose, 2 mM L-glutamine, 10% FCS, 100 units/mL penicillin and 0.1 mg/mL streptomycin and maintained at 37°C and 5% CO_2.

7.1.2 Transfection protocol

Cell transfection was performed using FuGene® transfection reagents (Promega) as recommended by the manufacturer. Eighty percent confluent cells were washed twice with free-serum medium and the mix of FuGene and plasmid DNA was added. In every experimental condition 6-8 μg of plasmid DNA per Petri (10 cm^2) were used. Cells were grown for 48 h post-transfection before use. In co-transfection experiments, half amount of each plasmid DNA was used.

Cells were transfected using Effectene transfection reagent (QIAGEN) according to the manufacturer's instructions. Cells cultured in 15 cm dishes were split at a 1:36 ratio into 6-well plates containing poly-D-lysine (PDL)-coated 24 mm glass coverslips. Cells seeded on PDL-coated coverslips in 6-well plates were transfected 16 hours after seeding with 0.6 μg plasmid/well.

7.1.3 Generation of M368A hiPSC clone

The human induced pluripotent stem cell (hiPSC) line BIHi005- A (https://hpscreg.eu/cell-line/BIHi005-A) was used to generate an isogenic iPSC clone (BIHi005-A-39) with M368A mutation. Small guide RNA (sgRNA) targeting the M_2 gene close to the mutation site to be corrected were designed using the http://crispor.tefor.net/ webpage and the sgRNA (5`- AGTCATCTTCACAATCTTGC-3`) were synthesized by Integrated DNA technologies (https://eu.idtdna.com). The donor ssODN template was designed to convert the ATG to GCT and was synthesized as an Ultramar DNA oligo by IDT.

(5´AAAAGTGACTCATGTACCCCAACTAATACCACCGTGGAGGTAGTGGGGT CTTCAGGTCAGAATGGAGATGAAAAGCAGAATATTGTAGCCCGCAAGATTG TGAAGGCTACTAAGCAGCCTGCAAAA-3´).

The Ribonucleoprotein (RNP) complexes were prepared by incubating of 1.5µg Cas-9 protein and 360 ng gRNA for 10 minutes at RT. For delivery of RNPs and ssODN template, 10µL cell suspension containing Cas9 RNPs and ssODN and 100000 cells were electroporated using the Neon transfection System (ThermoFisher Scientific). The electroporated cells were plated in one well of 6 well plate with StemFlex media (ThermoFisher Scientific) supplemented CloneR™(Stemcell technologies). Three days after the transfection we analyzed the bulk population using the Sanger sequencing to estimate the editing efficiency. Thereafter, the automated single cell cloning of the genome edited cell pool was performed. The clones were screened by SANGER sequencing, the positive confirmed clones were banked and characterized for pluripotency and karyotype stability.

For pluripotency assay, single cells were labelled with conjugated antibodies. Surface markers (SSEA1, SSEA4 and TRA1-60) staining was performed in unfixed cells by incubation with antibodies diluted in 0.5% BSA/PBS (10 minutes, 4°C, dark). Intracellular markers (OCT3/4, NANOG) were stained by fixation/permeabilization solution (Miltenyi Biotec, 130-093-142) (30 minutes, 4°C, dark) followed by antibody incubation in permeabilization buffer (Miltenyi Biotec) (30 minutes, 4°C, dark). Analysis was done using the MACSQuantR AnalyzerVYB and FlowJo v10.4.

For karyotype stability, genomic DNA was isolated using the DNeasy blood and tissue kit (Qiagen, Valencia, CA, United States) and samples were analyzed using the human Illumina OMNI EXPRESS-8v1.6 BeadChip. First, the genotyping was analyzed

using GenomeStudio 1 genotyping module (Illumina). Thereafter, KaryoStudio 1.3 (Illumina) was used to perform automatic normalization and to identify genomic aberrations utilizing settings to generate B-allele frequency and smoothened Log R ratio plots for detected regions. The stringency parameters used to detect copy number variations (CNVs) were set to 75 kb (loss), 100 kb (gain) and CN-LOH (loss of heterozygosity) regions larger than 3 MB.

7.1.3.1 Culture and handling of hiPSCs cells

A hiPSCs were cultured on Geltrex (Thermo Fisher) coated plates using: Essential 8 medium (Thermo Fisher). The culture was routinely monitored for mycoplasma contamination using a PCR assay. 10 μM ROCK Inhibitor Y-276322 HCl (Selleck Chemicals, #SELS1049) was added after cell splitting to promote survival. hiPSC cultures were kept in a humidified atmosphere of 5% CO_2 at 37°C and 5% oxygen. hiPSCs were undirectedly differentiated to a mixture of three lineages (ectodermal, endodermal and mesodermal) by replacing Essential 8 medium with DMEM-F12 medium supplemented with 10% FBS for seven days. 10 μM ROCK Inhibitor Y-276322 HCl (Selleck Chemicals) was added after cell splitting to promote survival.

7.2 Plasmid

M_2stop228: this plasmid was created by substituting codon 228 (CAA) with a stop codon (TAA) at the N-terminal of the i3 loop of the wild type M_2 receptor.

M_2trunk(1-228): this plasmid was created by substituting codon 228 (CAA) with a stop codon (TAA) at the N-terminal of the i3 loop of the wild type M_2 receptor followed by removal of the downstream sequence.

M_2trunk(1-283): the expression plasmid referred as M_2trunk(1-283) containing transmembrane domains I-V and the N-terminal portion of the third cytoplasmic loop were described previously [27]**(Maggio et al., 1993)**.

M_2tail(281-466): plasmid containing transmembrane domains VI and VII, and the C-terminal portion of the third cytoplasmic loop were described previously [27] **(Maggio et al., 1993)**.

M_2stop400: this plasmid was created by substituting codon 400 (TGG) with a stop codon (TAA) in the TM region VI of the wild type M_2 receptor.

M_2stop228/stop400: this plasmid was created by inserting an additional stop codon TGG was substituted with TAA at the position codon 400 of the TM region VI of the M_2stop228 mutant.

M_2stop196/stop400: This plasmid was created by substituting codon 196 TAT with a stop codon TAA in the TM region V of the wild type M_2 receptor and inserting an additional stop codon in the TM region VI of the M2stop196 mutant, where TGG was substituted with TAA at position of the codon 400.

M_2WT-EGFP: The wild type M_2 muscarinic receptor was cloned into the pEGFP-N1 expression cassette, between the restriction sites HindIII and XbaI.

M_2stop228-EGFP: The construct M_2stop228 has been fused to EGFP.

M_2stop400-EGFP: The construct M_2stop400 has been fused to EGFP

M_2fr.sh.-EGFP: single base insertion (G) upstream of nucleotide 1102 of the wild type M_2 receptor, just before the third in-frame methionine of the i3-loop (M368), induces a frame shift that, following 2 amino acids, generates a stop codon (TAA) in the amino acid position 370 of the new reading frame. The construct is then fused to EGFP

M_2stop228/fr.sh.: This plasmid was created by inserting four bases (AATT) fifteen nucleotides downstream of the stop codon to create a shift in the correct reading frame of the M2stop228 mutant.

M_2stop228/stop248,M_2stop228/stop296 and M_2stop228/stop368: These constructs were obtained by substituting the three in-frame ATG codons: ATG248,

ATG296 and ATG368, with the stop codon TAA downstream of the stop228 of the M_2stop228 mutant.

Sirius-M_2i3(417nt)-EGFP: this bicistronic construct was created by inserting the i3 loop of the muscarinic M_2 receptor, from nucleotide 685 to nucleotide 1101, between the ultramarine fluorescent protein Sirius and the EGFP. Eight nucleotides corresponding to the recognition site of the PacI enzyme were inserted between Sirius and the i3 loop of the wild type M_2 receptor to alter the reading frame downstream of the Sirius stop codon.

Sirius-H-EGFP: this bicistronic construct was created by inserting a 42 nucleotides hairpin loop between Sirius and the EGFP fluorescent protein. The hairpin loop was spaced from the Sirius stop codon by inserting a PacI recognition sequence and 15 nucleotides of the M_2 i3 loop sequence comprised between nucleotide 685 and nucleotide 699. A G nucleotide was also inserted following the 42 nucleotides of the hairpin loop and upstream of the initial ATG triplet of the EGFP to restore a correct reading frame.

Sirius-H- M_2i3(417nt)-EGFP: this bicistronic construct was created by adding 417 nucleotides of the i3 loop of M_2 from nucleotide 685 to nucleotide 1101 to the plasmid Sirius-H-EGFP. An additional PacI restriction site was also inserted upstream of this segment of the i3 loop.

Sirius-H-M_2i3(15nt)-GFP: this bicistronic construct was created by adding 15 nucleotides of the i3 loop of M_2 from nucleotide 685 to nucleotide 699 to the plasmid Sirius-H-EGFP. An additional PacI restriction site was also inserted upstream of this short segment of the i3 loop.

Sirius-H-M_2i3(387nt)-GFP: this bicistronic construct was created by adding 387 nucleotides of the i3 loop of M_2 from nucleotide 685 to nucleotide 1071 to the plasmid Sirius-H-EGFP. An additional PacI restriction site was also inserted upstream this long segment of the i3 loop.

Sirius-H-M_2i3(15/30nt)-GFP: this bicistronic construct was created by deleting from the plasmid Sirius-Hairpin- M_2i3(417n)-EGFP 372 nucleotides of the M_2 i3 loop, from nucleotide 700 to nucleotide 1071.

Sirius-H-M_2i3(15n/30n)Mut#1-GFP,Sirius-H-M_2i3(15n/30n)Mut#2-EGFP, Sirius-H-M_2i3(15n/30n)Mut#3-EGFP, Sirius-H-M_2i3(15n/30n)Mut#4-EGFP, Sirius-H-M_2i3(15n/30n)Mut#5-EGFP, Sirius-H- M_2i3(15n/30n)Mut#6-EGFP: all these construct have been created mutating the Sirius-H-M_2i3(15/30nt)-GFP as listed above in the text in the chapter 2.2 Use of bicistronic constructs to mark out IRES sequence.

M_2tail(368-466)-EGFP: this construct was created so that the receptor protein would start from the third in-frame methionine of the M_2 i3 loop (M368). The EGFP gene was fused C-terminally following a short restriction site sequence TCTAGA of the XbaI enzyme.

M_2mRuby2: the wild type M_2 muscarinic receptor was cloned into the mRuby2 vector (Addgene plasmid #40260).

M_2-mRuby2-STOP-M_2-i3-tail-EGFP: this mega construct was obtained by fusing two preceding constructs, M_2-mRuby2 and M_2tail(368-466)-EGFP, in a unique plasmid, but the M_2tail started at codon 229 M2tail(229-466)-EGFP. After the stop codon of mRuby2 and before the codon 229 of M2tail was inserted a short restriction site sequence TCCGGA of the BspEI enzyme.

M_2(M368A)-mRuby2-STOP- M_2-i3-tail-EGFP: this mega construct is analogous to M_2-mRuby2-STOP- M_2-i3-tail-EGFP, but the third in-frame methionine of the i3-loop of the M_2 muscarinic receptor was mutated to alanine (M368A).

M_2WT-myc, M_2tail(368-466)-myc, M_2M368A-myc, M_2stop400-myc, M_2stop228-myc: M_2-myc was purchased from OriGene. This plasmid encodes the human M_2 receptor with a myc tag at the C-terminus of the protein. M_2stop228-myc was obtained by replacing the 0.9 Kb BmtI-PspOMI fragment of the M_2stop228 mutant with the corresponding fragment of M_2-myc. M_2stop400-myc was obtained by substituting the codon 400 TGG with a stop codon TAA of the M_2-Myc. All the constructs have an

additional DDK tag after the c-Myc. Subsequently, all c-Myc constructs were extracted by PCR and subcloned into a bicistronic pVitro2-MCS plasmid (Invivogen), allowing for the expression of a reporter gene (in our case the red fluorescent protein mRuby2) after an IRES sequence, in order to check for transfection efficiency.

M_2-GFP11: short peptide 16 amino acids long from the GFP protein, GFP11, was fused to the C-terminus of the muscarinic M_2 receptor. GFP11 was custom synthetized and inserted as a linker between the XbaI and XhoI restriction sites in the plasmid backbone of M_2-EGFP.

Mito-GFP1-10: the mitochondrial targeting sequence of the cytochrome c oxidase subunit 8A (COX8A) was fused to the N-terminal of GFP1-10 fragment of GFP. GFP1-10 was purchased from Addgene as Addgene plasmid 70219.

M_2tail(368-466)-GFP11: the GFP11 fragment was fused to the C-terminus of the muscarinic M_2tail(368-466) receptor fragment.

7.3 Radioligand binding assay

Cells were lysed 48 h post-transfection with ice-cold 2 mM EDTA, 1 nM Na-HEPES (pH 7.4), scraped with a rubber policeman in the presence of ~4 mL rinsing medium, and homogenized with a Polytron homogenizer (ULTRA-TURRAX) in binding assay buffer (50 mM Tris-HCl, pH 7.4, 155 mM NaCl, 0.01 mg/mL bovine serum albumin). Radioligand bindings were carried out at 37°C for 3 h in a final volume of 1 mL. Non-specific binding was determined in presence of 1 μM atropine. For competition binding assays, increasing concentrations of carbachol (from 0.01 μM up to 10 μM) were used in presence of 200 ρM [^{3}H]N-Methylscopolamine ([^{3}H]NMS; 78.9 Ci/mmol; PerkinElmer). The bound ligand was separated from the unbound ligand using glass-fiber filters (Whatmann, GF/B) with a Brandel Cell Harvester, and filters were counted with a scintillation β-counter. K_d values of [^{3}H]NMS were calculated in direct saturation experiments, whereas carbachol IC_{50} values were calculated in competition curves, against 400 ρM [^{3}H]NMS, fitted to one binding models using the iterative, non-linear least-squares regression analysis of OriginPro 7.5 software (OriginLab Corporation).

7.4 Adenyl cyclase assay

COS-7 cells were transfected with plasmids containing the receptor of interest plus adenyl cyclase V. 24 h after transfection the cells were detached with trypsin and re-cultured in 24-well plates. Following an additional period of 24 h culture, they were assayed for adenyl cyclase activity, the assay was performed in triplicate**.** Cells were incubated in 24-well plates for 2 h with 0.25 mL/well of fresh growth medium containing 5 μCi/mL [^{3}H]adenine (PerkinElmer). The medium was then replaced with 0.5 mL/well of DMEM containing 20 mM HEPES, pH 7.4, 0.1 mg of bovine serum albumin, and the phosphodiesterase inhibitors 1-methyl-3-isobutylxanthine (0.5 mM) and Ro-20‑1724 (0.5 mM). AC activity was stimulated by the addition of 1 μM forskolin in the presence or absence of carbachol. After 10 min of incubation at 30°C the medium was removed, and the reaction terminated by addition of perchloric acid containing 0.1 mM unlabeled cAMP followed by neutralization with KOH. The amount of [^{3}H]cAMP formed under these conditions was determined by a two-step column separation procedure.

7.5 Detection of phophorylated ERK

On day zero, COS-7 cells were plated on 6-well plates (70000 cells/well). On day 1, the cells were transiently transfected with the plasmid of interest (1 μg DNA/well). On day 3, the cells were exposed to serum-free medium until the day of assay. On day 4, the cells were treated with 100 μM carbachol (time 0'; 1'; 5' and 20') at 37°C. The cells were then lysed in a buffer containing 50 mM TrisHCl (pH 7.8), 1% Triton X100, 0.1% SDS, 250 mM NaCl, 5 mM EDTA, 100 mM NaF, 2 mM NaPPi, 2 mM Na_3VO_4, 1 mM PMSF. Samples were incubated on ice for 30 min and then centrifuged at 17,000 rpm for 15 min at 4 °C. The supernatants were recovered and assayed for protein concentration. Protein extracts were run on a 10% SDS-PAGE and transferred on a PVDF membrane. The membrane was then blocked in 5% non-fat dry milk in 1xTBS plus 0.1% Tween 20 and the extent of phosphorylation of ERK was determined by immunoblotting with anti-p-ERK diluted 1:1000. The blots were stripped and re-blotted with the anti-ERK, diluted 1:1000 in blotto, to control the total amount of kinase loaded. Blot bands were detected

using a ChemiDoc XRSplus imaging system, and their optical densities determined using a computer-assisted densitometer.

7.6 Reverse transcription

Reverse transcription was performed using a 24-nucleotide antisense oligo (TTACCTTGTAGCGCCTATGTTCTT) directed against the last 24 nucleotides at the 3' end of the M_2 open reading frame. cDNA amplification was carried out with the same antisense oligo used for reverse transcription, together with a 24 nucleotides sense oligo (ATGAATAACTCAACAAACTCCTCT) directed against the first 24 nucleotides at the 5' end of the M_2 open reading frame.

7.7 Fluorescence microscopy

Fluorescence microscopy experiments were performed either on a Leica SP5 (or SP8) Confocal Microscopes, using HyD photon counting detectors and an Argon/Ion laser (or white light laser) source for 488 nm/633 nm excitation and a solid-state diode laser (or white light laser) for 561 nm excitation. A solid-state diode laser was used for 405 nm excitation. A 40x 1.3 NA objective was used, and the electronic zoom was set to achieve a pixel size of 50 nm. For visualization, mitochondria of transfected cells were labelled for 30 minutes at 37°C with 50nM MitoTrackerR Deep Red FM (Invitrogen™, Thermo Scientific).

7.8 Split-GFP complementation assay

To perform the sequential split GFP complementation assay 300000 HEK cells were seeded on a 10% poly-D-lysine (PDL)-coated 25mm coverslip in each well of a FalconR 6-well flat-bottom plate (StemCell™) and cultured overnight. Cells were transfected using Effectene with a 0.4 μg Mito-GFP1-10 plasmid. The cells were then washed once with fresh 2 mL PBS first and supplemented with 1.5 mL fresh DMEM medium (ScienCell™) supplemented with 10% FBS and 1% P/S. After adding the transfection mixture, the cells were cultured overnight. After the first transfection, a

second transfection of a 0.6 μg plasmid encoding either the C-terminal GFP11 tagged M_2tail(368-466) or M_2 receptor was performed using the Effectene Transfection Reagent (Qiagen). After washing each well with 2 mL PBS, the old medium was exchanged with 1.5 mL low glucose Minimum Essential Medium (MEM) (Gibco™, Thermo Scientific) supplemented with 1% P/S, in order to create a stress-like cell starvation condition. After a four hours starvation, the cells were fixed using 4% polyformaldehyde (PFA)/PBS at 37°C for 30 minutes and washed twice with PBS before imaging.

7.9 Quantification of M_2tail(368-466) mitochondrial import kinetics

250000 HEK-TSA cells were seeded in each PDL-coated well of the μ-Slide 8 well (Ibidi) with DMEM (ScienCell™) supplemented with 10% FBS and 1% P/S overnight, and transfected with a total of 2 μg C-terminal EGFP tagged M_2tail, after washing with 200 μL PBS and refreshing with 100 μL DMEM (ScienCell™) supplemented with 10% FBS and 1% P/S. After transfection for five hours, mitochondria of transfected cells were rapidly labelled with 50nM MitoTrackerR Deep Red FM (Invitrogen™, Thermo Scientific) in FluoroBrite DMEM medium (Thermo Scientific) supplemented with 1% P/S for 20 minutes after the removal of old culture medium. After mitochondria labeling, the μ-Slide were washed twice with FluoroBrite DMEM medium (Thermo Scientific) and subsequently mounted onto the TCS SP8 confocal microscope (Leica). Firstly the acquisition mode was set to the tile scanning and after storing the position of each desired transfected cells, the imaging mode was set to XYT and a HC PLAPO CS2 40×/NA1.3 oil immersion objective was selected. Both DIC channel and HyD were utilized to obtain 512×512 pixels images. Laser wavelengths were set as described above, all settings remained the same throughout the whole measurement. Images were taken every 30 minutes over a 5h interval. The images were afterwards analyzed by ImageJ software, using the Plugin JACoP. Briefly, the degree of colocalization between EGFP-tagged M_2tail(368-466) (CH1) and mitotracker stained mitochondria (CH2) was quantified by Mander's colocalization coefficients. A threshold was determined for individual channel in order to distinguish specific signals from nonspecific ones. Due to their sensitivities to thresholds, the Pearson correlation

coefficient (PCC), as well as the faster decaying attribute of nonspecific signals, were also considered while estimating thresholds for each channel. For the analysis of each cell, the threshold for mitotracker channel was kept constant the threshold for EGFP channel was evaluated based on the PCC value.

7.10 Immunoelectron Microscopy

Samples were fixed for 3 hours at 4°C with a mixture of 4% PFA and 0,05% GA in 0,1M PB, pH 7.4. After rinsing in the same buffer, samples were dehydrated in a graded series of ethanol and embedded in medium grade LR White resin, following addition of the LR White accelerator (London Resin Company, Berkshire, England). The resin was then polymerized for 20 min at room temperature in tightly capped gelatine capsules. Ultrathin sections were obtained using a Reichert Ultracut ultramicrotome equipped with a diamond knife and collected on nickel grids. For immunogold labelling, 60-80 nm thick sections were processed following the incubation protocol originally developed by Aurion (Vageningen, the Netherlands). Unspecific binding was prevented by treating sections for 20 minutes with 0.05 M glycine in PBS, at pH 7.4. A subsequent block step was made by washing sections for 30 minutes in 5% BSA, 5% normal goat serum and 0.1% cold water fish skin gelatine. Sections were soaked overnight 4°C in incubation buffer (PBS and 0.1% BSA-cTM, pH 7.4) 3x5 minutes in a moist chamber containing the anti myc-Tag (9B11) mouse primary antibody (Cell Signaling) diluted 1:50 with incubation buffer. Sections were then washed in incubation buffer 6x5 minutes and incubated for 1 h with a secondary goat anti-mouse antibody conjugated to 10 nm gold particles (British BioCell International, UK), diluted 1:10 in incubation buffer. After rinsing in incubation buffer 6x5 minutes, grids were washed in PBS 6x5 minutes. Sections were subsequently stained with uranyl acetate and observed with a Jeol JEM EXII Transmission Electron Microscope at 100kV. Micrographs were acquired by the Olympus SIS VELETA CCD camera equipped the iTEM software. Control sections were obtained by omitting the primary antibody from the incubation mixture.

7.11 Western Blot assay

7.11.1 Immunoblot of muscarinic M_2 receptor transfected in COS-7 cells

COS-7 cells were collected 48 h after transfection and treated with lysis buffer (50 mM TrisHCl pH 7.8, 1% Triton X100, 0.1% SDS, 250 mM NaCl, 5 mM EDTA, 100 mM NaF, 2 mM NaPPi, 2 mM Na_3VO_4, 1 mM PMSF). Cell lysates were then centrifuged at 16000 g for 15 min at 4 °C and supernatants, containing solubilized receptors resolved by SDS-PAGE or stored at -80°C. Samples were mixed with 65 mM Tris, 10% glycerol, 2% SDS, 0.1 M DTT, 0.001% bromophenol blue, pH 6.80 with HCl, boiled for 5 min and applied to a 10% SDS-PAGE.

Resolved proteins were transferred to a PVDF membrane. The membrane was blocked in 5% non-fat dry milk in 1xTBS plus 0.1% Tween 20 and the expression level of the M_2 receptor was assayed with 1:1000 anti myc-Tag (9B11) mouse primary antibody (Cell Signaling) and thereafter in a HRP-conjugated secondary antibody diluted 1:1000. Membranes were then incubated in SuperSignal West Pico chemiluminescent substrate and the bands detected using a ChemiDoc XRSplus imaging system. Optical densities of blot bands were finally determined using a computer-assisted densitometer (ImageJ U. S. National Institutes of Health, Bethesda, Maryland, USA), normalized versus the tubulin internal control.

7.11.2 Immunoblot of muscarinic M_2 receptor mutants transfected in HEK cells

Cells were seeded in 10 cm plates and transfected after 24h according to manufacturer protocols (Effectene, Qiagen) using 2 μg of plasmid DNA. 48h after transfection cells were washed (2x) in ice cold PBS, 200 μL per plate of ice-cold lysis buffer were added. Lysis buffer was a RIPA buffer: 50 mM Tris-HCL pH 8, 150 mM NaCl, 1% TRITON, 0.5% sodium deoxycholate and 0.1% SDS. 100x Halt Protease Inhibitor Cocktail (Thermo Fisher), 100x 0.5 M EDTA and (10x) 10 mM PMSF were added to the buffer to a final 1x dilution. Cells were then scraped and the cell lysate transferred to pre-cooled 1.5 mL Eppendorf tubes; the tubes were placed in a Thermomixer at 4 °C, 300 rpm for 30 minutes. Then the tubes were centrifuged for 30

minutes at 14000 rpm at 4 °C. Protein concentration in the cell lysates was quantified by a BCA assay (Pierce BCA Protein Assay Kit, from Thermo Fisher) according to manufacturer instructions. Cell lysates were loaded into 10% polyacrylamide gels. Cell lysates were loaded using Laemmli Buffer 2x (Sigma Aldrich) in equal mass. As a reference marker we loaded 5 μL of PageRuler Prestained Protein Ladder (Thermo Fisher). Gels were mounted into a Mini Protean Tetra Cell kit (BioRad) using 1x SDS running buffer. Gels were ran using a constant voltage of 90V for approximately 15 minutes, and afterwards at 130V for 45 minutes. Gels were transferred to PVDF membranes, wet transfer was achieved by using the Mini Trans Blot Module (BioRad) in Wet Transfer Buffer (25 mM Tris pH 8.3, 192 mM Glycine and 20% MetOH) at 350 mA for 90 minutes. The immunoblotted membranes were then blocked in 5% milk in TBS-T for 1 hour at room temperature. The membrane was then incubated overnight at 4°C with primary antibody solution using the following concentrations depending on the antibody used: 1:1000 anti myc-Tag (9B11) mouse primary antibody (Cell Signaling), 1:1000 anti β-actin (13E5) rabbit primary antibody (Cell Signaling), 1:1000 anti myc-Tag (9B11) mouse primary antibody (Cell Signaling). After overnight incubation, the membranes were washed 3x10 minutes in TBS-T and incubated at RT for 1 h with a secondary antibody (1:10000 anti-mouse IgG/(anti rabbit) HRP-linked antibody from Cell Signaling). After the incubation with the secondary antibody, the membrane was washed 3x10 minutes in TBS-T. The membrane was incubated with SuperSignal WestFemto solution (Thermo Fisher) according to the manufacturer’s instructions and imaging the membrane using a c600 Transilluminator from Azure Biosystems.

7.11.3 Isolation of mitochondrial fractions and immunodetection

Cells were seeded in 10 cm plates and transfected after 24h according to manufacturer protocols (Effectene, Qiagen) using 5 μg of plasmid DNA. 48h after transfection cells were harvested and centrifuged at 1000 rpm for 10 minutes, resuspended in NaCl 0.9% (w/v) and centrifuged at 1000 rpm for 10 minutes. For mouse tissue were freshly excised and placed in ice cold PBS (1x) . The samples were washed with NaCl 0.9% (w/v). The homogenization steps were performed with Precellys Evolution Homogenizer, at 4500 rpm for 10 seconds. The samples were processed according to manufacturer protocols (Qproteome Mitochondria Isolation Kit, Qiagen).

From the different steps were obtained three different fractions: the cytosolic, the microsomal and the mitochondrial fraction. The fresh mitochondrial pellet was resuspended in 150µL of ice-cold lysis buffer and the protein concentration of the three fractions from each sample was quantified with a BCA assay. Cell lysates were loaded into 12% polyacrylamide gels using an SDS loading buffer (6x solution: 2.28g Tris-HCl, 2.313 DTT, 6g SDS, 30% Glycerol and 0.03% bromophenol blue in a final volume of 50 mL) in equal mass. The membrane was then incubated overnight at 4°C with primary antibody solution using the following concentrations: 1:1000 anti myc-Tag (9B11) mouse primary antibody (Cell Signaling), 1:1000 anti β-actin (13E5) rabbit primary antibody (#4970 from Cell Signaling), 1:1000 anti β-tubulin mouse primary antibody, 1:1000 anti GAPDH mouse primary antibody (s.c.-47724 from Santa Cruz Biotechnology), 1:1000 anti COXIV mouse primary antibody (#ab33985 from abcam).

7.12 Animal experiments

All animal experiments were carried out according to the German animal welfare act, considering the guidelines of the National Institute of Health and the 2010/63/EU Directive of the European Parliament on the protection of animals used for scientific purposes. The animals had free access to food and water and were kept in individually ventilated cages under a 12h:12h light/dark regime (light from 6:30 am to 6:30 pm), a constant 22 ±2°C temperature and 55 ±10% humidity. The transgenic line B6.Cg-Chrm2tm1.1Hze/J, also known as Chrm2-tdT-D knock-in, was obtained from 'The Jackson Laboratory' (Stock No: 030330). They are heterozygous animals, designed to have expression of a Chrm2/tdTomato fusion protein directed by the endogenous M_2 muscarinic acetylcholine receptor promoter/enhancer sequences.

7.12.1 Immunoblot of endogenous M_2 receptor in Chrm2-tdT-D knock-in mice

Mouse tissues were weighed out and ice-cold lysis buffer was added to approx. 0.2-0.5mg tissue/ml buffer (10mM K_2HPO_4, 150mM NaCl, 5mM EDTA, 5mM EGTA, 1% Triton X-100, 0.2% sodium deoxycholate. Fresh protease inhibitors PMSF 0.5mM, Na_3VO_4 0.1mM, NaF 50mM, Jenny's mix (Soybean trypsin inhibitor 3.2 μg/ml, Aprotinin 2µg/ml, Benzamidin 0.5mM) were added to the buffer. Samples were first

homogenized, and then pellet debris were centrifuged at 4°C for 30 minutes at max speed (tabletop) and the supernatant (soluble proteins) was transferred into fresh tube (pellets = non soluble proteins) Protein concentration were determined with BCA assay. Cell lysates were loaded using Laemmli Buffer 2x (Sigma Aldrich) in equal mass (see above for the immunoblot procedure) into 8% polyacrylamide gels. The membrane was then incubated overnight at 4°C with primary antibody solution 1:1000 anti β-actin (13E5) rabbit primary antibody #4970 from Cell Signaling, 1:1000 anti GAPDH (s.c.-47724 from Santa Cruz Biotechnology), 1:1000 anti-TdTomato rabbit primary antibody (#632496 from Takara).

7.12.2 Isolation of mitochondrial fractions and immunodetection

Mouse tissues were freshly excised and placed in ice cold PBS (1x) . The samples were washed with NaCl 0.9% (w/v). The homogenization steps were performed with Precellys Evolution Homogenizer, at 4500 rpm for 10 seconds. The samples were processed according to manufacturer protocols (Qproteome Mitochondria Isolation Kit, Qiagen). From the different steps were obtained three different fractions: the cytosolic, the microsomal and the mitochondrial fraction. The fresh mitochondrial pellet was resuspended in 150µL of ice-cold lysis buffer and the protein concentration of the three fractions from each sample was quantified with a BCA assay. Cell lysates were loaded into 12% polyacrylamide gels using an SDS loading buffer (6x solution: 2.28g Tris-HCl, 2.313 DTT, 6g SDS, 30% Glycerol and 0.03% bromophenol blue in a final volume of 50 mL) in equal mass. The membrane was then incubated overnight at 4°C with primary antibody solution using the following concentrations: 1:1000 anti myc-Tag (9B11) mouse primary antibody (Cell Signaling), 1:1000 anti β-actin (13E5) rabbit primary antibody (#4970 from Cell Signaling), 1:1000 anti β-tubulin mouse primary antibody, 1:1000 anti GAPDH mouse primary antibody (s.c.-47724 from Santa Cruz Biotechnology), 1:1000 anti COXIV mouse primary antibody (#ab33985 from abcam).

7.13 Oxygen consumption assay

7.13.1 Clark electrode method

In a 2 ml volume chamber kept under continuous stirring at the constant temperature of 37°C, after determination of the baseline of oxygen consumption in the presence of the sole culture medium, 6000000 of transfected cells were added, and the disappearance of oxygen was monitored through a Yellow Springs Instruments Model 53 Oxygen Monitor device (YSI Inc., Yellow Springs, OH). Since the electrode consumes oxygen during measurement, the rate of oxygen decrease in 2 mL of DMEM media with no cells was subtracted from the sample's oxygen consumption rates. Results are expressed as ng-atom of oxygen/min/10^6cells. For the evaluation of oxygen consumption rate in the absence of oxidative phosphorylation, the ATP synthase inhibitor oligomycin was added to the measurement vessel through a fine needle.

7.13.2 Sea Horse assay

50000 COS-7 cells were seeded in seahorse 24 MW plates with complete media, DMEM supplemented with 10% FBS and 1X P/S and then incubated for about 4 h at 37°C in a cell incubator. After this incubation cells were washed twice with Seahorse media supplemented with glutamate (1 mM), pyruvate (1 mM) and glucose (20 mM) and then incubated for 1 h at 37°C in an incubator without CO_2 before being analyzed in the Seahorse XF Analyzers. The baseline cell oxygen consumption rate, OCR, was measured at the beginning of the assay, followed by measurements of ATP linked respiration and maximal respiratory capacity after the addition of respectively oligomycin (1 μM) and the FCCP protonophore (1 μM); finally, rotenone (1 μM), an inhibitor of complex I, and antimycin (1 μM), inhibitor of complex III, were added to shut down completely the electron transport chain (ETC) function, revealing the non-mitochondrial respiration.

7.13.3 Extracellular oxygen consumption

HEK293 cells 24h after transfection and hiPSCs were harvested and seeded respectively in 96 MW black plate and pre-coated (Geltrex A1413302, Thermo Fisher) 96 MW black plate, 50000 cells for well; after incubation O.N. at 37°C and in 5% CO_2,

the cell culture medium was replaced by HBSS and the assay were performed according to the manufacturer protocols (abcam Extracellular Oxygen Consumption Assay).

7.14 Statistical analysis

Significance values reported in the graphs, in comparing tabulated values, were determined by a one-tailed Student t-test using Prism 9 (GraphPad Software), and significance values (p-values) are indicated according to the following legend: **** $p<0.0001$; *** $0.0001<p<0.001$; ** $0.001<p<0.01$; * $0.01<p<0.05$. p-values larger than 0.05 are deemed non-significant. Unless otherwise indicated, bar charts and scatter plots indicate average value with s.e.m.

References

1. Fasciani I., Petragnano F., Wang Z., Edwards R., Telegu N., Pietrantoni I., Zauber H., Rossi M., Zabel U., Grieben M., Terzenidou M.E., Di Gregorio J., Pellegrini C., Santini Jr S., Taddei A.R., Pöhl B., Aringhieri S., Marco Carli M., Aloisi G., Marampon F., Roman A., Diecke S., Flati V., Giorgi F., Amicarelli F., Tobin A.B., Scarselli M., Tokatlidis K., Lohse M.J., Maggio R., Annibale P., One gene - two proteins: The C-terminus of the prototypical M_2 muscarinic receptor localizes to the mitochondria. BioRxiv (2022)

2. Komar A.A. & Hatzoglou M., Cellular IRES-mediated translation. The war of ITAFs in pathophysiological states. Cell Cycle. 10, 229-240 (2011)

3. Jackson R.J. & Hellen C.U.T., Pestova T.V., The mechanism of eukaryotic translation initiation and principles of its regulation. Nat Rev Mol Cell Biol. 11(2):113-27 (2010)

4. Hinnebusch A.G., Transcriptional and translational regulation of gene expression in the general control of amino-acid biosynthesis in Saccharomyces cerevisiae. Prog Nucleic Acid Res Mol Biol. 38, 195-240 (1990)

5. Yueh A. & Schneider R.J., Translation by ribosome shunting on adenovirus and hsp70 mRNAs facilitated by complementarity to 18S rRNA. Gene Dev. 14, 414-42 (2000)

6. Jackson R. J. & Kaminski A., Internal initiation of translation in eukaryotes: the picornavirus paradigm and beyond. RNA 1, 985-1000 (1995).

7. Hellen C. U. & Sarnow P., Internal ribosome entry sites in eukaryotic mRNA molecules. Genes Dev 15, 1593-1612 (2001).

8. Kaminski A., Howell M.T., Jackson R.J., Initiation of encephalomyocarditis virus RNA translation: The authentic initiation site is not selected by a scanning mechanism. EMBO J. 9, 3753-3759 (1990)

9. Sangar D.V., Newton S.E., Rowlands D.J., Clarke B.E., All foot and mouth disease virus serotypes initiate protein synthesis at two separate AUGs Nucleic Acids Res. 15,3305-15 (1987)

10. Belsham G.J., Dual initiation sites of protein synthesis on foot-and-mouth disease virus RNA are selected following internal entry and scanning of ribosomes in vivo. EMBO J. 11, 1105-1110 (1992)

11. Komar A.A., Lesnik T., Cullin C., Merrick W.C., Trachsel H., Altmann M., Internal initiation drives the synthesis of Ure2 protein lacking the prion domain and affects [URE3] propagation in yeast cells. EMBO J. 22,1199-209 (b) (2003)

12. Baird S.D., Lewis S.M., Turcotte M., Holcik M., A search for structurally similar cellular internal ribosome entry sites. Nucleic Acids Res. 35, 4664-77 (2007)

13. Fitzgerald K.D. & Semler B.L., Bridging IRES elements in mRNAs to the eukaryotic translation apparatus. Biochim Biophys Acta. 1789, 518-528 (2009)

14. Lewis S.M. & Holcik M., For IRES trans-acting factors, it is all about location. Oncogene. 27,1033-5 (2008)

15. Coleman J. & Miskimins W.K., Structure and activity of the internal ribosome entry site within the human p27Kip1 5'-untranslated region. RNA Biol. 6,84-9 (2009)

16. Dorsam R.T. & Gutkind J.S., G-protein-coupled receptors and cancer. Nat Rev Cancer. 7, 79-94 (2007)

17. Clementi F., Fumagalli G., Paoletti R., Nicosia S., Farmacologia generale e molecolare. Ed. UTET (1996)

18. Wettschureck N. & Offermanns S., Mammalian G proteins and their cell type specific functions. Physiol Rev. 85, 1159-1204 (2005)

19. Rossi F., Cuomo V. e Riccardi C., Farmacologia principi di base e applicazioni terapeutiche. Ed. MINERVA (2005)

20. Jöhren K. & Höltje H.D., A model of the human M_2 muscarinic acetylcholine receptor. Journal of Computer-Aided Molecular Design. 16, 795–801 (2002)

21. Wess J., Eglen R.M., Gautam D., Muscarinic acetylcholine receptors: mutant mice provide new insights for drug development. Nat Rev Drug Discov. 6, 721-33 (2007)

22. Weston-Green K., Huang X.F., Lian J., Deng C., Effects of olanzapine on muscarinic M_3 receptor binding density in the brain relates to weight gain, plasma insulin and metabolic hormone levels. Eur Neuropsychopharmacol. 22, 364-73 (2012)

23. Peralta E.G., Ashkenazi A., Winslowl J.W., Smith D.H., Ramachandran J., Capon D.J., Distinct primary structures, ligand-binding properties and tissue specific expression of four human muscarinic acetylcholine receptors. The EMBO Journal. 6, 3923 -3929 (1987)

24. Eglen R.M., Choppin A., Watson N., Therapeutic opportunities from muscarinic receptor research. Trends Pharmacol. Sci. 22, 409-14 (2001)

25. Wise H., The roles played by highly truncated splice variants of G protein-coupled receptors. J Mol Signal. 7, 13 (2012)

26. Maggio R., Vogel Z., Wess J., Co-expression studies with mutant muscarinic/adrenergic receptors provide evidence for intermolecular “cross-talk” between G-protein linked receptors. Proc Natl Acad Sci. 90, 3103-3107 (1993a)

27. Maggio R., Fasciani I., Rossi M., Di Gregorio J., Pietrantoni I., Puca V., Flati V., Scarselli M., Variants of G protein-coupled receptors: a

reappraisal of their role in receptor regulation. Biochem Soc Trans 44, 589-594, doi:10.1042/BST20150239 (2016)

28. Maggio R., Vogel Z., Wess J., Reconstitution of functional muscarinic receptors by co-expression of amino- and carboxyl-terminal receptor fragments. FEBS Lett. 319, 195–200 (1993b)

29. Maggio R., Barbier P., Colelli A., Salvadori F., Demontis G., Corsini G.U., G protein-linked receptors: pharmacological evidence for the formation of heterodimers. J. Pharmacol. Exp. Ther. 291, 251–257 (1999).

30. Schueren F., Lingner T., George R., Hofhuis J., Dickel C., Gärtner J., Thoms S., Peroxisomal lactate dehydrogenase is generated by translational readthrough in mammals. eLife 3, e03640 (2014)

31. Kozak, M., Constraints on reinitiation of translation in mammals. Nucleic Acids Res 29, 5226- 5232, doi:10.1093/nar/29.24.5226 (2001)

32. Kozak M., Circumstances and mechanisms of inhibition of translation by secondary structure in eucaryotic mRNAs. Mol Cell Biol 9, 5134-5142, doi:10.1128/mcb.9.11.5134 (1989)

33. Loughran G., Chou M.Y., Ivanov I.P., Jungrei I., Kellis M., Kiran A.M., Baranov P.V., Atkins J.F., Evidence of efficient stop codon readthrough in four mammalian genes. Nucleic Acids Res. 42, 8928–8938 (2014)

34. Park P.S.H. & Wells J.W., Monomers and oligomers of the M_2 muscarinic cholinergic receptor purified from Sf9 cells. Biochemistry 42, 12960–12971 (2003)

35. Taylor A.B., Smith B.S., Kitada S., Kojima K., Miyaura H., Otwinowski Z., Ito, A., Deisenhofer J., Crystal structures of mitochondrial processing peptidase reveal the mode for specific cleavage of import signal sequences. Structure 9, 615–625 (2001)

36. Davies C.W., Vidal S.E, Phu L., Sudhamsu J., Hinkle T.B., Rosenberg S.C., Schumacher F., Zeng Y.J., Schwerdtfeger C., Peterson A.S., Lill

J.R., Rose C.M., S Shaw A.S., Wertz I.E., Kirkpatrick D.S., Koerber J.T., Antibody toolkit reveals N-terminally ubiquitinated substrates of UBE2W. Nat Commun 29;12(1):4608 (2021)

37. Zhang J., Nuebel E., Wisidagama D.R., Setoguchi K., Hong J.S., Van Horn C.M., Imam S.S., Vergnes L., Malone C.S., Koehler C.M., Teitell M.A., Measuring energy metabolism in cultured cells, including human pluripotent stem cells and differentiated cells. Nat. Protoc. 7, 1068–1085 (2012)

38. Holcik M. & Sonenberg N., Translational control in stress and apoptosis. Nat. Rev. Mol. Cell Biol. 6, 318–327 (2005)

39. Thakor N. & Holcik M., IRES-mediated translation of cellular messenger RNA operates in eIF2α- independent manner during stress. Nucleic Acids Res. 40, 541–552 (2012)

40. Newman L. E., Schiavon C., Kahn R. A., Plasmids 1337 for variable expression of proteins targeted to the mitochondrial matrix or intermembrane space. Cell Logist 6, e1247939, doi:10.1080/21592799.2016.1247939 (2016)

41. Bonfili L., Cecarini V., Cuccioloni M., Angeletti M., Flati V., Corsetti G., Pasini E., Dioguardi F.S., Eleuteri A.M., Essential amino acid mixtures drive cancer cells to apoptosis through proteasome inhibition and autophagy activation. FEBS J 284, 1726-1737, doi:10.1111/febs.14081 (2017)

42. Richardson C.D., Ray G.J., DeWit M.A., Curie, G.L., Corn, J.E., Enhancing homology directed genome editing by catalytically active and inactive CRISPR-Cas9 using asymmetric donor DNA. Nat Biotechnol 34, 339-344, doi:10.1038/nbt.3481 (2016)

43. Vallone V.F., Vallone V.F., Telugu N.S., Fischer I., Miller D., Schommer S., Diecke S., Methods for Automated Single Cell Isolation and Sub-Cloning of Human Pluripotent Stem Cells. Curr Protoc Stem Cell Biol 55, e123, doi:10.1002/cpsc.123 (2020)

44. Metzler E., Telugu N., Diecke S., Spuler S., Escobar H. Generation of two human induced pluripotent stem cell lines derived from myoblasts (MDCi014-A) and from peripheral blood mononuclear cells (MDCi014-B) from the same donor. Stem Cell Res 48, 101998, doi:10.1016/j.scr.2020.101998 (2020)

45. Ishizuka T., Ozawa A., Katsuura M., Nomura S., Satoh Y., Effects of muscarinic acetylcholine receptor stimulation on the differentiation of mouse induced pluripotent stem cells into neural progenitor cells. Clin Exp Pharmacol Physiol 45, 1198-1205, doi:10.1111/1440-1681.12993 (2018)

46. Hoogduijn M.J., Cheng A., Genever, P.G., Functional nicotinic and muscarinic receptors on mesenchymal stem cells. Stem Cells Dev 18, 103-112, doi:10.1089/scd.2008.0032 (2009)

47. Marti-Solano M., Crilly S.E., Malinverni D., Munk C., Harris M., Pearce A., Quon T., Mackenzie A.E., Wang X., Peng J., Tobin A.B, Ladds G., Milligan G., Gloriam D.E., A Puthenveedu M.A., Babu M.M., Combinatorial expression of GPCR isoforms affects signalling and drug responses. Nature 587, 650-656, doi:10.1038/s41586-020-2888-2 (2020)

48. van Heesch S., Witte F.,Schneider-Lunitz V., Schulz J.F., Adami E., Faber A.B., Kirchner M., Maatz H., Blachut S., Sandmann C., Kanda M., Worth C.L., Schafer S., Calviello L., Merriott R., Patone G., Hummel O., Wyler E., Obermayer B., Mücke M.B., Lindberg E.L., Trnka F., Memczak S., Schilling M., Felkin L.E., Barton P.J.R., Quaife N.M., Vanezis K., Diecke S., Mukai M., Mah N., Oh S., Kurtz A., Schramm C., Schwinge D., Sebode M., Harakalova M., Asselbergs F.W., Vink A., de Weger R.A, Viswanathan S., Widjaja A.A., Gärtner-Rommel A., Milting H., Remedios C., Knosalla C., Mertins P., Landthaler M., Vingron M., Linke W.A., Seidman J.G., Seidman C.E., Rajewsky N., Ohler U., Cook S.A., Hubner N., The translational landscape of the human heart. Cell 27;178(1):242-260.e29. doi: 10.1016/j.cell.2019.05.010 (2019)

49. Chappell S.A., Edelman G.M., Mauro V.P. A 9-nt segment of a cellular mRNA can function as an internal ribosome entry site (IRES) and when

present in linked multiple copies greatly enhances IRES activity. Proc. Natl. Acad. Sci. 97, 1536–1541 (2000)

50. Schöneberg, T., Liu, J., Wess, J., Plasma membrane localization and functional rescue of truncated forms of a G protein-coupled receptor. J. Biol. Chem. 270, 18000–18006 (1995)

51. Stojanovski D., Bohnert M., Pfanner N., van der Laan M., Mechanisms of protein sorting in mitochondria. Cold Spring. Harb. Perspect. Biol. 4, 1–18 (2012)

52. Vögtle F.N., Wortelkamp S., Zahedi R.P., Becker D., Leuthold C., Gevaert K., Kellermann J., Voos W., Sickmann A., Pfanner N., Meisinger C., Global analysis of the mitochondrial N-proteome identifies a processing peptidase critical for protein stability. Cell 139, 428–439 (2009)

53. Taylor A.B., Smith B.S., Kitada S., Kojima K., Miyaura H., Otwinowski Z., Ito A., Deisenhofer J., Crystal structures of mitochondrial processing peptidase reveal the mode for specific cleavage of import signal sequences. Structure 9, 615–625 (2001)

54. Weinberg Z.Y. & Puthenveedu M.A., Regulation of G protein-coupled receptor signaling by plasma membrane organization and endocytosis. Traffic 20, 121-129,1348 doi:10.1111/tra.12628 (2019)

55. Lyssand J.S. & Bajjalieh S.M., The heterotrimeric G protein subunit $G_{\alpha i}$ is present on mitochondria. FEBS Lett. 581, 5765–5768 (2007)

56. Zhang J., Liu W., Liu J., Xiao W., Liu L., Jiang C., Sun X., Liu P., Zhu Y., Zhang C., Chen Q., G-protein β_2 subunit interacts with mitofusin 1 to regulate mitochondrial fusion. Nat. Commun. 1, 101 (2010)

57. Wang Q., Zhang H., X H., Guo, D., Shi H., Li Y., Zhang W., Gu Y., 5-HTR_3 and 5-HTR_4 located on the mitochondrial membrane and functionally regulated mitochondrial functions. Sci. Rep. 6, 37336 (2016)

58. Wang X., Sirianni A., Pei Z., Cormier K., Smith K., Jiang J., Zhou S., Wang H., Zhao R., Yano H., Kim J.E., Li W., Kristal B.S., Ferrante R.J., Friedlander R.M., The melatonin MT_1 receptor axis modulates mutant Huntingtin-mediated toxicity. J. Neurosci. 31, 14496–507 (2011)

59. Suofu Y., Li W., Jean-Alphonse F.G., Jia J., Khattar N.K., Li J., Baranov S.V., Leronni D., Mihalik A.C., He Y., Cecon E., Wehbi V.L., Kim J., Heath B.E., Baranova O.V., Wang X., Gable M.J., Kretz E.S., Di Benedetto G., Lezon T.R., Ferrando L.M., Larkin T.M., Sullivan M., Yablonska S., Wang J., Minnigh M.B., Guillaumet G., Suzenet, F., Richardson, R.M., Poloyac S.M., Stolz D.B., Jockers R., Witt-Enderby P.A., Carlisle D.L., Vilardaga J.P., Friedlander R.M., Dual role of mitochondria in producing melatonin and driving GPCR signaling to block cytochrome c release. Proc. Natl. Acad. Sci. USA 114, E7997–E8006 (2017)

60. Benard, G., Massa F., Puente N., Lourenço J., Bellocchio L., Soria-Gómez E., Matias I., Delamarre A., Metna-Laurent M., Cannich A., Hebert-Chatelain E., Mulle C., Ortega-Gutiérrez S., Martín-Fontecha M., Klugmann M., Guggenhuber S., Lutz B., Gertsch J., Chaouloff F., López-Rodríguez M.L., Grandes P., Rossignol R., Marsicano G., Mitochondrial CB_1 receptors regulate neuronal energy metabolism. Nat Neurosci 15, 558-564, doi:10.1038/nn.3053 (2012)

61. Murphy M.P., How mitochondria produce reactive oxygen species. Biochem. J. 417, 1–13 (2009)

62. Guo C., Sun L., Chen X., Zhang D., Oxidative stress, mitochondrial damage and neurodegenerative diseases. Neural Regen. Res. 8, 2003–2014 (2013)

63. Zhang J., Nuebel E., Daley G.Q., Koehler C.M., Teitell M.A., Metabolic regulation in pluripotent stem cells during reprogramming and self-renewal. Cell Stem Cell 11, 589-595, doi:10.1016/j.stem.2012.10.005 (2012)

Acknowledgments

I would like to thank Pharmacology Lab, for having been part of this course during the years, the ones that are still present but also all the people had share this adventure with me.

A special thank goes to prof. Maggio for giving me the chance to take up this career.

I want to thank also the Lohse's group of Max Delbrück Center for giving me the chance to measure myself within a stimulating environment, in particular Dr. Annibale for guiding me during my months in Berlin. I want to thank all the members of the group for having been not only colleagues but also great company to spend time with, you have made my days more interesting.